Linköping Studies in Science and Technology. Dissertations.
No. 1180

Efficient Simulation and Optimal Control for Vehicle Propulsion

Anders Fröberg

Department of Electrical Engineering
Linköpings universitet, SE–581 83 Linköping, Sweden
Linköping 2008

Efficient Simulation and Optimal Control for Vehicle Propulsion

froberg@isy.liu.se
www.vehicular.isy.liu.se
Division of Vehicular Systems
Department of Electrical Engineering
Linköpings universitet
SE–581 83 Linköping
Sweden

ISBN 978-91-7393-904-1 ISSN 0345-7524

Printed by LiU-Tryck, Linköping, Sweden 2008

To my dear family, Carolina, Viktor and Arvid

Abstract

Efficient drive cycle simulation of longitudinal vehicle propulsion models is an important aid for design and analysis of power trains. Tools on the market today mainly use two different methods for such simulations, forward dynamic or quasi-static inverse simulation. Here known theory for stable inversion of non linear systems is used in order to combine the fast simulation times of the quasi-static inverse simulation with the ability of including transient dynamics as in the forward dynamic simulation. The stable inversion technique with a new implicit driver model together forms a new concept, inverse dynamic simulation. This technique is demonstrated feasible for vehicle propulsion simulation and specifically on three powertrain applications that include important dynamics that can not be handled using quasi-static inverse simulation. The extensions are engine dynamics, drive line dynamics, and gas flow dynamics for diesel engines, which also are selected to represent important properties such as zero dynamics, resonances, and non-minimum phase systems. It is shown that inverse dynamic simulation is easy to set up, gives short simulation times, and gives consistent results for design space exploration. This makes inverse dynamic simulation a suitable method to use for drive cycle simulation, especially in situations requiring many simulations, such as optimization over design space, powertrain configuration optimization, or development of powertrain control strategies.

Optimal vehicle propulsion control is developed with special focus on heavy trucks used for long haulage. The power to mass ratio for a typical heavy duty truck makes even moderate road slopes significant in the sense that it is impossible to keep a constant cruising speed. This gives an interesting problem how to control vehicle speed such that fuel consumption is minimized. Todays telematic systems together with three dimensional road maps can provide the vehicle control system with information of the road topography. This enables intelligent cruise controllers that utilize this information to control engine fueling and gear shifting such that an optimal speed trajectory is obtained.

First the optimal control problem is solved numerically by dynamic programming, giving a controller with real time capabilities that can be used on-line in the vehicles control system. Simulations of such a system on authentic road profiles show that it has potential for significant fuel savings. To achieve knowledge about the underlying physics that affects the optimal solution, the optimal control problem is solved in detail and analytical expressions for the conditions of optimality are derived. Those expressions are then used to find optimal solutions on constructed test road profiles. Such test cases point out the typical behavior of an optimal solution and also which parameters that are decisive for the fuel minimization problem, and also how they quantitatively influence the behavior. It is for example shown that small non-linearities in the engine torque characteristics have significant effect on the optimal control strategy. The solutions for the non linear engine model have a smoother character but also require longer prediction horizons. For optimal gear ratio control it is shown that the maximum fueling function is essential for the solution. For example, in the case of a continuously variable transmission it is shown that the gear ratio never is chosen such that engine speed exceeds the speed of maximum engine power. For a discrete step transmission the gear shifting losses are essential for the optimal shift positions, but over all the solutions are close to continuous solutions.

Sammanfattning

Effektiv körcykelsimulering av longitudinella fordonsframdrivningsmodeller är ett viktigt hjälpmedel för design och analys av drivlinor. Tillgängliga verktyg på marknaden idag använder huvudsakligen två metoder för sådan simulering, framåtdynamisk simulering eller kvasistatisk inverssimulering. Kända metoder för stabil invertering av olinjära system används här för att kombinera de snabba beräkningseffektiva kvasistatiska inverssimuleringarna med den framåtdynamiska simuleringens möjlighet att inkludera transient dynamik. Metoden för stabil invertering tillsammans med en ny implicit förarmodell skapar tillsammans ett nytt koncept, inversdynamisk simulering. Denna metods användbarhet för simulering av fordonsframdrivning demonstreras på tre drivlineexempel som innehåller viktig transient dynamik som inte kan hanteras med kvasistatisk inverssimulering. Utvidningarna är motordynamik, drivlinedynamik och gasflödesdynamik för dieselmotorer. Dessa har också valts för att representera viktiga egenskaper såsom nolldynamik, resonanser och icke-minfas-beteende. Det visas att inversdynamisk simulering är enkel att sätta upp, ger korta simuleringstider och ger konsistenta resultat vid parameterstudier. Detta gör att inversdynamisk simulering är en passande metod för körcykelsimulering särskilt i situationer som kräver många simuleringar, såsom parameteroptimering, optimering av drivlinekonfiguration eller utveckling av reglerstrategier för drivlinor.

Optimal styrning av fordonsframdrivning utvecklas med särskilt fokus på landsvägskörning med tunga lastbilar. Förhållandet mellan motoreffekt och fordonsmassa för en typisk tung lastbil gör att det inte är möjligt att hålla en konstant marschfart ens i relativt små väglutningar. Därför är det ett intressant reglerproblem att styra fordonets hastighet så att bränsleförbrukningen minimeras. Dagens telematiksystem tillsammans med tredimensionella vägkartor kan levera information om vägtopografi till fordonets styrsystem. Denna information ger möjligheten att skapa intelligenta farthållare för att styra bränsleinsprutning och växling så att en optimal hastighetstrajektoria erhålls.

Först löses det optimala styrnings-problemet numeriskt med dynamisk programmering vilket ger en regulator med realtidsegenskaper som kan användas on-line i fordonets styrsystem. Simulering av ett sådant system på autentiska vägprofiler visar på potential för signifikanta bränslebesparingar. Det optimala styrnignsprobelemet löses sedan i detalj för att få kunskap om den påverkande underliggande fysiken och analytiska uttryck för optimalitetsvillkoren härleds. Dessa uttryck används för att hitta optimala lösningar på konstruerade testvägprofiler. Sådana testfall pekar ut typiskt beteende för en optimal lösning och också vilka parametrar som är bestämmande för bränsleminimeringsproblemet. Till exempel visas att små olinjäriteter i motorns momentkaraktäristik har stor betydelse för den optimala reglerstrategin. Lösningarna för den olinjära motormodellen har en mjukare karaktär men kräver också längre prediktionshorisont. För optimal växlingsreglering visas det att bränslebegränsingsfunktionen är viktig för lösningen. I till exempel fallet med kontinuerligt variabelt utväxlingsförhållande visas det att utväxling aldrig väljs så att varvtalet för motorns maxeffekt överskrids. För en stegad växellåda så är växlingsförlusterna viktiga för de optimala växlingspunkterna, men som helhet är lösningarna liknande de kontinuerliga lösningarna.

Acknowledgments

This work has been carried out under the guidance of Professor Lars Nielsen at Vehicular Systems, Department of Electrical Engineering, Linköpings Universitet, Sweden.

The Swedish Energy Agency through the Center for Automotive Propulsion Simulation CAPSIM, and the Swedish Foundation for Strategic Research, through the VISIMOD project and the Excellence Center in Computer Science and Systems Engineering ECSEL, are gratefully acknowledged for their funding.

I would like to express my gratitude to a number of people:

Professor Lars Nielsen for letting me join this group, for supervision and guidance of this work, and for the many interesting discussions along the way.

My assistant supervisors Jan Åslund and Lars Eriksson for interesting research discussions. My colleague Erik Hellström for his contributions to our collaborative work and for his many interesting ideas on the fuel optimal control problem. All other colleagues at the division of vehicular systems for making it a nice place to work at.

Most of all I would like to thank my wife, Carolina and our sons, Viktor and Arvid, for sharing life with me and making me happy. You mean everything for me. I love you!

Contents

1 Introduction

For road vehicles performance, cost, and safety have traditionally been important factors to optimize. Also environmental aspects has emerged as a top priority, where one main focus of the industry has been to reduce fuel consumption and thereby CO_2 emission. In this strive, the power trains and the vehicle's control systems have become more and more complex. One example is hybrid vehicles where two or more power sources, in a coordinated fashion, propels the vehicle. Another example is advanced traffic information systems that provides information to the driver and/or the vehicle control system. Then the current road and traffic situation can be used in an intelligent way, such that the vehicle can be driven more fuel efficiently. Systems that can adapt to current situation and operate in the most fuel efficient way for that situation are for example cruise controllers, gear shifting programs for automatic transmissions, and energy management systems for hybrid vehicles.

In the development of such complex systems simulation and optimization have become necessary tools when designing a competitive product that is optimized with respect to many criteria. The way to handle this is to use mathematical models of the vehicle, and simulation of such models can to a high extent replace physical prototypes when testing different design choices. To find an optimal design of the physical vehicle and/or its control system, simulation of the mathematical models can be used to evaluate different criteria. This process can be automatized by coupling the simulation with an optimization algorithm. Simulation and optimization also shortens the product development cycle which is necessary to cut development costs. A recent case where simulation studies replaced most prototype testing is the new Fiat 500 with a total development time of 18 months. Simulation is also an important part of many control algorithms where predictions of future vehicle states are made by simulation, and then used to find the optimal control signals.

In this thesis simulation methods and optimization of vehicle propulsion has been studied with the main focus on fuel consumption. The first part of the thesis treats ef-

ficient vehicle propulsion simulation methods that are suitable to for example parameter optimization and control strategy evaluation. The second part treats fuel optimal driving of heavy trucks, and special attention is given to optimal control of engine fueling and optimal gear shifting strategies under the assumption that the road topography ahead of the vehicle is known. The results of the thesis can for example be used to design fuel optimal control strategies, but the methods presented are also applicable for other purposes where one important example is emission minimization.

1.1 Contributions

The contributions of the thesis will here shortly be summarized for each appended paper. A more detailed description is given in the introduction for the respective parts of the thesis.

Efficient Drive Cycle Simulation, Anders Fröberg and Lars Nielsen, IEEE Transactions on Vehicular Technology, accepted for publication, 2008. The paper proposes a new method for inverse dynamic vehicle simulation. The new method is compared to forward dynamic simulation regarding for example simulation setup effort, consistency for parameter exploration, and simulation time. Also, a new driver model for inverse dynamic simulation has been developed that makes it easy to define drive cycle tracking that is independent of vehicle properties.

Inverse Dynamic Simulation of Non-Quadratic MIMO Powertrain Models -Application to Hybrid Vehicles, Anders Fröberg, IEEE Vehicle Power and Propulsion Conference 2006. Extending the previous paper, it is demonstrated how typical non-quadratic MIMO power train models can be reformulated enabling inverse dynamic simulation. It is also demonstrated how time variant system order and time variant relative degree is handled.

Controlling Gear Engagement and disengagement on heavy trucks for minimization of fuel consumption, Anders Fröberg, Lars Nielsen, Lars-Gunnar Hedström, and Magnus Pettersson, IFAC World Congress 2005. This paper treats fuel optimal use of neutral gear using preview information of road topography. The contribution is to show the magnitude of possible fuel savings by making the correct decision in steep downhill slopes whether to disengage the gear or to cut the fuel injection.

A Real-Time Fuel-Optimal Cruise Controller for Heavy Trucks using Road Topography Information, Erik Hellström, Anders Fröberg, and Lars Nielsen, SAE World Congress 2006. It is shown how a predictive cruise controller with real time performance can be designed using dynamic programming, and the magnitude of possible fuel savings is demonstrated.

Explicit Fuel Optimal Speed Profiles for Heavy Trucks on a Set of Topograhic Road Profiles, Anders Fröberg, Erik Hellström, and Lars Nielsen SAE World Congress 2006. To gain knowledge of decisive parameters affecting fuel consumption, fueling control is here studied on constructed road profiles. The simple test cases together with analytical solutions to vehicle motion gives valuable insight into the properties of the optimal control.

Optimal Control Utilizing Analytical Solutions for Heavy Truck Cruise Control, Anders Fröberg and Lars Nielsen, technical report that is an extended version of the paper *Optimal fuel and gear ratio control for heavy trucks with piece wise affine engine charac-*

teristics, Anders Fröberg and Lars Nielsen, Fifth IFAC symposium on advances in automotive control, California, 2007. The fuel optimal control problem treated in the previous paper is solved in more detail. Engine torque is a piece wise affine function of fueling, and optimal gear choice is presented both for a continuously variable transmission as well as for a discrete stepped transmission. The theoretical results are used in a simple rule based predictive cruise controller and the possible fuel savings for that method is demonstrated in simulations on authentic road profiles.

The following work have also been published by the author, but are not included here:

Dynamic Vehicle Simulation -Forward, Inverse and New Mixed Possibilities for Optimized Design and Control, Anders Fröberg and Lars Nielsen in Modeling: Diesel Engines, Multi-Dimensional Engine, and Vehicle and Engine Systems. Volume 2002-01-1619 of SAE Technical paper series SP-1826.

A Method to Extend Inverse Dynamic Simulation of Powertrains with Additional Dyanmics , Anders Fröberg and Lars Nielsen in 1:st IFAC symposium on Advances in Automotive Control.

Extending the Inverse Vehicle Propulsion Simulation Concept-To Improve Simulation Performance, Anders Fröberg, Licentiate thesis.

Optimal Fuel and Gear Ratio Control for Heavy Trucks with Piece Wise Affine Engine Characteristics, Anders Fröberg and Lars Nielsen, Fifth IFAC Symposium on Advances in Automotive Control 2007.

Part I

Efficient vehicle propulsion simulation

2
Inverse dynamic simulation

Modeling and simulation are today widely used tools when designing new power trains and control systems. In for example optimization of a power train, a candidate design is evaluated by use of an objective function. When optimizing complex systems the calculation of the objective function can not always be done by calculation of analytical expressions, instead a simulation of the model has to be done to calculate the objective function. Using simulation in this way possibly a large number of simulations have to be performed of the same model, where some parameters are varied from simulation to simulation. For these situations computational efficiency and consistency between simulations are important properties for the simulation method. The aim in this part of the thesis is to find a simulation method that has good behavior with respect to these properties.

When certifying a vehicle with respect to fuel consumption and emission levels, the vehicle is driven according to a given speed profile, a drive cycle. Hence, a typical task for vehicle propulsion simulation is drive cycle simulation which is the main topic of this part of the thesis. Another typical task for vehicle propulsion simulation is performance simulations which are done to test for example acceleration performance or the vehicles ability to keep speed in steep grades. Although it is not exemplified here, the methods presented in this part can be used for such simulations as well.

Mainly two different methods have been used for vehicle propulsion simulation. Forward dynamic simulation and quasi-static inverse simulation. The forward dynamic simulation typically uses models that consist of a set of ordinary differential equations, ODEs, that uses the drivers input, e.g. throttle, brakes, and steering input, to calculate the vehicles states and speed. Since the method is capable of handling dynamic systems, the prediction of for example fuel consumption and emissions can be accurate. Quasi-static inverse simulation uses speed and acceleration given from the speed profile to calculate the required torque and speed at the wheels. The computation then goes backward through the driveline to compute the generating variables to produce the given torque and speed. Each component uses a static model and hence the prediction ability for this type of sim-

ulation is not as good as for the forward dynamic simulation. On the other hand, due to the static models the simulation time for these models are very short, which makes it a suitable method for initial concept studies and parameter optimizations. This first part of the thesis suggests that known theory for inversion of non-linear systems is used to combine the merits of forward dynamic simulation and quasi-static inverse simulation.

2.1 Overview and contributions of simulation

This thesis part on simulation consists of two papers. *Efficient Drive Cycle Simulation*, Anders Fröberg and Lars Nielsen, IEEE Transactions on Vehicular Technology, accepted for publication, 2008, and *Inverse Dynamic Simulation of Non-Quadratic MIMO Powertrain Models -Application to Hybrid Vehicles*, Anders Fröberg, IEEE Vehicle Power and Propulsion Conference 2006. In the first paper a new inverse dynamic simulation method is proposed. A comparison of forward and inverse simulation of vehicle propulsion models is presented. The comparison is done in order to evaluate how well different simulation methods are suited for different tasks. For example how well the method can capture transients, how suitable it is for optimization, and how computationally efficient the method is. A new driver model for inverse dynamic simulation has been developed that makes it easy to define drive cycle tracking that is independent of vehicle properties. This work has also been presented more thoroughly in *Extending the Inverse Vehicle Propulsion Simulation Concept-To Improve Simulation Performance*, Licentiate thesis, Anders Fröberg.

The second paper is an extension to the first and deals with some practical issues for vehicle propulsion simulation. For example, inverse dynamic simulation in general requires a quadratic system, i.e. a system with equally many inputs and outputs. This paper demonstrates how this requirement can be relaxed for typically non-quadratic vehicle propulsion models. It is also demonstrated how vehicle propulsion models with time variant system order and time variant relative degree can be simulated.

2.1.1 Related publications

The following publications by the author also treats the subject of this part, but are not included here.

Dynamic Vehicle Simulation -Forward, Inverse and New Mixed Possibilities for Optimized Design and Control, Anders Fröberg and Lars Nielsen in Modeling: Diesel Engines, Multi-Dimensional Engine, and Vehicle and Engine Systems. Volume 2002-01-1619 of SAE Technical paper series SP-1826.

A Method to Extend Inverse Dynamic Simulation of Powertrains with Additional Dyanmics , Anders Fröberg and Lars Nielsen in 1:st IFAC symposium on Advances in Automotive Control.

Extending the Inverse Vehicle Propulsion Simulation Concept-To Improve Simulation Performance, Anders Fröberg, Licentiate thesis.

Paper A

EFFICIENT DRIVE CYCLE SIMULATION[1]

Anders Fröberg[⋆]**, Lars Nielsen**[⋆]

[⋆] *Dep. of Electrical Engineering, Linköpings universitet,*
SE-*581 83 Linköping, Sweden.* {froberg, lars}@isy.liu.se.

Abstract

Drive cycle simulations of longitudinal vehicle models is an important aid for design and analysis of power trains, and tools on the market today mainly use two different methods for such simulations, forward dynamic or quasi-static inverse simulation. Here known theory for stable inversion of non linear systems is used in order to combine the fast simulation times of the quasi-static inverse simulation with the ability of including transient dynamics as in the forward dynamic simulation. The stable inversion technique with a new implicit driver model together form a new concept, inverse dynamic simulation. This technique is demonstrated feasible for vehicle propulsion simulation and specifically on three powertrain applications that include important dynamics that can not be handled using quasi-static inverse simulation. The extensions are engine dynamics, drive line dynamics, and gas flow dynamics for diesel engines, which also are selected to represent important properties such as zero dynamics, resonances, and non-minimum phase systems. It is shown that inverse dynamic simulation is easy to set up, gives short simulation times, and gives consistent results for design space exploration. This makes inverse dynamic simulation a suitable method to use for drive cycle simulation, especially in situations requiring many simulations, such as optimization over design space, powertrain configuration optimization, or development of powertrain control strategies.

[1] This is an edited version of [11], Efficient drive cycle simulation, accepted for publication in IEEE Transactions on Vehicular Technology.

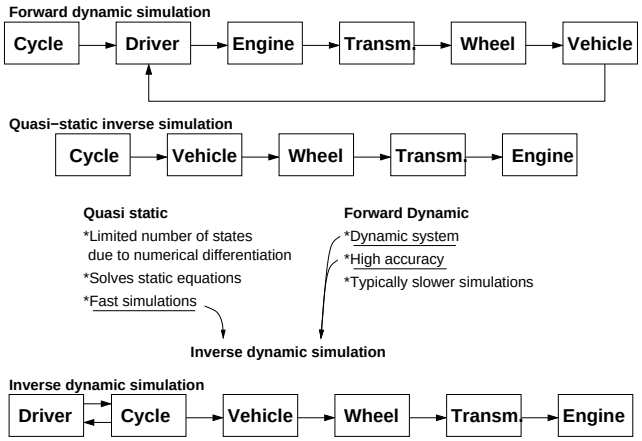

Figure 1: *Schematic depiction of different computational schemes, also illustrating goal of the paper.*

1 Introduction

There are a number of important uses of drive cycle simulations, and among all applications there are many where simulation time is important. It has been used a lot in concept studies [31, 14, 21], and other examples where drive cycle simulation is used is in optimization over a design space of parameters [14, 19], in optimization of powertrain configuration [24, 2], and in design of powertrain control systems, [3], [25]. Drive cycle simulation is also used in controllers such as model predictive cruise controllers, [13].

There are two main ways to do longitudinal vehicle simulation, quasi-static inverse simulation and forward dynamic simulation. The quasi-static inverse simulation uses vehicle speed and acceleration to calculate required torques and speeds backwards through the driveline. Finally fuel flow is calculated. See Figure 1 for a typical computational scheme of quasi-static inverse simulation. No driver model is used and drive cycle tracking is explicit. In existing tools today the following *quasi-static approach* [15], [30] to inverse simulation is taken. The speed, $v(t)$, and acceleration, $\dot{v}(t)$, are approximated by $v(t) = (v(kh+h) + v(kh))/2$, $\dot{v}(t) = (v(kh+h) - v(kh))/h$. In this way only static equations are solved when the input is computed, and a major advantage of this method is that simulation time is low. On the other hand, in forward dynamic simulation, differential equations are solved using, e.g., throttle position or fuel flow as input, and vehicle speed as output. Given an initial value of the vehicle's states and the input, the system is numerically integrated to compute the speed trajectory. This type of simulation also requires a driver model, a controller, to track a given speed trajectory (drive cycle) as depicted in Figure 1. For forward dynamic simulation drive cycle tracking is implicit since it is obtained using an explicit driver model, and it is straight forward to include additional significant dynamics. However, the differential equations that have to be solved typically gives an order of magnitude longer simulation times for drive cycle simulations than what is typical for quasi-static simulation.

Because of the importance of drive cycle simulation it is natural that there are several

tools for simulation of longitudinal vehicle models on the market today. Example of quasi-static inverse tools are, e.g., Advisor [30] and QSS-TB [15], and examples of forward dynamic simulation tools are, e.g., PSAT [23], Capsim [1], and, V-Elph [5]. All these tools use Matlab/Simulink.

1.1 Goal of paper

It would of course be of considerable value to be able to extend the time-efficient quasi-static simulation with important dynamics without significantly loosing simulation performance. The goal of this paper is to find a simulation method with such properties. Guiding principles in this development have been to make extensions to the quasi-static method that are sufficiently general to include dynamics of the powertrain, such that important transients can be captured in the simulation. Quasi-static inverse simulation uses only one state, vehicle speed $v(t)$, so that the control is determined by $u(t) = f(v(t), \dot{v}(t))$. If more dynamics needs to be added to the models, then the inverse simulation strategy has to be extended. More states z have to be included, and they have to be obtainable from the velocity profile, which means that higher derivatives of the speed, or drive-cycle, may be needed. This can formally be written as $u(t) = F(v(t), \dot{v}(t), z(t), \dot{z}(t)) = \mathcal{F}(v(t), \dot{v}(t), \ddot{v}(t), \ldots)$, where either additional states or higher derivatives may be used. Such simulation, here named *inverse dynamic simulation*, is the main topic of this paper.

Given the main objective of the paper, i.e. combining the good properties of quasi-static and forward dynamic simulation, see Figure 1, there are a number of ramifications of the problem that have to be considered and the rest of the paper is outlined as follows. In Section 2 inversion of non linear systems with added dynamics is described. Since drive cycles in general are non smooth, tracking within limits is an issue in drive cycle simulations. This together with driver models is treated in Section 3. In Section 4 the proposed method of inverse dynamic simulation is demonstrated feasible on powertrain models. This includes additional dynamics that has significant influence on fuel consumption and emissions, and also that internal variables are captured. Last, in Section 5 simulation performance measures such as simulation time, set up effort, and consistency in design space exploration are discussed, and inverse dynamic simulation is compared to forward dynamics simulation.

2 Inversion of nonlinear systems

Inverse dynamic simulation is to compute generating variables like fuel flow and engine torque when the output, the velocity profile, is given, which means that it is a problem of system inversion. This section will present the theory to be used, whereas the practical use of the theory will be demonstrated on important powertrain models in Section 4.

Various domain specific solutions to system inversion have been developed, e.g. in rigid body dynamics, [22], [29], [32]. A review of methods for inverse dynamic simulation of nonlinear systems in aerospace applications is given in [20] where a method based on numerical differentiation followed by algebraic inversion is presented, and an application of that method is presented in [26]. This method is limited in that it uses an Euler approximation of the derivatives. Another way to perform system inversion is to

use a tool for non-causal simulation like e.g. Dymola, where the method is based on a structural manipulation of equations. However, only minimum phase systems are treated and numerical differentiation of the inputs is used [4].

A different possibility utilized in this paper, is to use the theory of stable inversion of nonlinear systems. Drivecycles need not be continuously differentiable, but for physical powertrains, having finite forces and torques, simulation signals will be smooth, and it turns out that it is not a limitation to assume smoothness. Therefore, the method described in [6] and [16] can fruitfully be adapted. Related theory is presented in [17]. The rest of this section presents the method by showing how a system of ordinary differential equations is manipulated in order to perform an inverse dynamic simulation of it. The method handles minimum- as well as non-minimum phase systems, and in the next section it will be shown how numerical differentiation of the inputs is avoided. A large class of systems that can be simulated in the forward dynamic way can thereby also be simulated in the inverse dynamic way.

2.1 Stable inversion of nonlinear systems

A short review of the used inversion method will be given here. Let $u(t)$ be the inputs, $y(t)$ the outputs, and $x(t)$ the states of a given system. Suppose that the system can be written in input-affine form

$$\dot{x}(t) = f(x(t)) + g(x(t))u(t) \quad (1)$$
$$y(t) = h(x(t)) \quad (2)$$

Assume that the number of inputs, q, equals the number of outputs. This is not a crucial assumption as demonstrated for example in [12], where redundancy is used to cast the problem in this formulation. Consider also a system where variables with suffix d corresponds to a system where variables are smooth, corresponding to tracking of a velocity profile within tracking limits. Given a desired output $y_d(t)$ that is smooth, the problem is to solve

$$\dot{x}_d(t) = f(x_d(t)) + g(x_d(t))u_d(t) \quad (3)$$
$$y_d(t) = h(x_d(t)) \quad (4)$$

for the input $u_d(t)$, and possibly also the states $x_d(t)$. With the notion smooth, it is here meant that a signal is sufficiently many times continuously differentiable. From here on it will be assumed that all functions are smooth such that the necessary derivatives exist and can be computed. It will also be assumed that $f(0) = 0$ and $h(0) = 0$. This can always be achieved for systems like (3)-(4) by a simple change of coordinates.

Let L be the standard notation for Lie-derivatives according to

$$L_f h(x) = \sum_i f_i(x) \frac{\partial}{\partial x_i} h(x) \quad (5)$$
$$L_f^r h(x) = L_f \left(L_f^{r-1} h(x) \right) \quad (6)$$

If for all $1 \leq i, j \leq q$, for all $k < r_i - 1$, and for all x in a neighborhood of x^0

$$L_{g_j} L_f^k h_i(x) = 0 \quad (7)$$

and the $q \times q$ matrix

$$\tilde{\beta}(x) = \begin{pmatrix} L_{g_1} L_f^{r_1-1} h_1(x) & \dots & L_{g_q} L_f^{r_1-1} h_1(x) \\ L_{g_1} L_f^{r_2-1} h_2(x) & \dots & L_{g_q} L_f^{r_2-1} h_2(x) \\ \vdots & \ddots & \vdots \\ L_{g_1} L_f^{r_q-1} h_q(x) & \dots & L_{g_q} L_f^{r_q-1} h_q(x) \end{pmatrix} \tag{8}$$

is nonsingular, then the system is said to have a vector relative degree $r = (r_1, r_2, \dots, r_q)$ at the point x^0. That is, the relative degree of the system is the number of times one has to differentiate the outputs for at least one input to appear explicitly.

The first step in the inversion procedure is to compute the relative degree. The next step is to partially linearize the system. This is done by differentiating $y_i(t)$ until at least one $u_j(t)$ appears explicitly. Define $\xi_k^i = y_i^{(k-1)}(t)$ for $i = 1, \dots, q$ and $k = 1, \dots, r_i$ and let

$$\begin{aligned} \xi(t) &= \left(\xi_1^1(t), \xi_2^1(t), \dots, \xi_{r_1}^1(t), \xi_1^2(t), \dots, \xi_{r_2}^2(t), \dots, \xi_{r_q}^q(t)\right)^T \\ &= \left(y_1(t), \dot{y}_1(t), \dots, y_1^{(r_1-1)}(t), y_2(t), \dots, y_2^{(r_2-1)}(t), \dots, y_q^{(r_q-1)}(t)\right)^T \end{aligned} \tag{9}$$

Now the change of coordinates can be defined. Since y is a function of x, it can be written as

$$\left(\xi^T, \eta^T\right)^T = \psi(x) \tag{10}$$

where η are variables needed, and the only constraint in the choice of η is that the jacobian matrix of $\psi(x)$ must be nonsingular at x^0 so that it is a local coordinates transformation in a neighborhood of x^0. It is always possible to find such a $\psi(x)$ [17]. With this choice of coordinates the following system which is partially linear in ξ is achieved

$$\begin{aligned} &\left\{ \begin{array}{rcll} \dot{\xi}_1^i(t) &=& \xi_2^i(t) & \\ &\vdots & & \text{for } i = 1, \dots, q \\ \dot{\xi}_{r_i-1}^i(t) &=& \xi_{r_i}^i(t) & \\ \dot{\xi}_{r_i}^i(t) &=& \alpha_i(\xi(t), \eta(t)) + \beta_i(\xi(t), \eta(t)) u(t) & \end{array} \right. \\ &\dot{\eta}(t) = s_a(\xi(t), \eta(t)) + s_b(\xi(t), \eta(t)) u(t) \end{aligned} \tag{11}$$

where the vector α and the matrix β are

$$\alpha(\xi, \eta) = L_f^r h(\psi^{-1}(\xi, \eta)) \tag{12}$$

$$\beta(\xi, \eta) = L_g L_f^{r-1} h(\psi^{-1}(\xi, \eta)) \tag{13}$$

and the functions $s_a(\xi, \eta)$ and $s_b(\xi, \eta)$ are given by the choice of η.

Denote $y^{(r)} = \left(y_1^{(r_1)}, \dots, y_q^{(r_q)}\right)$. Then it can be seen in the first part of (11) that $y^{(r)}(t) = \alpha_i(\xi(t), \eta(t)) + \beta_i(\xi(t), \eta(t)) u(t)$. By the definition of relative degree, $\beta(\xi, \eta)$ is nonsingular. Given a desired output trajectory $y_d(t)$ the required control input $u_d(t)$ can be calculated as

$$u_d(t) = \beta_i(\xi(t), \eta(t))^{-1} (y_d^{(r)}(t) - \alpha_i(\xi(t), \eta(t))) \tag{14}$$

Here it is seen that in order to calculate the required input for the system to follow the prescribed trajectory, not only $y_d(t)$ has to be known, but also the trajectories of $\eta(t)$ and the r first derivatives of $y_d(t)$. If the state trajectories producing the desired output are of interest they can be calculated from the inverse coordinate change

$$x(t) = \psi^{-1}(\xi(t), \eta(t)) \tag{15}$$

How the zero dynamics is to be solved depends on the system studied. There are three classes of systems that can be written in the form (11). The first class is all systems where the relative degree equals the dimension of the system, which means that there are no zero dynamics. The second class is all systems with stable zero dynamics, i.e., minimum phase systems, and the third class is systems with unstable zero dynamics, i.e., non-minimum phase systems. For the class of systems without zero dynamics, (14) becomes a system of static equations where the required input can be calculated from the desired output and its derivatives. In the case of stable zero dynamics the procedure is also straight forward. Substitute (14) in (11),

$$\begin{aligned}\dot{\eta}(t) &= s_a(\xi(t), \eta(t)) + s_b(\xi(t), \eta(t))\beta_i(\xi(t), \eta(t))^{-1}(y_d^{(r)}(t) - \alpha_i(\xi(t), \eta(t))) \\ &\equiv s(\eta(t), Y_d(t))\end{aligned} \tag{16}$$

where

$$Y_d(t) = \left(y_1(t), \dot{y}_1(t), \ldots, y_1^{(r_1)}(t), y_2(t), \ldots, y_2^{(r_2)}(t), \ldots, y_q^{(r_q)}(t)\right) \tag{17}$$

Choose appropriate initial values for $\eta(t)$, and solve the system of differential equations, (16), in order to find the trajectories of the zero dynamics.

In the case of unstable zero dynamics however, there is no such straight forward way, since then (16) can not be integrated as an initial value problem. It is not possible to solve the unstable zero dynamics in the general case, but in drive cycle simulations the desired output trajectory is known before hand. This gives the possibility of computing a non causal solution of (16) and still receive a stable result. In Devasia et al. [6] a Picard-like iteration is used to find the zero dynamics of a nonlinear non-minimum-phase system. To illustrate that method a linear system is first studied

$$\dot{\eta}(t) = A\eta(t) + Bu(t); \quad \eta(\pm\infty) = 0 \tag{18}$$

where A has no eigenvalues on the $j\omega$-axis. For such systems it is possible to find a similarity transformation $\eta = T\tilde{\eta}$, where T is invertible, that brings the system on a form where

$$\begin{pmatrix}\dot{\tilde{\eta}}_1 \\ \dot{\tilde{\eta}}_2\end{pmatrix} = \begin{pmatrix}\tilde{A}_n & 0 \\ 0 & \tilde{A}_p\end{pmatrix}\begin{pmatrix}\tilde{\eta}_1 \\ \tilde{\eta}_2\end{pmatrix} + \begin{pmatrix}\tilde{B}_1 \\ \tilde{B}_2\end{pmatrix} u; \ \eta(\pm\infty) = 0 \tag{19}$$

where $\tilde{A}_n$ has all eigenvalues in the left half plane and $\tilde{A_p}$ has all eigenvalues in the right half plane. The solution to the boundary value problem (19) is

$$\tilde{\eta}(t) = \int_{-\infty}^{\infty} \phi(t-\tau)\tilde{B}u(\tau)d\tau \tag{20}$$

where

$$\phi(t) = \begin{pmatrix} 1(t)e^{\tilde{A}_n t} & 0 \\ 0 & -1(-t)e^{\tilde{A}_p t} \end{pmatrix} \tag{21}$$

and $1(t)$ is the unit step function. Solving for the first states $\eta_1(t)$ in (19) is easy. The system is stable and the solution

$$\tilde{\eta}_1 = \int_0^\infty e^{\tilde{A}_n \tau} \tilde{B}_1 u(t-\tau) d\tau \tag{22}$$

can be computed with numerical solvers for ODE:s. If the input signal is known before hand, the solution to the last states $\eta_2(t)$ can be computed in a stable way by reversing time as

$$\tilde{\eta}_2 = \int_{-\infty}^0 -e^{\tilde{A}_p \tau} \tilde{B}_2 u(t-\tau) d\tau \tag{23}$$

or a non causal numerical solution can be used. Hence a stable simulation of the system can be done. For a nonlinear system such as (16), a separation of the system in a stable and unstable part as in (19) can not be done in general. The approach in Devasia et al. [6] is to write the nonlinear zero dynamics (16) as

$$s(\eta, Y_d) = A\eta + (s(\eta, Y_d) - A\eta) \tag{24}$$

which can be interpreted such as that the nonlinearities is seen as disturbances to a linear system. In the above equation A gives a linear approximation of $s(\cdot)$, typically $\frac{\partial s}{\partial \eta}|_{(0,0)}$. The iteration method simulates the linear system with the disturbances (nonlinearities) as inputs according to

$$\eta_{m+1}(t) = \int_{-\infty}^\infty \phi(t-\tau)[s(\eta_m(\tau), Y_d(\tau) - A\eta_m(\tau)] d\tau \tag{25}$$

where $\phi(t)$ is the state transition matrix for the linear system. If a change of coordinates that brings the linearization in the form of (19) is applied, the system becomes

$$\dot{\tilde{\eta}}(t) = T^{-1}AT\tilde{\eta}(t) + T^{-1}(s(T\tilde{\eta}(t), Y_d(t)) - AT\tilde{\eta}(t)) \tag{26}$$

and the iteration (25) can be separated in the form (19)

$$\begin{pmatrix} \tilde{\eta}_{1,m+1}(t) \\ \tilde{\eta}_{2,m+1}(t) \end{pmatrix} = \int_{-\infty}^\infty \phi(t-\tau) T^{-1}[s(T\tilde{\eta}_m(\tau), Y_d(\tau) - AT\tilde{\eta}_m(\tau)] d\tau \tag{27}$$

where $\phi(t)$ is defined by (21). For this iteration to converge to a solution of (25), there are restriction on the area of attraction that has to be handled, [6].

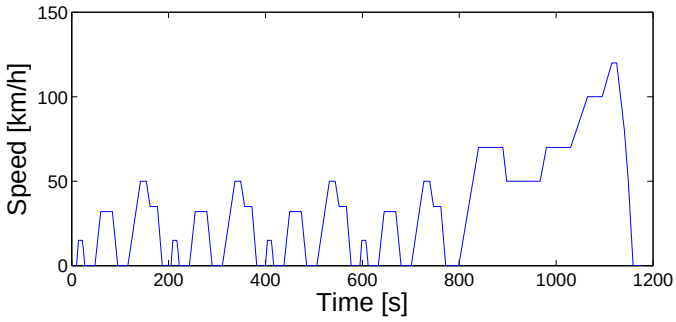

Figure 2: *The New European Drive Cycle, NEDC.*

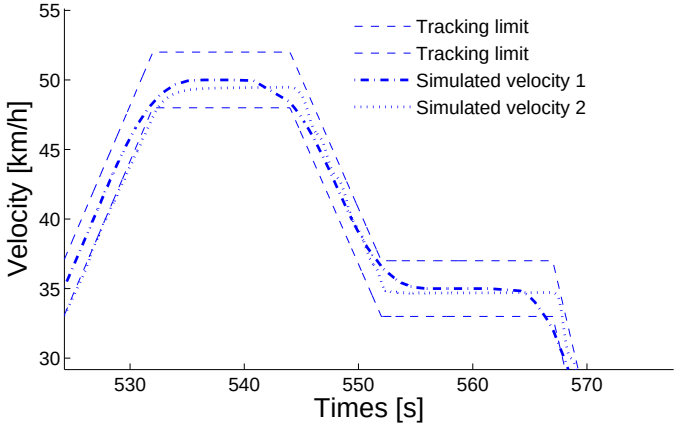

Figure 3: *Two different simulations of NEDC. Both are within tracking limits but result in different fuel consumption.*

3 Tracking performance and driver models

A drive cycle is a speed profile where speed is given as a function of time, see Figure 2 for an example, and as can be seen in the figure a drive cycle can not be expected to be continuously differentiable. This means that for models including additional dynamics, it is impossible to follow, or track, a drive cycle exactly, and hence, the speed has to be controlled to track the drive cycle in a desired way. When drive cycles are used for emission legislations the cycle is tracked by a human driver within certain limits. It is therefore logical, also in simulation, to design driver models to track cycles within defined limits. As will be shown later, results in for example fuel consumption can differ between two different velocity trajectories that both are within prescribed limits, see Figure 3, and it is thus important to study how a drive cycle is tracked and not only that the tracking is within limits.

To achieve good drive cycle tracking, more or less sophisticated driver models are needed, and here driver models for both forward and inverse dynamic simulation will

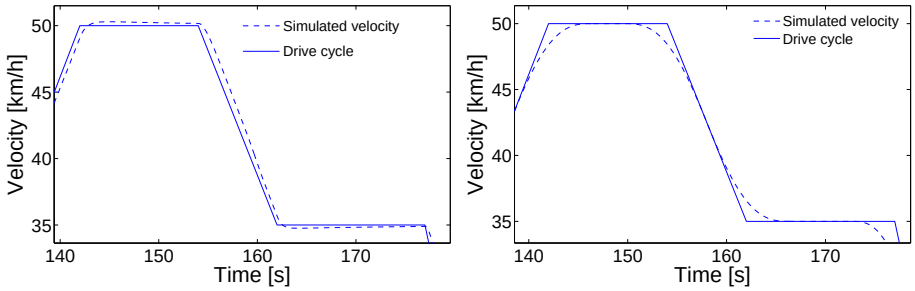

Figure 4: *Driver behavior for forward dynamic simulation (left) and inverse dynamic simulation (right) for a part of NEDC.*

be discussed. To compare tracking and behavior, the different driver models are in the following tested on the New European Drive Cycle, NEDC, see Figure 2.

3.1 Tracking in forward dynamic simulation

In forward dynamic simulation a driver model acts as a controller to track the reference speed trajectory, and as seen in Figure 1 the driver model compares the drivecycle with the actual speed and decides how to control the inputs, e.g., accelerator pedal, brake pedal, clutch, and gear selector, in order to follow the prescribed drive cycle within defined limits. A driver model can be as simple as a PID-controller [7] or a more sophisticated controller with prediction abilities [18]. The parameters of the driver model determines driver alertness, which in this type of simulation results in tightness of cycle tracking. For an example of tracking behavior for forward driver models, see Figure 4.

3.2 Enabling Tracking in inverse dynamic simulation

In inverse dynamic simulation, the reference speed trajectory is followed exactly if the physics of the model allows it, provided that the reference speed trajectory is continuously differentiable as many times as the relative degree of the system, as mentioned in [9], [8] or as can be seen in Equation (14), see also [17]. If it is not sufficiently differentiable, then the trajectory has to be smoothed to create a reference speed that the simulated model can follow with bounded states and inputs [9]. This smoothing of the drive cycle is in real life done by a test driver, but is here done by mathematical smoothing that will be given the interpretation of an implicit driver model. There are several possibilities to smooth the drive cycle, and the shape of the smoothed speed profile is decided by the behavior of the driver model. One way is to filter the drive cycle with a standard linear low pass filter with relative degree of at least the same order as the system. This will ensure that the filtered drive cycle is differentiable sufficiently many times for Equation (14) to be solvable, see [17]. Using a non causal linear filter gives the driver look ahead properties. Another way to smooth the drive cycle, $v_c(t)$, is to compute the desired trajectory, $v_d(t)$,

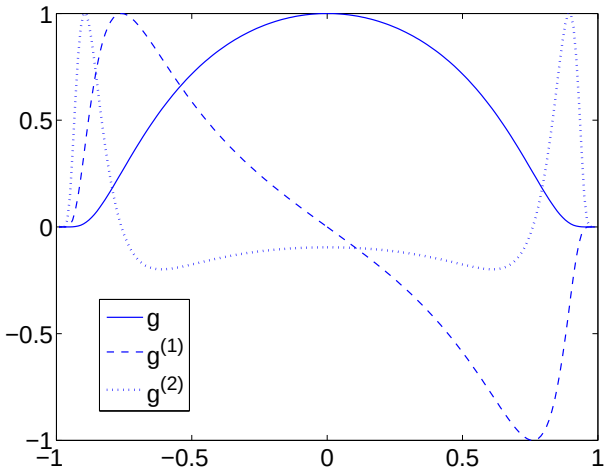

Figure 5: *Convolution kernel and its first derivatives (normalized curves).*

as the convolution

$$v_d(t) = \frac{1}{C}\int_{-\infty}^{\infty} g(t-\tau)v_c(\tau)d\tau \tag{28}$$

A good choice for the convolution kernel, $g(t)$, see Figure 5, is to use the definition

$$g(t) = \begin{cases} e^{\frac{-a^2}{a^2-t^2}}, & |t| \leq a; \\ 0, & \text{otherwise} \end{cases} \tag{29}$$

where the parameter a is a tracking time constant. Linear filtering of the drive cycle gives only asymptotically exact tracking while the use of (29), due to compact support, gives exact tracking on large parts of the drive cycle, as seen in Figure 4. A smaller a gives "tighter" tracking which corresponds to a more aggressive or alert driver behavior.

Since the choice (29) of the convolution kernel $g(t)$ has compact support and is infinitely many times continuously differentiable, the resulting trajectory $v_d(t)$ is infinitely many times continuously differentiable. Moreover, the calculation of the derivatives does not require numerical differentiation. Instead the derivatives are calculated using the following convolution

$$v_d^{(r)}(t) = \int_{-\infty}^{\infty} g^{(r)}(t-\tau)v_c(\tau)d\tau \tag{30}$$

where the different derivatives $g^{(r)}$ are obtained by analytical differentiation of (29). See Figure 5 for some examples with the parameter $a = 1$.

Driver model. The new driver model for inverse dynamic simulation is defined by Equations (28)-(30).

Inverse dynamic simulation. The driver model presented above together with the inversion procedure presented in Section 2 is an extension to quasi-static simulation and forms a new concept of inverse dynamic vehicle simulation. See Figure 1.

Thus, the smoothing of the drive cycle is interpreted as an implicit driver model, where the tracking behavior is specified in the velocity domain and is independent of the vehicle. In fact, this way of specifying tracking behavior can be argued to be closer to human behavior when performing drive cycle tests on a chassis dynamometer, since the tracking of a human driver is not specified by controller parameters, but rather in terms of tracking smoothness.

4 Typical Powertrain model examples

When using drive cycle simulation it may be desired to capture the behavior in transients to achieve sufficient precision in the processes generating fuel consumption and emissions. Therefore it is necessary to be able to include the dominant dynamics, and not only use quasi-static simulation like in Advisor [30] or the QSS-toolbox [15].

In this section three of the most important dynamics [18] that capture such transients will be presented, and the feasibility of the inversion procedure presented in Section 2 will be demonstrated on these models. One example is the dynamics of the air filling in the intake manifold when using throttle position as input to the powertrain. Another example is resonances in the driveline mainly caused by torsion in the drive shafts. These are modeled in Section 4.1. The third example comes from diesel engines with exhaust gas recycling where the gas flow in the engine is important for emissions modeling. This flow is modeled in Section 4.2. The models are only briefly presented here and for a more detailed presentation the reader is referred to [10].

Even though the examples in this section are motivated from the application they each impose interesting and illustrative mathematical characteristics. The first example introduces intake manifold pressure to illustrate the extension with one extra state compared to quasi-static modeling. The second example additionally includes drive shaft torsion which includes a resonant system and zero dynamics. The third example with gas flow for diesel engines includes non-minimum phase, i.e. unstable zero dynamics. The model examples will be used for comparison of different simulation methods in Section 5.

4.1 Powertrain with intake dynamics and driveline dynamics

This section will describe the two first examples, and it will be done by first giving the most complex example which is a power train with both intake pressure dynamics and drive shaft flexibility. Then the model will be specialized to exclude the drive shaft flexibility.

The main dynamic variable of a vehicle is vehicle speed v, which is the only one used in quasi-static models. Including drive shaft torsion θ_d decouples vehicle speed v and engine speed ω_e. Also the dynamics of intake manifold pressure p_i is included. The model, see Figure 6, is more thoroughly described in Fröberg [10], and will be referred to as the flexible powertrain model, FP. The tractive input is effective throttle area A_{eff}. From ambient pressure p_a and intake manifold pressure p_i the flow past the throttle is calculated via a flow restriction model Ψ. Then the gasflow into the cylinders is calculated, giving gross work. Subtracting pump work and friction gives the output torque from the engine. The rest of the driveline is modeled as standard inertias, torsion springs, dampers, and

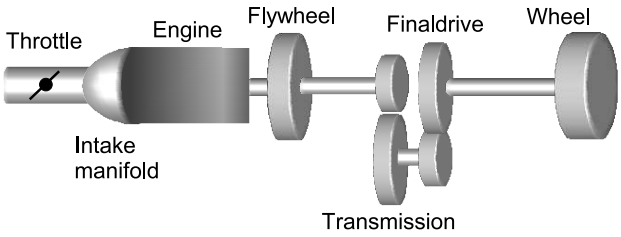

Figure 6: *Components of the powertrain model.*

gears, giving driving force on the wheels. This driving force reduced by air resistance and rolling resistance gives vehicle speed. When needed a brake torque proportional to driver input is applied to the wheels, and the simulation is handled as in [12]. During the tractive part of the drive cycle the model has input $u = A_{eff}$, states $x = [v, \omega_e, \theta_d, p_i]^T$, and output $y = v$. The model parameters are lumped into the coefficients c_i. Let the functions f_i, g_i, h be defined by the model equations that are

$$\dot{v} = c_1 v^2 + c_2 v + c_3 \omega_e + c_4 \theta_d + c_5 \equiv f_1(x) \tag{31}$$

$$\dot{\omega}_e = c_6 v + c_7 \omega_e + c_8 \omega_e^{1.8} + c_9 \theta_d + c_{10} p_i + c_{11} \equiv f_2(x) \tag{32}$$

$$\dot{\theta}_d = c_{12} v + c_{13} \omega_e \equiv f_3(x) \tag{33}$$

$$\dot{p}_i = c_{14} \omega_e + c_{15} \omega_e p_i + c_{16} \Psi \left(\frac{p_i}{p_a} \right) A_{eff} \equiv f_4(x) + g_4(x) u \tag{34}$$

$$y = v \equiv h(x) \tag{35}$$

The relative degree of this system is $r = 3$. Hence the zero dynamics, and the inverse dynamic model, has order 1.

The coordinate change (10) is chosen as

$$(\xi_1, \xi_2, \xi_3, \eta)^T = (v, \dot{v}, \ddot{v}, p_i)^T \tag{36}$$

Using (14) in the zero dynamics gives

$$\dot{\eta} = f_4(\psi^{-1}(\xi, \eta)) + g_4(\psi^{-1}(\xi, \eta)) \beta^{-1} (v_d^{(3)} - \alpha) \tag{37}$$

using (12)-(13) which are

$$\alpha = L_f^3 h \tag{38}$$

$$\beta = L_g L_f^2 h \tag{39}$$

The zero dynamics (37) is stable for this model, and hence can be solved as an initial value problem. It is seen that only the output $v_d(t)$ and the first three derivatives thereof have to be known when solving for the zero dynamics and the resulting required input (14)

$$A_{eff,d} = \beta^{-1}(\xi, \eta)(v_d^{(3)} - \alpha(\xi, \eta)) \tag{40}$$

See Figures 7 and 8 for simulations of this model. The figures show both forward dynamic and inverse dynamic simulation. The results are comparable which demonstrates the feasibility of the proposed new method. A more detailed evaluation is done in Section 5.

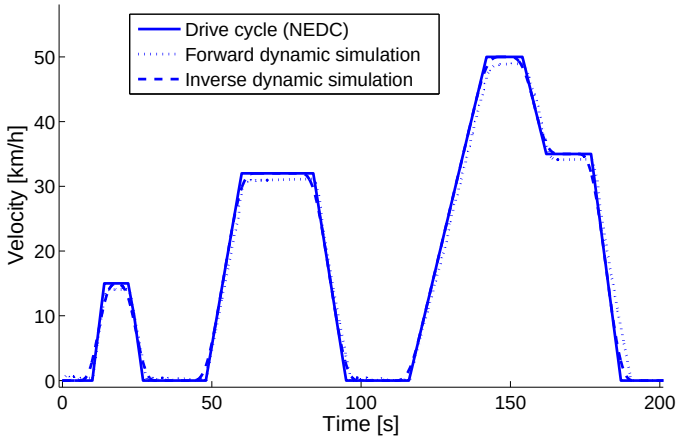

Figure 7: *Velocity of a simulation of the powertrain model with flexible driveshaft from Section 4.1.*

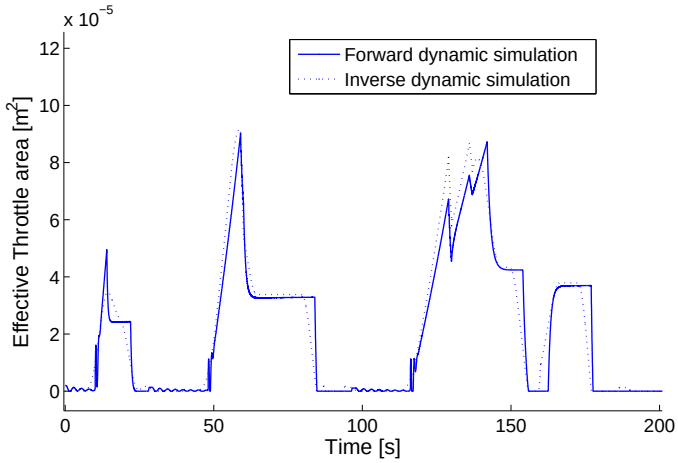

Figure 8: *Effective throttle area of a simulation of the powertrain model with flexible driveshaft from Section 4.1.*

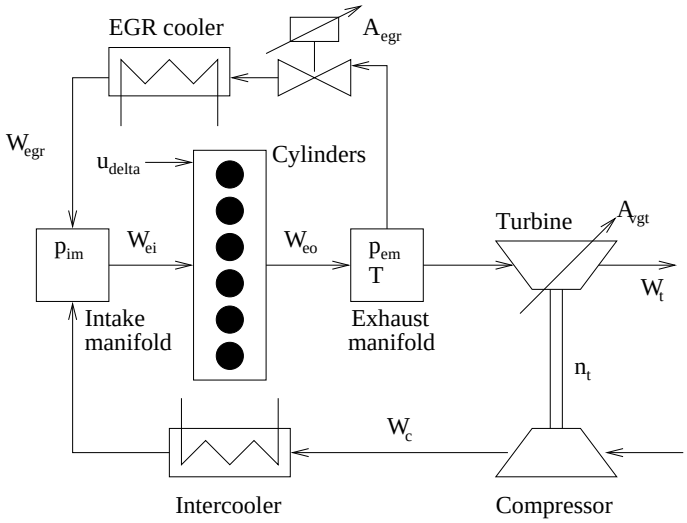

Figure 9: *A schematic picture of a diesel engine with EGR and VGT. The figure is adapted from [27].*

Powertrain with intake dynamics

The stiff powertrain, SP, includes the dynamics of intake manifold pressure p_i but not the drive shaft torsion. This simplified version of the model (31)-(35) with stiff driveshafts is written as

$$\dot{v} = c_1 v^2 + c_2 v^{1.8} + c_3 p_i + c_4 \equiv f_1(x) \tag{41}$$

$$\dot{p}_i = c_5 v + c_6 v p_i + c_7 \Psi\left(\frac{p_i}{p_a}\right) A_{eff} \equiv f_4(x) + g_4(x)u \tag{42}$$

$$y = v \equiv h(x) \tag{43}$$

The inversion of this system follows the same procedure as for the previous example. The system's relative degree is $r = 2$, giving an inverse model that consists of static equations.

4.2 Gas flow control in a diesel engine

As mentioned earlier non-minimum-phase systems may be challenging, and one important powertrain component that has this property is the gas flow for a diesel engine with exhaust gas recycling, EGR and variable geometry turbine, VGT, see Figure 9. Such a system is modeled in Wahlström [27], and the simplified version that is used here is detailed in Fröberg [10], and will here be referred to as DE. Control variables are the EGR valve u_{egr} and the area of the VGT A_{vgt}. These two inputs are used to control the mass flow and its composition into the cylinder. Here the fuel flow and engine speed are considered as model parameters. Outputs are normalized air fuel ratio, λ, and EGR ratio, x_{egr}. This is a non minimum phase system for many operating points, and intuitively it can be reasoned as follows: When the VGT is closed, initially, the flow past the turbine will

decrease, which results in a decrease of compressor flow and a decrease in λ. However, there will be a build up of pressure in the exhaust manifold, and after a while this will result in a higher flow past the turbine, speeding up the turbo, and after a while results in an increase of fresh air flow, which means that λ increases. The model has four states $x = [p_i, p_e, \omega_t, A_{egr}]^T$, i.e. intake manifold pressure, exhaust manifold pressure, turbine speed, and EGR valve area. As before the, coefficients c_i are lumped model parameters, and functions f_i, g_i, h are defined in the model equations that are written as

$$\dot{p}_i = c_1 p_i + c_2 \omega_t + c_3 A_{egr} p_e \Psi\left(\frac{p_i}{p_e}\right) \equiv f_1(x) \tag{44}$$

$$\dot{p}_e = c_4 p_i + c_5 A_{egr} p_e \Psi\left(\frac{p_i}{p_e}\right) + c_6 + c_7 p_e \sqrt{1 - \frac{c_8}{p_e^{c_9}}} A_{vgt} \equiv f_2(x) + g_2(x)u \tag{45}$$

$$\dot{\omega}_t = c_{10} p_i^{c_{11}} + c_{12} + \left(c_{13} + \frac{c_{14}}{p_e^{c_{15}}}\right) \sqrt{1 - \frac{c_8}{p_e^{c_9}}} \frac{p_e}{\omega_t} A_{vgt} \equiv f_3(x) + g_3(x)u \tag{46}$$

$$\dot{A}_{egr} = c_{16} A_{egr} - c_{16} u_{egr} \equiv f_4(x) + g_4(x)u \tag{47}$$

The outputs are $y = [\lambda, x_{egr}]^T$

$$\lambda = c_{17} \omega_t \equiv h_1(x) \tag{48}$$

$$x_{egr} = \frac{c_{18} A_{egr} p_e \Psi\left(\frac{p_i}{p_e}\right)}{c_{19}\omega_t + c_{18} A_{egr} p_e \Psi\left(\frac{p_i}{p_e}\right)} \equiv h_2(x) \tag{49}$$

Computing Lie-derivatives for this system gives the vector relative degree as $r = (1,1)$, which means that the systems zero dynamics has order two. As was mentioned earlier it is assumed in the inversion procedure that $f(0) = 0$ and $h(0) = 0$, which is easily achieved for this system by a simple coordinate change where the origin is moved to a stationary point, like $\tilde{p}_i = p_i - p_{i,stat}$. When this is done the coordinate change to ξ and η can be chosen as

$$(\xi_1, \xi_2, \eta_1, \eta_2)^T = \left(\tilde{\lambda}, \tilde{x}_{egr}, \tilde{p}_i, \tilde{p}_e\right)^T \tag{50}$$

Using (14) the zero dynamics can be written as

$$\eta_1 = f_1(\psi^{-1}(\xi, \eta)) \tag{51}$$

$$\eta_2 = f_2(\psi^{-1}(\xi, \eta)) + g_2(\psi^{-1}(\xi, \eta))\beta(\xi, \eta)^{-1}(\dot{\xi} - \alpha(\xi, \eta)) \tag{52}$$

where

$$\alpha = L_f h \tag{53}$$

$$\beta = L_g h \tag{54}$$

For the stationary point $p_i = 2.06 \cdot 10^5$ Pa, $p_e = 2.41 \cdot 10^5$ Pa, $\omega_t = 7001$ rad/s, and $A_{egr} = 1 \cdot 10^{-4}\text{m}^2$, this zero dynamics is linearized

$$\dot{\eta} = A\eta \tag{55}$$

and the eigenvalues of A become $\sigma_1 = -6.8$ and $\sigma_2 = 15.8$, so clearly the zero dynamics is unstable. The iterative technique described by (27) is used to solve for the trajectories

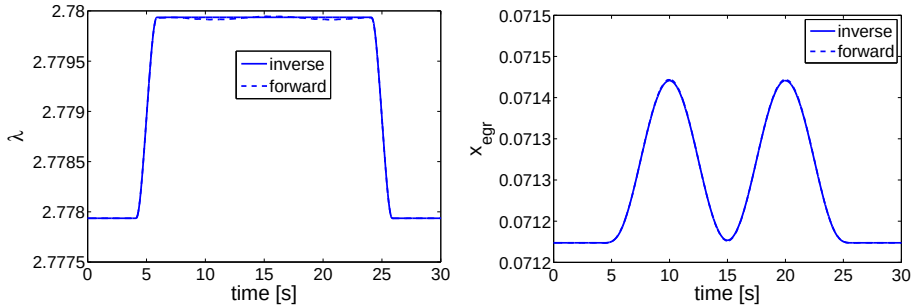

Figure 10: *Specified output trajectories for λ and x_{egr} (solid). A corresponding forward dynamic simulation (dashed) is also seen.*

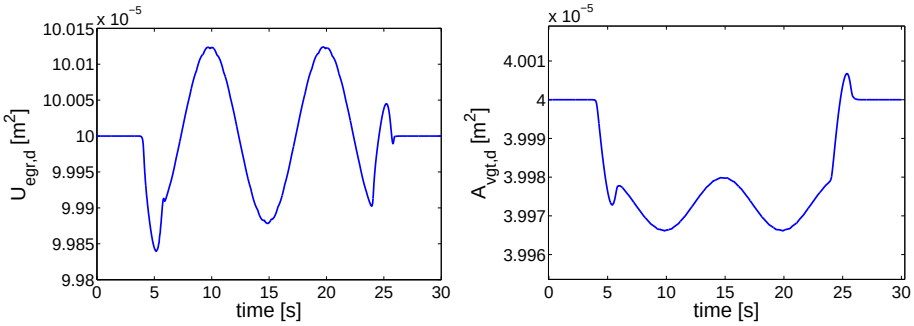

Figure 11: *Required inputs from an inverse dynamic simulation of the diesel engine with desired outputs according to Figure 10.*

of the zero dynamics. No measures like e.g. multiple linearizations are used to optimize performance. Having obtained the trajectories the required input is calculated as in (14) which here becomes

$$\begin{pmatrix} \tilde{u}_{egr,d} \\ \tilde{A}_{vgt,d} \end{pmatrix} = \beta^{-1}(\xi,\eta)\left(\begin{pmatrix} \ddot{\tilde{\lambda}}_d \\ \dot{\tilde{x}}_{egr,d} \end{pmatrix} - \alpha(\xi,\eta)\right) \tag{56}$$

Forward dynamic simulations of the diesel engine is non trivial [28], since it is hard to design a controller for the non minimum phase multivariable system. Instead, the procedure here is first to specify desired outputs, the drivecycle, then to perform an inverse simulation, and finally to use the resulting inputs as inputs to the forward dynamic simulation. See Figures 10 - 11 for simulations of the model, which demonstrates feasibility since the results are almost identical for forward and inverse simulation.

5 Simulation usability and performance

The extended concept of inverse dynamic vehicle simulation summarized in Sections 2 and 3.2 was in the previous section demonstrated to be feasible. However, as has been

mentioned, the goal of the paper is increased performance by combining the advantages of forward dynamic simulation and quasi-static inverse simulation in a new method, inverse dynamic simulation, see Figure 1. This section is devoted to a comparison with standard forward simulation, realizing that when performing a simulation there a several properties that are important. This regards the set-up effort, consequences of tracking performance, consistency when scanning a parameter set, and of course simulation time, which are the topics of the following sections.

5.1 Simulations

The simulation study for investigating properties and for making comparisons has been set up in the following way. The powertrain models from Section 4 are used, with parameter values corresponding to a typical personal sedan car except for the diesel example which is a typical heavy truck diesel. Detailed parameter values can be found in [10]. Regarding driver models, the forward model is controlled with a driver model implemented as a PID-controller that is connected to the vehicle model as depicted in Figure 1. The PID-parameters are $K_p = 8 \cdot 10^{-5}$, $K_i = 1 \cdot 10^{-6}$ and $K_d = 0$. The inverse dynamic simulation, see Figure 1, uses a driver model as described by (28) - (29) with the parameter $a = 5$. To get comparable tracking, the parameter setting of the driver models has been done as follows: First an inverse dynamic driver model has been designed that has a suitable tracking behavior. Then, a forward dynamic PID-type driver model has been designed such that it has comparable response time as the inverse driver model. The models are simulated in the New European Drive Cycle, Figure 2.

5.2 Simulation setup effort

It was seen in Section 4.1 that both the inverse and forward dynamic simulation produced qualitatively the same result. However, it can be seen in Figure 8 that the forward dynamic simulation in that example has an oscillating behavior in throttle position. This stems from the driver model, since for this example it is not sufficient with a single PID-controller due to the non-linearities in the system. It may take quite some effort to design a driver model that adapts to the vehicle's behavior in different operating points. On the other hand, it is seen that the inverse dynamic simulation has a smooth control that better resembles the behavior of a real driver. Thus, the complexity of designing a driver model may be a drawback for the forward dynamic simulation considering setup effort.

It is straight forward to implement a forward dynamic model in a simulation tool like Matlab/Simulink, whereas an inverse dynamic simulation requires manipulations with the differential equations describing the system before it can be simulated. These manipulations are however systematic as described in Section 2, and can be automatized. The systematic conversion reduces the need to build dedicated inverse models as those used in, e.g., Advisor. In this way the new simulation concept is a bridge that ties forward dynamic simulations as in, e.g., PSAT, to quasi-static inverse simulations as in, e.g., Advisor, in the sense that common model data bases can be used.

Sim Method	Driver model	Fuel cons [l/100km] r=0.3m	Fuel cons [l/100km] r=0.45m
Forward	Kp = $1.5 \cdot 10^{-4}$ Ki = $1 \cdot 10^{-5}$	8.619	7.315
Forward	Kp = $5 \cdot 10^{-4}$ Ki = $5 \cdot 10^{-6}$	8.634	7.293
Inverse	a=2	8.595	7.265
Inverse	a=1	8.627	7.271

Table 1: *Consistency in simulation with change in wheel radius.*

5.3 Consistency for parameter exploration

An important use of drive cycle simulation is for design space exploration like optimizing gear ratios of the transmission, optimizing the size of the engine for minimal fuel consumption, or tuning of control system parameters. Then, it is important to have consistency when some parameters vary between simulations, so that correct conclusions can be drawn.

A first complication is that tracking may vary as described already in Section 3 and illustrated in Figure 3. Using the model from Section 4.1, it is seen in Figures 7 and 8 that both the forward and inverse dynamic simulation produces qualitatively comparable results. In [10] an experiment with parameter changes in this model is done by keeping the driver parameters, but the engine size is changed from 2.3 to 1.6 liters and the vehicle mass is changed from 1700 to 1100kg. It turns out that the tracking behavior in the forward simulations is different in the two cases but is by construction exactly the same for the inverse dynamic simulations. Further, even though all simulations are within tracking limits, the different behaviors of the forward simulation give oscillations in the light weight vehicle case. This shows that it can be difficult to run a set of forward dynamic simulations and get a consistent fuel consumption calculations without retuning the driver model when the vehicle parameters are changed.

An even more important point will now be demonstrated. The same model is used again but now with a stiff driveline. It is simulated to study the fuel consumption in the NEDC driving cycle. The fuel consumption is taken as the integral of the maximum of the fuel flow given by the model and an idle flow. Simulations are performed both with the inverse dynamic method and the forward dynamic method. Keeping the same driver models, the simulations are performed with two different wheel radius namely 0.3m and 0.45m. The results are shown in Table 1. For the forward case the order between the two cases are reversed ($8.619 < 8.634$ compared to $7.315 > 7.293$), which means that the order in fuel consumption between the driver models is not preserved when wheel radius is changed. This indicates that it can be difficult to evaluate simulations where model parameters change if the tracking characteristics is not preserved. For the inverse case the order is consistent ($8.595 < 8.627$ and $7.265 < 7.271$).

The examples above show effects in forward dynamic simulation that deteriorates the usefulness for the set of simulations as a design space exploration. However, for inverse dynamic simulation, due to the computational scheme with the implicit driver model the

behavior within tracking limits is consistent. The conclusion is that inverse dynamic simulation has an advantage regarding consistency in design space exploration.

5.4 Simulation time

Recall that the main goal was to extend quasi-static inverse simulation with additional dynamics while still keeping the low simulation time.

In order to study the simulation speed of inverse and forward dynamic simulation the three models from Section 4 will be used again in a more elaborate study including more cases than in the previous sections. Besides the drive cycle NEDC also FTP 75 has been used. Further, different driver models have been used as summarized in Table 3. Twentysix combinations of vehicle models, driver models, and drive cycles have been simulated and they are listed in the presentation of the results in Table 2. The "SP" models is the model from Section 4.1 with a stiff drive shaft and engine dynamics. The "FP" models is the model of a powertrain with a flexibility in the driveshaft from Section 4.1. The diesel engine model, "DE", is the one with unstable zero dynamics described in Section 4.2. One iteration has been used to find the zerodynamics of the inverse diesel engine model. The number of integration steps in the inverse simulation of the diesel engine is the sum of steps for the simulations of the zero dynamics and for finding the required inputs.

Approach in comparisons

The inverse dynamic simulations are setup in order to resemble an automatic conversion from the corresponding forward model using only the conversion described in Section 2. This means that there is additional potential for speed up, like regarding choice of coordinates or to see if all or at least some of the variables in the inverse coordinate change can be solved analytically.

For each case in both inverse and forward simulation the fastest solver has been chosen, and the resulting choice is listed in a column of the result presentation in Table 2.

Timing results

The main result that can be seen in Table 2 is that the inverse dynamic simulation has a considerable speed advantage compared to the forward dynamic simulation. This holds for all three powertrain applications that have different added dynamics. Going a bit more into detail there are a number of interesting observations to be made in the comparisons. There are mainly two things that affect the simulation time, the number of steps required in the integration, and the number of calculations in each step. In Table 2 it is seen that the inverse dynamic simulation takes at least an order of magnitude fewer steps than the forward dynamic simulation.

One reason for the difference in number of integration steps relates to characteristics of the vehicle model. The number of steps in the integration is mainly depending on the eigenvalues of the simulated system, where large eigenvalues, i.e., far away from the imaginary axis, will require small steps and thus more steps. This means that when the eigenvalues of the zero dynamics are smaller than the eigenvalues for the forward dynamic

model, the inverse dynamic simulation will require fewer steps than the forward and for many systems this is the case. For example, in the diesel engine model the eigenvalues of the forward model in the linearization point are -18.2, -12.7, -5.00, -1.26, and for the zero dynamics the eigenvalues are 15.8 and -6.8. For the stiff powertrain model there is no zero dynamics, so the inverse model is correct in each sample point independent of how few steps that are taken. Also for the flexible powertrain model, the zero dynamics, stemming from the drive shaft flexibility, is slower than e.g. the intake pressure dynamics.

Another reason for the advantage in simulation time are the calculations needed in each integration step. If there is a need to solve the inverse coordinate change numerically online, the number of calculations in each step can increase some for the inverse dynamic models. However, since the dimension of the zero dynamics is smaller than the number of states in the forward dynamic models the number of calculations in each step are fewer in most cases.

A further reason for the relatively slow simulations of the forward models of the basic powertrain and the flexible powertrain is the need for extra dynamics in the form of a controller, the driver model. Typically, such a controller may have ten times faster dynamics than the controlled system. Plots from such simulations presented in Table 2 have been presented in Section 4. In those plots the forward dynamic simulation is unnecessarily oscillating in some cases due to the driver model, but this is not the main reason for long simulation times. The trends in simulation time reported in Table 2 are still valid for other tunings of the forward driver models.

6 Conclusions

The importance and characteristics, e.g. regarding tracking and repeatability, of drive cycle simulation have been presented. Aiming especially for repeated drive cycle simulations, the new implicit driver model presented in Section 3.2 together with the inversion procedure presented in Section 2 forms a new concept of inverse dynamic vehicle simulation. The use of the new driver model is a good way of specifying tracking behavior. Compared to specifying tracking using the forward driver model it is closer to human behavior when performing drive cycle tests on a chassis dynamometer, since it is not specified by controller parameters, but rather in terms of tracking smoothness.

In Section 4 three powertrain applications were presented that included important dynamics that can not be handled using quasi-static inverse simulation. The extensions were engine dynamics, drive line dynamics, and gas flow dynamics around diesel engines. These three cases also represented interesting mathematical properties such as zero dynamics, resonances, and non-minimum phase systems, i.e. unstable zero dynamics. The feasibility of inverse dynamic simulation of these systems was shown.

Besides feasibility more importantly also good characteristics was demonstrated regarding consistency and simulation speed. It was found that specifying the parameter a in the interpolating driver model is simpler than retuning the forward driver model (PID-controller) for each model parameter setting, which is necessary to achieve consistency in design space exploration. Simulation comparisons demonstrated that the new method has good performance with faster simulations compared to standard forward simulation. This means that the goals of Section 1 and Figure 1 are achieved. Inverse dynamic simula-

Model	Drivecycle	Sim. Time [s]	#steps	Solver	Forw./ Inv.
SP 1	NEDC	18.0	7653	ode45	F
SP 1	FTP75	31.8	13594	ode45	F
SP 2	NEDC	13.5	6287	ode45	F
SP 2	FTP75	22.2	9819	ode45	F
SP 3	NEDC	12.1	5637	ode45	F
SP 3	FTP75	22.6	9730	ode45	F
SP 4	NEDC	0.33	50	ode45	I
SP 4	FTP75	0.078	50	ode45	I
SP 5	NEDC	0.076	50	ode45	I
SP 5	FTP75	0.084	50	ode45	I
SP 6	NEDC	0.057	50	ode45	I
SP 6	FTP75	0.090	50	ode45	I
FP 1	NEDC	409	308207	ode23tb	F
FP 1	FTP75	216	140183	ode45	F
FP 2	NEDC	320	244053	ode23tb	F
FP 2	FTP75	197	130734	ode45	F
FP 3	NEDC	263	201583	ode23tb	F
FP 3	FTP75	188	124498	ode45	F
FP 4	NEDC	60.0	10207	ode23tb	I
FP 4	FTP75	161	26763	ode23tb	I
FP 5	NEDC	30.5	5164	ode23tb	I
FP 5	FTP75	100	16806	ode23tb	I
FP 6	NEDC	117	16294	ode23tb	I
FP 6	FTP75	66.9	10899	ode23tb	I
DE	-	12.9	3596	ode23tb	F
DE	-	8.66	2201	ode23tb	I

Table 2: *Simulation times.*

Model	K_p	K_i	a
SP 1, 4	$6 \cdot 10^{-4}$	$1 \cdot 10^{-5}$	1
SP 2, 5	$1.5 \cdot 10^{-4}$	$1 \cdot 10^{-5}$	2
SP 3, 6	$8 \cdot 10^{-5}$	$1 \cdot 10^{-6}$	5
FP 1, 4	$1.5 \cdot 10^{-4}$	$2.5 \cdot 10^{-6}$	1
FP 2, 5	$1.2 \cdot 10^{-4}$	$2 \cdot 10^{-6}$	2
FP 3, 6	$8 \cdot 10^{-5}$	$1 \cdot 10^{-6}$	5

Table 3: *Driver model parameters.*

tion was favorably compared to forward dynamic simulation regarding simulation set-up effort, simulation time, and consistency for parameter exploration. This makes inverse dynamic simulation a suitable method to use for drive cycle simulation, especially in situations requiring many simulations, such as optimization over design space, powertrain configuration optimization, or development of powertrain control strategies.

Bibliography

[1] *Center for automotive propulsion simulation.* http://www.capsim.se.

[2] A. I. Antoniou, J. Komyathy, J. Bench, and A. Emadi. Modeling and simulation of various hybrid-electric configurations of the high-mobility multipurpose wheeled vehicle (HMMWV). *IEEE Transactions on Vehicular Technology*, 56(2), 2007.

[3] M. Back, S. Terwen, and V Krebs. Predictive powertrain control for hybrid electric vehicles. *First IFAC Symposium on Advances in Automotive Control*, 2004.

[4] Johann Bals, Gerhard Hofer, Andreas Pfeiffer, and Christian Schallert. Object-oriented inverse modelling of multi-domain aircraft equipment systems and assessment with modelica. *Proceedings of the 3rd International Modelica Conference, Linköping*, November 2003.

[5] Karen L. Butler, Mehrdad Ehsani, and Preyas Kamath. A matlab-based modeling and simulation package for electric and hybrid electric vehicle design. *IEEE Transactions on vehicular technology*, 48(6):1770–1778, 1999.

[6] S. Devasia, D. Chen, and B. Paden. Nonlinear inversion-based output tracking. *IEEE Transactions on Automatic Control*, 41:930–942, 1996.

[7] Lars Eriksson. Simulation of a vehicle in longitudinal motion with clutch lock and clutch release. *3rd IFAC workshop on Advances in automotive control*, pages 65–70, 2001.

[8] A. Fröberg and L Nielsen. Dynamic vehicle simulation -forward, inverse and new mixed possibilities for optimized design and control. *SAE Technical Paper Series SP-1826, 2004-01-1619*, 2004.

[9] A. Fröberg and L Nielsen. A method to extend inverse dynamic simulation of powertrains with additional dynamics. *First IFAC Symposium on Advances in Automotive Control*, April 2004.

[10] Anders Fröberg. *Extending the inverse vehicle propulsion simulation concept -to improve simulation performance*. Licentiate thesis, LiU-TEK-LIC-2005:36, Linköping Institute of Technology, Linköping, 2005.

[11] Anders Fröberg and Lars Nielsen. Efficient drive cycle simulation. *IEEE Transactions on Vehicular Technology*, Accepted for publication(-), 2008.

[12] A. Fröberg. Inverse dynamic simulation of non-quadratic mimo powertrain models -application to hybrid vehicles. *IEEE Vehicle power and propulsion conference, Windsor, UK*, 2006.

[13] A. Fröberg, L. Nielsen, L-G. Hedström, and M. Pettersson. Controlling gear engagement and disengagement on heavy trucks for minimization of fuel consumption. *IFAC World Congress. Prague, Czech Republic*, 2005.

[14] L. Guzella and A. Sciaretta. *Vehicle Propulsion Systems.* Springer, 2005.

[15] L. Guzzella and A. Amstutz. Cae tools for quasi-static modeling and optimization of hybrid powertrains. *IEEE Transactions on Vehicular Technology*, 48:1762–1769, 1999.

[16] L. R. Hunt and G. Meyer. Stable inversion for nonlinear systems. *Automatica*, 33:1549–1554, 1997.

[17] A. Isidori. *Nonlinear Control Systems.* Springer-Verlag, 1995.

[18] U. Kiencke and L. Nielsen. *Automotive Control Systems, 2nd ed.* Springer-Verlag, 2005.

[19] S. M. Lukic and A. Emadi. Effects of drivetrain hybridization on fuel economy and dynamic performance of parallel hybrid electric vehicles. *IEEE Transactions on Vehicular Technology*, 53(2), 2004.

[20] D.J. Murray-Smith. The inverse simulation approach: a focused review of methods and applications. *Mathematics and Computers in Simulation*, 53:239–247, 2000.

[21] S. Onoda and A. Emadi. PSIM-based modeling of automotive power systems: Conventional, electric, and hybrid electric vehicles. *IEEE Transactions on Vehicular Technology*, 53(2), 2004.

[22] G Rodriguez. Kalman filtering, smoothing, and recursive robot arm forward and inverse dynamics. *IEEE Journal of Robotics and Automation*, RA-3(6), 1987.

[23] A. Rousseau, P. Sharer, and F. Besnier. Feasability of reusable vehicle modeling: Application to hybrid vehicle. *SAE Technical Paper Series SP-1826, 2004-01-1618*, 2004.

[24] Tony Sandberg. *Heavy Truck Modeling for Fuel Consumption Simulations and Measurments.* Licentiate thesis, LiU-TEK-LIC-2001:61, Linköping Institute of Technology, Linköping, 2001.

[25] A. Sciaretta, L. Guzella, and C. H. Onder. On the power split control of parallell hybrid vehicles: from global optimization towards real-time control. *Automatisierungstechnik*, 51(5), 2003.

[26] Douglas G. Thomson and Roy Bradley. The principles and practical application of helicopter inverse simulation. *Simulation Practice and Theory*, 6:47–70, 1998.

[27] Johan Wahlström. *Control of EGR and VGT for emission control and pumping work minimization in diesel engines.* Licentiate thesis, LiU-TEK-LIC-2006:52, Linköping Institute of technology, Linköping, Sweden, 2006.

[28] Johan Wahlström, Lars Eriksson, Lars Nielsen, and Magnus Pettersson. PID controllers and their tuning for EGR and VGT control in diesel engines. *IFAC World Congress, Prague Czech Republic*, 2005.

[29] C.W. Wampler. Manipulator inverse kinematic solutions based on vector formulations and damped least-squares methods. *IEEE Transactions on systems, man, and, cybernetics*, smc-16(1), 1986.

[30] K. B. Wipke, M. R. Cuddy, and S. D. Burch. Advisor 2.1: A user-friendly advanced powertrain simulation using a combined backward/forward approach. *IEEE Transactions on Vehicular Technology*, 48:1751–1761, 1999.

[31] R. P. Wolfson and J. H. Gower. The role of computer modeling and simulation in electric and hybrid vehicle research and development. *IEEE Transactions on Vehicular Technology*, VT-32(1), 1983.

[32] G.D. Wood. Simulating mechanical systems in simulink with SimMechanics. *www.mathworks.com*, 2003.

Paper B

INVERSE DYNAMIC SIMULATION OF NON-QUADRATIC MIMO POWERTRAIN MODELS -APPLICATION TO HYBRID VEHICLES[1]

Anders Fröberg[⋆]

[⋆] *Dep. of Electrical Engineering, Linköpings universitet,*
SE*-581 83 Linköping, Sweden.* froberg@isy.liu.se.

Abstract

The method for stable inversion of nonlinear systems has earlier been demonstrated as an efficient tool in inverse dynamic vehicle propulsion simulation. However, that method is restricted to quadratic systems, i.e. systems with equally many inputs and outputs. Here that restriction is relaxed for typical vehicle propulsion simulation where the number of inputs, e.g. accelerator pedal and brake pedal, are greater than the number of outputs, e.g. vehicle speed. Also restrictions to states and inputs resulting in time varying system order and relative degree is discussed. A model of a parallel hybrid vehicle is used for demonstration.

[1] This is an edited version of [7], Inverse Dynamic Simulation of Non-Quadratic MIMO Powertrain Models - Application to Hybrid Vehicles, published in the preprints of the IEEE Vehicle Power and Propulsion Conference 2006.

1 Introduction

Simulation of longitudinal vehicle models is a commonly used tool for driveline design, driveline optimization, and, design of driveline control strategies. There are two common ways to do this, quasi-static as, e.g., in Advisor [13] and QSS-TB [8], and forward dynamic simulation as, e.g. in PSAT [12] and Capsim [1]. The quasi-static simulation uses vehicle speed and acceleration to calculate required torques and speeds backwards through the driveline, and from that engine input is calculated. The model consists of static equations and efficiency maps of the components which results in low simulation time making the method suitable for design space exploration and optimization loops. In forward dynamic simulation, differential equations are solved using, e.g., throttle position as input, and vehicle speed as output, resulting in typically an order of magnitude longer simulation times for drive cycle simulations than what is typical for Advisor or QSS [6]. The advantage is that dynamic effects can be included making the modeling more accurate than in quasi-static simulation. In Fröberg [6] and Fröberg and Nielsen [5], [4] it is shown that inverse dynamic simulation is a good compromise between accuracy and simulation speed. There the method for stable inversion of nonlinear system [2], [9] is used to systematically transform a forward dynamic model to an inverse dynamic model. In contrast to the quasi-static approach this method treats the same kind of dynamics as the forward dynamic simulation, and it also handles zero dynamics and non-minimum phase systems, while keeping a low computational time.

The method for stable inversion of nonlinear systems requires a quadratic system, i.e. a system with equally many inputs and outputs. For a typical longitudinal vehicle simulation the number of inputs is greater than the number of outputs. Typically, there is one output, vehicle speed, and at least three inputs, accelerator pedal, brake pedal, and gear selector. It will here be shown how this MISO system, with minimal restrictions, can be transformed to a quadratic system that can be inverted.

A characteristic property in system inversion is the system relative degree [10], i.e. the number of times the output has to be differentiated in order for the input to appear explicitly. When for example putting restrictions on states or controls, the relative degree typically varies over time. It will here be discussed how this is treated and in a simulation example it will be demonstrated how this is handled in typical vehicle propulsion simulation.

First, the method of inverse dynamic powertrain simulation will be described, and it will be discussed what extensions that are necessary to simulate non quadratic powertrain models and systems of time varying order and time varying relative degree.

2 Inversion of non linear systems

The inverse dynamic simulation method is based on two things, inversion of differential equations that describes the system, and design of a driver model. The inversion uses the method of stable inversion of nonlinear systems [2], [9]. The method is based on a change of coordinates that enables computation of the input as a function of the output, its derivatives, and the trajectories of the zero dynamics.

A short review of the method [2, 9] will be given here. Let $u(t)$ be the inputs, $y(t)$ the

outputs, and $x(t)$ the states of a given system. Suppose that the system can be written in input-affine form and that the number of inputs, q, equals the number of outputs.

$$\begin{aligned} \dot{x}_d(t) &= f(x_d(t)) + g(x_d(t))u_d(t) && (1)\\ y_d(t) &= h(x_d(t)) && (2) \end{aligned}$$

Here suffix d corresponds to variables which by some means are smooth, corresponding to tracking of a velocity profile. Given a desired output $y_d(t)$ that is smooth, the problem is to solve for the input $u_d(t)$, and possibly also the states $x_d(t)$. With the notion smooth, it is here meant that a signal is sufficiently many times continuously differentiable. From here on it will be assumed that all functions are smooth such that the necessary derivatives exist and can be computed. It will also be assumed that $f(0) = 0$ and $h(0) = 0$. This can always be achieved for systems like (1)-(2) by a simple change of coordinates.

Let L be the standard notation for Lie-derivatives according to

$$L_f h(x) = \sum_i f_i(x)\frac{\partial h(x)}{\partial x_i},\ L_f^r h(x) = L_f\left(L_f^{r-1}h(x)\right) \tag{3}$$

If for all $1 \leq i, j \leq q$, for all $k < r_i - 1$, and for all x in a neighborhood of x^0

$$L_{g_j} L_f^k h_i(x) = 0 \tag{4}$$

and the $q \times q$ matrix

$$\tilde{\beta}(x) = \begin{pmatrix} L_{g_1}L_f^{r_1-1}h_1(x) & \dots & L_{g_q}L_f^{r_1-1}h_1(x) \\ L_{g_1}L_f^{r_2-1}h_2(x) & \dots & L_{g_q}L_f^{r_2-1}h_2(x) \\ \vdots & \ddots & \vdots \\ L_{g_1}L_f^{r_q-1}h_q(x) & \dots & L_{g_q}L_f^{r_q-1}h_q(x) \end{pmatrix} \tag{5}$$

is nonsingular, then the system is said to have a vector relative degree $r = (r_1, r_2, \dots, r_q)$ at the point x^0. That is, the relative degree of the system is the number of times one has to differentiate the outputs for at least one input to appear explicitly.

The first step in the inversion procedure is to compute the relative degree. The next step is to partially linearize the system. This is done by differentiating $y_i(t)$ until at least one $u_j(t)$ appears explicitly. Define $\xi_k^i = y_i^{(k-1)}(t)$ for $i = 1, \dots, q$ and $k = 1, \dots, r_i$ and let

$$\begin{aligned} \xi &= \left(\xi_1^1, \xi_2^1, \dots, \xi_{r_1}^1, \xi_1^2, \dots, \xi_{r_2}^2, \dots, \xi_{r_q}^q\right)^T \\ &= \left(y_1, \dot{y}_1, \dots, y_1^{r_1-1}, y_2, \dots, y_2^{r_2-1}, \dots, y_q^{r_q-1}\right)^T && (6) \end{aligned}$$

Now the change of coordinates can be defined. Since y is a function of x, it can be written as

$$\left(\xi^T, \eta^T\right)^T = \psi(x) \tag{7}$$

where η are variables needed, and the only constraint in the choice of η is that the Jacobian matrix of $\psi(x)$ must be nonsingular at x^0 so that it is a local coordinates transformation in

a neighborhood of x^0. It is always possible to find such a $\psi(x)$ [10]. With this choice of coordinates the following system which is partially linear in ξ is achieved

$$\begin{cases} \dot{\xi}_1^i(t) &= \xi_2^i(t) \\ &\vdots \\ \dot{\xi}_{r_i-1}^i(t) &= \xi_{r_i}^i(t) \\ \dot{\xi}_{r_i}^i(t) &= \alpha_i(\xi(t),\eta(t)) + \beta_i(\xi(t),\eta(t))u(t) \end{cases} \tag{8}$$
$$\dot{\eta}(t) = s_a(\xi(t),\eta(t)) + s_b(\xi(t),\eta(t))u(t)$$

where the vector α and the matrix β are

$$\alpha(\xi,\eta) = L_f^r h(\psi^{-1}(\xi,\eta)) \tag{9}$$
$$\beta(\xi,\eta) = L_g L_f^{r-1} h(\psi^{-1}(\xi,\eta)) \tag{10}$$

and the functions $s_a(\xi,\eta)$ and $s_b(\xi,\eta)$ are given by the choice of η.

Denote $y^{(r)} = \left(y_1^{(r_1)},\ldots,y_q^{(r_q)}\right)$. Then it can be seen in the first part of (8) that $y^{(r)}(t) = \alpha_i(\xi(t),\eta(t)) + \beta_i(\xi(t),\eta(t))u(t)$. By the definition of relative degree, $\beta(\xi,\eta)$ is nonsingular. Given a desired output trajectory $y_d(t)$ the required control input $u_d(t)$ can be calculated as

$$u_d(t) = \beta_i(\xi(t),\eta(t))^{-1}(y_d^{(r)}(t) - \alpha_i(\xi(t),\eta(t))) \tag{11}$$

Here it is seen that in order to calculate the required input for the system to follow the prescribed trajectory, not only $y_d(t)$ has to be known, but also the trajectories of $\eta(t)$ and the r first derivatives of $y_d(t)$. If the state trajectories producing the desired output are of interest they can be calculated from the inverse coordinate change

$$x(t) = \psi^{-1}(\xi(t),\eta(t)) \tag{12}$$

How the zero dynamics is to be solved depends on the system studied. There are three classes of systems that can be written in the form (8). The first class is all systems where the relative degree equals the dimension of the system, which means that there are no zero dynamics. The second class is all systems with stable zero dynamics, i.e., minimum phase systems, and the third class is systems with unstable zero dynamics, i.e., non-minimum phase systems. For the class of systems without zero dynamics, (11) becomes a system of static equations where the required input can be calculated from the desired output and its derivatives. In the case of stable zero dynamics the procedure is also straight forward. Substitute (11) in (8),

$$\dot{\eta} = s_a(\xi,\eta) + s_b(\xi,\eta)\beta_i(\xi,\eta)^{-1}(y_d^{(r)} - \alpha_i(\xi,\eta)) \equiv s(\eta, Y_d) \tag{13}$$

where

$$Y_d = \left(y_1,\dot{y}_1,\ldots,y_1^{(r_1)},y_2,\ldots,y_2^{(r_2)},\ldots,y_q^{(r_q)}\right) \tag{14}$$

Choose appropriate initial values for $\eta(t)$, and solve the system of differential equations, (13), in order to find the trajectories of the zero dynamics.

In the case of unstable zero dynamics however, there is no such straight forward way, since then (13) can not be integrated as an initial value problem. It is not possible to

solve the unstable zero dynamics in the general case, but in drive cycle simulations the desired output trajectory is known before hand. This gives the possibility of computing a non causal solution of (13) and still receive a stable result. In Devasia et al. [2] a Picard-like iteration is used to find the zero dynamics of a nonlinear non-minimum-phase system. See also Fröberg [6] for a simulation example of a diesel engine with non-minimum phase properties.

In summary the algorithm is as follows. Consider a system of order n. First, find the relative degree r of the system and differentiate the output r times. Then make a coordinate change (7) where the system outputs and its derivatives up to the order $r-1$ are used as states. Choose $n-r$ other states to form a complete base for state space. These $n-r$ states is the zero dynamics and is typically chosen from the original states. The zero dynamics is driven from the output and can be calculated from the output and its r first derivatives by combining Equations (11) and (8). The trajectories of zero dynamics are solved by numerical integration. Then Equation (11) is used to calculate the inputs from the trajectories of the zero dynamics and the r first derivatives of the output . The original states are found by the inverse of the coordinate change (12).

3 Driver model

The output y to the original system, and its derivatives, is used as input to the inverse dynamic simulation. In vehicle propulsion simulation this means that the reference vehicle speed has to be differentiated as many times as the systems relative degree. For a physically realistic system it is not a restriction to assume that the speed is sufficiently differentiable, since it would require infinite accelerations and torques in the driveline to produce a non differentiable vehicle speed. In inverse dynamic simulation the vehicle speed profile has to be smoothed to fulfill the differentiation requirements. The smoothing corresponds to driver behavior and in [5], [6] the smoothing is done based on desired driver behavior by calculating the desired speed profile $v_d(t)$ and its derivatives from a given drive cycle $v_c(t)$ as the following convolution

$$v_d^{(r)}(t) = \int_{-\infty}^{\infty} g^{(r)}(t-\tau) v_c(\tau) d\tau \tag{15}$$

By using this method when calculating $v_d^{(r)}(t)$ numerical differentiation of the speed profile is avoided since $g^{(r)}(t)$ can be analytically differentiated. Using the convolution kernel

$$g(t) = \begin{cases} e^{\frac{-a^2}{a^2-t^2}}, & |t| \leq a; \\ 0, & \text{otherwise} \end{cases} \tag{16}$$

a speed profile as in Figure 1 is achieved.

4 Application to hybrid vehicles

To demonstrate inverse dynamic powertrain simulation a model of a parallel hybrid electric vehicle is used. First, the powertrain model equations will be presented. Then, the

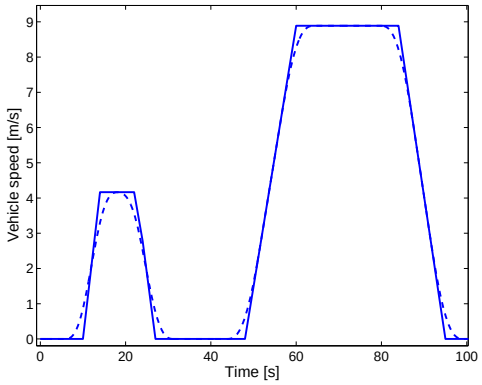

Figure 1: *Part of the European drive cycle NEDC. The solid line is the drive cycle and the dashed line is the desired speed profile given by the driver model (15) with the tracking time constant $a = 5$ seconds.*

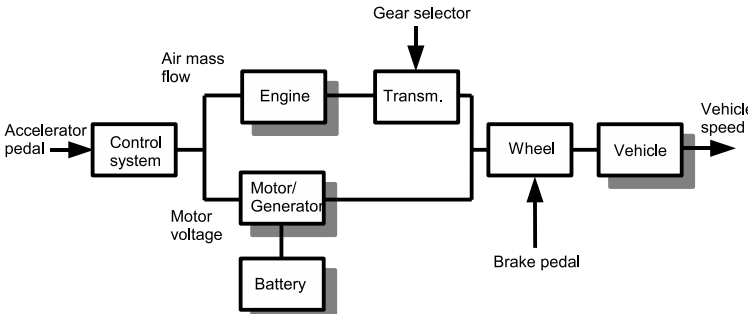

Figure 2: *Schematic description of an example model of a parallell hybrid electric vehicle.*

design of the control system necessary for inversion will be presented. The inversion algorithm for this system will be detailed, and last a simulation of the model will be presented.

The powertrain is a parallel hybrid electric vehicle consisting of an internal combustion engine, ICE, with transmission, and an electric motor coupled to the driveshafts. See Figure 2 for a schematic depiction. The vehicle and engine model are standard as described in Kiencke and Nielsen [11].

The motion of the vehicle is described by Newtons second law,

$$m\dot{v} = F_t - F_a - F_r - F_b \tag{17}$$

i.e., mass, m, times acceleration, $\dot{v}$, equals the tractive force, F_t, reduced by air resistance, F_a, rolling resistance, F_r, and force from the brakes, F_b. The resistances are given by

$$F_a = \frac{1}{2}\rho c_d A v^2,\ F_r = mgc_r \tag{18}$$

where ρ is air density, c_d drag coefficient, A vehicle cross sectional area, g gravitational acceleration, and c_r is rolling resistance coefficient.

The wheels are modeled without slip such that the tractive force is given from wheel torque T_w and wheel radius r, and vehicle speed is given from wheel speed ω_w according to

$$F_t r = T_w,\ \omega_w r = v \tag{19}$$

The wheel torque is the sum of the transmission torque $T_{t,out}$ and the electric motor torque T_{em}

$$T_w = T_{t,out} + T_{em} \tag{20}$$

The transmission is modeled as an ideal gear with gear ratio i_t and the ingoing torque to the transmission $T_{t,in}$ and engine speed ω_e are given by

$$T_{t,in} i_t = T_{t,out},\ \omega_e = i_t \omega_w \tag{21}$$

The rotating parts of the engine is modeled as a standard rotating inertia as

$$J_e \dot{\omega}_e = T_e - T_{t,in} \tag{22}$$

where J_e is engine inertia and T_e is the produced torque from the pistons. The engine torque is modeled as proportional to fuel mass per engine cycle m_f. Assuming that the engine runs at stoichiometric conditions, i.e. the normalized air fuel ratio $\lambda = 1$, fuel mass is given from air mass per engine cycle m_{ac} and stoichiometric air fuel ratio AFs

$$T_e = k_e m_f = k_e \frac{m_{ac}}{AFs\lambda} \tag{23}$$

The air mass flow into the cylinders is described by

$$\dot{m}_{ac} = \eta_{vol} \frac{V_d \omega_e p}{2\pi n_r R T_i},\ m_{ac} = \dot{m}_{ac} \frac{2\pi n_r}{\omega_e} \tag{24}$$

where η_{vol} is volumetric efficiency, V_d is engine displacement, p is intake manifold pressure, n_r is number of revolutions per engine cycle, R is the mass specific gas constant, T_i is intake manifold temperature.

The pressure derivative in the intake manifold is given by the difference of the inflow and the outflow, i.e. the flow past the throttle, $\dot{m}_{at}$, and the flow into the cylinders, according to

$$\dot{p} = \frac{RT_i}{V_i}(\dot{m}_{at} - \dot{m}_{ac}) \tag{25}$$

where V_i is intake manifold volume.

The electric traction motor is here assumed to work as a generator also and is modeled as a DC-motor where the torque is proportional to the electric current $\imath_{em}$.

$$T_{em} = \imath_{em} k_{em} \tag{26}$$

The motor is modeled as with internal inductance and resistance and the current derivative is given by

$$L_{em} i_{em} = U_{em} - R_{em}\imath_{em} - \omega_{em} k_{em} \tag{27}$$

where U_{em} is the applied voltage. Note that motor current is denoted $\imath_{em}$ and that its time derivative is denoted i_{em}.

The rate change of the battery charge is simply

$$\dot{q} = -\imath_{em} \tag{28}$$

Putting Equations (17)-(28) together results in a system with the states vehicle speed, v, intake manifold pressure, p, motor current, $\imath_{em}$, and battery charge, q. Inputs to the system is air flow past the throttle, $\dot{m}_{at}$, motor voltage, U_{em}, gear ratio, i_t, and braking force F_b. Output is vehicle speed. Lumping all model parameters into $c_i > 0$, the system can be written as

$$\dot{v} = \frac{-c_1 v^2 - c_2 - c_3 F_b + c_4 \imath_{em} + c_5 p i_t}{c_6 + c_7 i_t^2} \tag{29}$$

$$\dot{p} = c_8 \dot{m}_{at} - c_9 i_t v p \tag{30}$$

$$i_{em} = c_{10} U_{em} - c_{11} \imath_{em} - c_{12} v \tag{31}$$

$$\dot{q} = -\imath_{em} \tag{32}$$

4.1 Control system

Since the system (29)-(32) has four inputs and only one output inverse dynamic simulation as described in Section 2 can not be applied directly. However, for most vehicle propulsion simulation applications this problem can be solved by also considering an energy management system and a driver model. In a hybrid vehicle the driver does not decide how to combine the engine and motor to get a desired tractive force. This is done by an energy management system that in this case controls the motor voltage and the engine air mass flow from accelerator pedal position, $A_{p,pos}$, and the vehicles current state. Formally this can be written as $U_{em} = U_{em}(A_{p,pos}, v, p, \imath_{em}, q)$, and $\dot{m}_{at} = \dot{m}_{at}(A_{p,pos}, v, p, \imath_{em}, q)$. For most purposes it can also be assumed that the accelerator pedal and brake pedal never is used at the same time. It will also be assumed that the driver changes gear at for example given engine speed, i.e. $i_t = f(\omega_e)$. Using the above assumptions the system has one input at each time, either, accelerator pedal or brake pedal, and one output, vehicle speed. See Figure 3 for a schematic depiction of inverse dynamic simulation of the example vehicle.

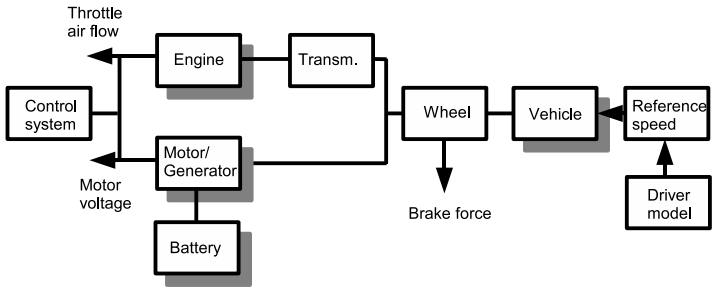

Figure 3: *Schematic description of inverse simulation of the model of a parallell hybrid electric vehicle depicted in Figure 2.*

Energy management system

The focus in this work have been to demonstrate the inverse dynamic simulation on typical system structure of a hybrid electric vehicle with varying relative degree and more inputs than outputs. No effort has been made on finding a fuel optimal energy management system.

The control strategy is as follows:

1. Use the electric motor at speeds below V_{lim}
2. Use both the electric motor and ICE at hard accelerations
3. Use the ICE above V_{lim}
4. Use the electric motor at braking (charging the battery)
5. Use the brakes if electric motor is not enough

No clutch is modeled between the engine and the rest of the driveline so the engine always rotates. When the electric motor is not used a switch is used to disconnect the motor from the battery. Also the charge and discharge current is limited to $\imath_{em,min} \leq \imath_{em} \leq \imath_{em,max}$.

For the five cases above the following systems are simulated: For case 1 and 4 the engine is dragged by the driveline, $\dot{m}_{at} = 0$, and U_{em} is the input to the model. This means that the system is of order $n = 4$, the relative degree becomes $r = 2$, and the dimension of the zero dynamics is $\dim \eta = 2$. The coordinate change (7) can be chosen as

$$\begin{bmatrix} \xi_1 & \xi_2 & \eta_1 & \eta_2 \end{bmatrix}^T = \begin{bmatrix} v & \dot{v} & \imath_{em} & q \end{bmatrix}^T \tag{33}$$

where $\dot{v}$ is given from Equation (29).

For case 2 the current of the motor is saturated at $\imath_{em,max}$ so the states to be simulated are v, p, and q, and the input to the model is $\dot{m}_{at}$. The system order is $n = 3$, the relative

degree $r = 2$, and $\dim \eta = 1$. The coordinate change can be chosen as

$$\begin{bmatrix} \xi_1 & \xi_2 & \eta_1 \end{bmatrix}^T = \begin{bmatrix} v & \dot{v} & q \end{bmatrix}^T \tag{34}$$

For case 3 the battery is disconnected from the motor, which gives $n = 2$, $r = 2$, and $\dim \eta = 0$. This means that there are no zero dynamics and the inverse model is a system of static equations according to Equation (11). The coordinate change is

$$\begin{bmatrix} \xi_1 & \xi_2 \end{bmatrix}^T = \begin{bmatrix} v & \dot{v} \end{bmatrix}^T \tag{35}$$

For case 5 the electric motor is saturated at $\imath_{em,min}$, $\dot{m}_{at} = 0$, and F_b is the input to the model. Since the motor current is given $n = 3$, $r = 1$, and $\dim \eta = 2$. The coordinate change can be chosen as

$$\begin{bmatrix} \xi_1 & \eta_1 & \eta_2 \end{bmatrix}^T = \begin{bmatrix} v & p & q \end{bmatrix}^T \tag{36}$$

When the coordinate changes have been decided, the zero dynamics can be simulated combining Equation (11) with the last equations of the system (8). Using the inverse coordinate change (12) the zero dynamics can be simulated using the original coordinates. When the zero dynamics is known the required inputs is given by Equation (11).

The terms α, (9) and β, (10) for the different cases when U_{em}, $\dot{m}_{at}$, or F_b is used as input becomes (expressed in the original coordinates):

$$\alpha_{EM} = \frac{1}{c_6 + c_7 i_t^2}\Big(\frac{-2c_1 v}{c_6 + c_7 i_t^2}\left(-c_1 v^2 - c_2 - c_3 F_b + c_4 \imath_{em} + c_5 p i_t\right) + c_4\left(-c_{11}\imath_{em} - c_{12} v\right) + c_5 i_t\left(c_8 \dot{m}_{at} - c_9 i_t v p\right)\Big) \tag{37}$$

$$\beta_{EM} = \frac{c_4 c_{10}}{c_6 + c_7 i_t^2} \tag{38}$$

$$\alpha_{ICE} = \frac{1}{c_6 + c_7 i_t^2}\Big(\frac{-2c_1 v}{c_6 + c_7 i_t^2}\left(-c_1 v^2 - c_2 - c_3 F_b + c_4 \imath_{em} + c_5 p i_t\right) + c_4\left(c_{10} U_{em} - c_{11}\imath_{em} - c_{12} v\right) + c_5 i_t\left(-c_9 i_t v p\right)\Big) \tag{39}$$

$$\beta_{ICE} = \frac{c_5 c_8 i_t}{c_6 + c_7 i_t^2} \tag{40}$$

$$\alpha_B = \left(-c_1 v^2 - c_2 + c_4 \imath_{em} + c_5 p i_t\right)\frac{1}{c_6 + c_7 i_t^2} \tag{41}$$

$$\beta_B = \frac{-c_3}{c_6 + c_7 i_t^2} \tag{42}$$

To perform an inverse dynamic simulation of this system, an inverse dynamic driver model, (15), is designed that specifies the desired velocity profile. Using the inverse driver model together with the powertrain model and its control system, the model has only one input, desired acceleration, i.e. accelerator or brake pedal position, and one output, vehicle speed. This system can be inverted using the method described in Sections 2 and 3 which results in an inverse dynamic model as depicted in Figure 3. An example simulation of the hybrid powertrain model is presented in Figures 4 and 5. When simulating the considered vehicle model there are some further considerations that will be discussed in the following subsections.

4.2 Change in system order and relative degree

As described above the system changes both order and relative degree when the energy management system switches operating mode. For some mode switches the coordinates for the zero dynamics is changed. Whenever a new coordinate is introduced it has to be properly initiated. For example, when switching from high to low speed, i.e. case 3 to 1, two new coordinates, ι_{em} and q is introduced and has to be properly initialized. This has to be done such that the system equations (29)-(32) is consistent over the mode switch. For the charge q the only constraint is the obvious fact that it has to be initialized to the value it had at the end of the period when it was last used. For ι_{em} continuity and smoothness of other variables also has to be considered. In this case it means that ι_{em} has to be initialized to a value consistent with Equation (29). Note that re-initializations of variables as described above can not be done for general non-minimum phase systems due to continuity restrictions [2].

4.3 Gear shifting and parameter jumps

The simplest way to model a gear change is as a parameter jump in gear ratio. This approach however can not be used without consideration in neither inverse nor forward simulation. As described in Section 2 there are smothness constraints on vehicle speed as well as on internal variables. This can be violated if gear changes are modeled as parameter jumps. In the vehicle model presented here the parameter jump approach is chosen. Since the model is a minimum phase system the simulation of the zero dynamics can be stopped just before a gear change, then all states are re-initialized to be consistent with the new gear ratio. For this example this causes a jump in intake manifold pressure. Since the intake pressure dynamics is much faster than the chassis dynamics this can be accepted for cases such as fuel consumption simulations. If an exact simulation of the engine dynamics is required the gear shifting has to be more carefully modeled, for example with a slipping clutch where a “drive cycle” is specified for the clutch, i.e. speed profiles for the clutch plates during release and lock has to be specified.

Results for parameter jumps in inversion of linear non-minimum phase systems is given by Devasia et.al. [3].

5 Conclusion

Inverse dynamic simulation based on stable inversion of nonlinear systems has earlier been demonstrated feasible on quadratic powertrain models, i.e. models with equally many outputs and inputs. Here it has been discussed how the inverse dynamic powertrain simulation of non quadratic systems is performed. Inverse dynamic simulation of MISO powertrains is shown possible by specifying a control system and a driver model which results in a total system of one input, i.e. the driver’s desired acceleration, and one output, the vehicle speed. It is shown that restrictions on states and controls can result in a system where the system order and relative degree changes at switch points. Proper handling of such systems in inverse dynamic simulation is discussed. Last, inverse dynamic simulation of non quadratic systems that changes order and relative degree at switch points,

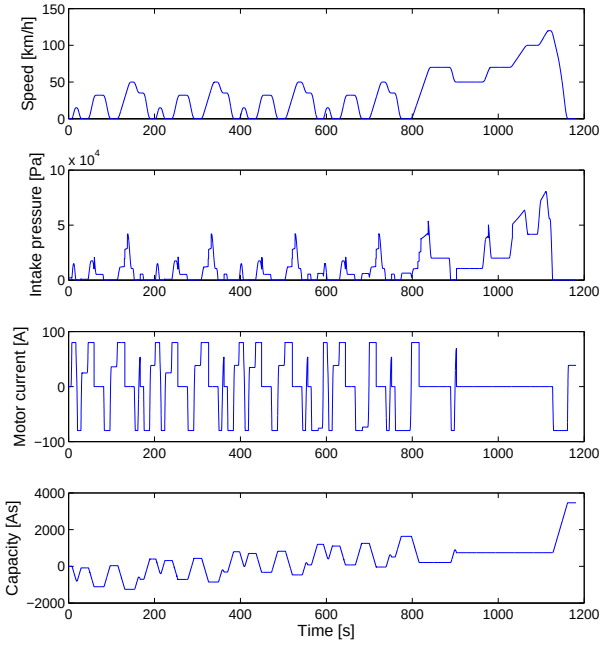

Figure 4: *Simulated states for the hybrid vehicle model.*

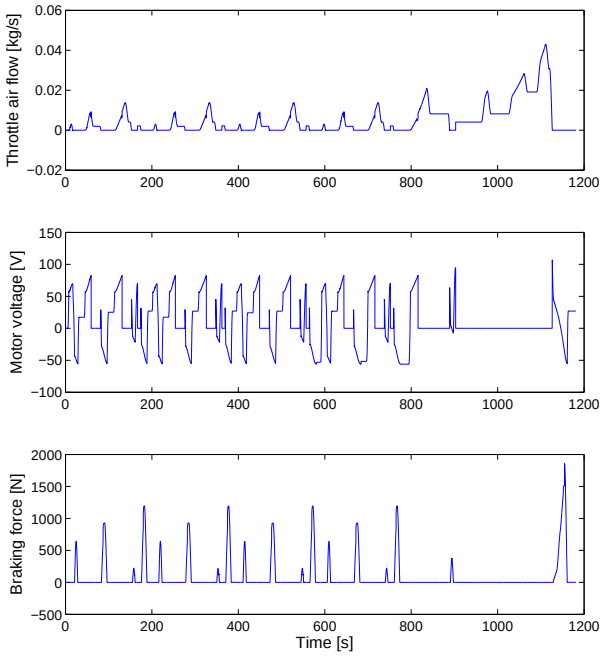

Figure 5: *Simulated controls for the hybrid vehicle model.*

is demonstrated feasible by simulation of an example model of a parallel hybrid electric vehicle.

Acknowledgment

The Swedish Energy Agency is gratefully acknowledged for the funding.

Bibliography

[1] *Center for automotive propulsion simulation.* http://www.capsim.se.

[2] S. Devasia, D. Chen, and B. Paden. Nonlinear inversion-based output tracking. *IEEE Transactions on Automatic Control*, 41:930–942, 1996.

[3] S. Devasia, B. Paden, and C. Rossi. Exact-output tracking theory for systems with parameter jumps. *International Journal of Control*, 67:117–131, 1997.

[4] A. Fröberg and L Nielsen. Dynamic vehicle simulation -forward, inverse and new mixed possibilities for optimized design and control. *SAE Technical Paper Series SP-1826, 2004-01-1619*, 2004.

[5] A. Fröberg and L Nielsen. A method to extend inverse dynamic simulation of powertrains with additional dynamics. *First IFAC Symposium on Advances in Automotive Control*, April 2004.

[6] Anders Fröberg. *Extending the inverse vehicle propulsion simulation concept -to improve simulation performance.* Licentiate thesis, LiU-TEK-LIC-2005:36, Linköping Institute of Technology, Linköping, 2005.

[7] A. Fröberg. Inverse dynamic simulation of non-quadratic mimo powertrain models -application to hybrid vehicles. *IEEE Vehicle power and propulsion conference, Windsor, UK*, 2006.

[8] L. Guzzella and A. Amstutz. Cae tools for quasi-static modeling and optimization of hybrid powertrains. *IEEE Transactions on Vehicular Technology*, 48:1762–1769, 1999.

[9] L. R. Hunt and G. Meyer. Stable inversion for nonlinear systems. *Automatica*, 33:1549–1554, 1997.

[10] A. Isidori. *Nonlinear Control Systems.* Springer-Verlag, 1995.

[11] U. Kiencke and L. Nielsen. *Automotive Control Systems, 2nd ed.* Springer-Verlag, 2005.

[12] A. Rousseau, P. Sharer, and F. Besnier. Feasability of reusable vehicle modeling: Application to hybrid vehicle. *SAE Technical Paper Series SP-1826, 2004-01-1618*, 2004.

[13] K. B. Wipke, M. R. Cuddy, and S. D. Burch. Advisor 2.1: A user-friendly advanced powertrain simulation using a combined backward/forward approach. *IEEE Transactions on Vehicular Technology*, 48:1751–1761, 1999.

Part II

Optimal control of vehicle propulsion

3
Look ahead powertrain control

The problem studied in this part is how to drive a given distance at a given time in the most fuel efficient way. Only highway-like driving for heavy trucks has been studied, but the results should be easily transferred to other driving missions and other vehicles by changing the problem parameters.

Driving a given distance with an average speed is equivalent to drive a given distance at a given time. The problem of minimizing fuel consumption under such conditions can be formulated as follows. Let $\dot{m}_f(t)$ be the fuel flow into the engine, let $v(t)$ be vehicle speed, and v_{avg} a desired average speed. Then minimization of fuel consumption over the time t_f is

$$\min \quad \int_0^{t_f} \dot{m}_f(t)dt \tag{3.1}$$

$$\text{such that} \quad \frac{1}{t_f}\int_0^{t_f} v(t)dt = v_{avg} \tag{3.2}$$

This problem is studied with slightly different view points in the following papers. First some background to the problem is presented, and then some theory on optimal control is summarized in a perspective used in the papers. Finally the papers are summarized and contributions are indicated.

3.1 Background

For heavy trucks even moderate slopes become significant. For a typical heavy truck, with weigth up to 60 metric tons, the mass of the vehicle makes it impossible to keep a constant cruising speed at most roads due to road slope. A typical road in Sweden has variations in slope between approximately -5% to 5%, see Figure 3.1. A negative slope here defines a downhill slope and a positive slope defines an uphill slope. As shown in Paper E the power to mass ratio for a typical vehicle that weighs 60 tons is too small for

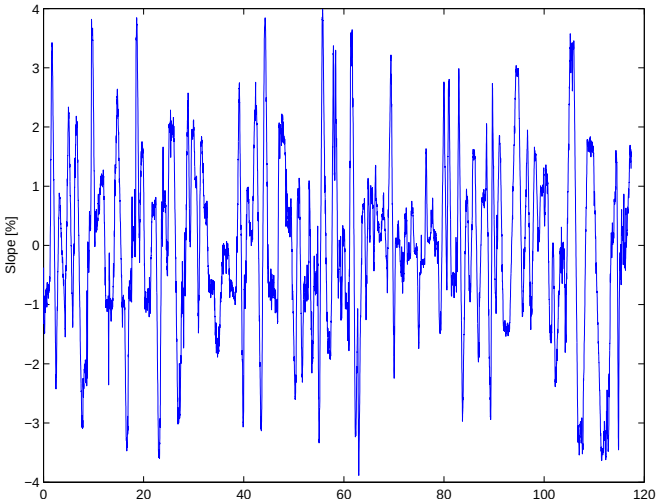

Figure 3.1: *Slope of the highway E4 in Sweden between the cities of Södertälje and Norrköping.*

the vehicle to keep cruising speed in uphill slopes with an inclination larger than about 1%. Further, in down hill slopes where the engine does not produce any work, the mass of the vehicle will make it accelerate if no brakes are applied, if the slope is steeper than about -1%. For driving missions on such roads there are several possible speed profiles that have the same average speed but with different fuel consumption. These facts make it interesting to study optimal speed profiles that minimizes fuel consumption on a given driving mission while keeping a desired average vehicle speed.

3.2 Optimal control theory

To solve the problem defined by Equations (3.1) and (3.2) optimal control theory is used. A short review of optimal control as described in the classical textbook [4] will now be given.

Let t_0, t_f be the initial and final time respectively. Let $x(t)$ be the state vector and $u(t)$ be the controls of the system defined by

$$\dot{x}(t) = f(x(t), u(t), t),\ x(t_0) = x_0 \tag{3.3}$$

Let $\varphi(x_f, t_f)$ and $L(x(t), u(t), t)$ be functions that are differentiable sufficiently many times. The optimal control problem is then to find the control law $u(t)$ that minimizes the performance index

$$J = \varphi(x(t_f), t_f) + \int_{t_0}^{t_f} L(x(t), u(t), t)dt \tag{3.4}$$

Now, adjoin the system dynamics, i.e. the constraint (3.3), to the performance index with multipliers $\lambda(t)$

$$\tilde{J} = \varphi(x(t_f), t_f) + \int_{t_0}^{t_f} \left(L(x(t), u(t), t) + \lambda^T(t) \left(f(x(t), u(t), t) - \dot{x}(t) \right) \right) dt \tag{3.5}$$

Define a scalar function called the Hamiltonian as

$$H(x(t), u(t), \lambda(t), t) = L(x(t), u(t), t) + \lambda^T(t) f(x(t), u(t), t) \tag{3.6}$$

In Chapter 2.3 in [4] the necessary optimality conditions are stated as follows: The adjoint dynamics for an optimal solution is

$$\dot{\lambda}^T = -\frac{\partial H}{\partial x} = -\frac{\partial L}{\partial x} - \lambda^T \frac{\partial f}{\partial x} \tag{3.7}$$

with boundary conditions

$$\lambda^T(t_f) = \frac{\partial \varphi}{\partial x(t_f)} \tag{3.8}$$

and for an extremum it must hold that

$$\frac{\partial H}{\partial u} = 0, \; t_0 \leq t \leq t_f \tag{3.9}$$

Equations (3.7), (3.8) and, (3.9) are often referred to as the Euler-Lagrange equations.

A more general result than (3.9) for optimal control is the maximum principle as stated in [7]. For a minimization problem as here the maximum principle becomes a "minimum principle". Let the set of allowed controls be $u \in U$, let the optimal control be $u^\star$, and let the optimal solution be $x^\star$. Then the optimal control is found from

$$\min_{u \in U} H(x^\star(t), u(t), \lambda(t)) = H(x^\star(t), u^\star(t), \lambda(t)) \tag{3.10}$$

Example 3.1

Consider a vehicle with air and rolling resistance forces F_l of the form $F_l = a + bv^2$ where v is vehicle speed. Let the resistance due to road slope be $c \sin\alpha(s)$, the total vehicle inertia J, the propulsive force F, and the distance traveled s. The system dynamics can then be written as

$$\dot{v} = \frac{1}{J} \left(F - a - bv^2 - c \sin\alpha(s) \right) \tag{3.11}$$

$$\dot{s} = v \tag{3.12}$$

The system state vector is thus $x = [v, s]^T$ and the control is $u = F$. If the total propulsive work for the driving time t_f is to be minimized, i.e.

$$\min \int_0^{t_f} F v dt \tag{3.13}$$

i.e. $L = Fv$. The Hamiltonian for this problem is

$$H = Fv + \lambda_v \frac{1}{J}(F - a - bv^2 - c\sin\alpha(s)) + \lambda_s v \tag{3.14}$$

and the adjoint dynamics is given by (3.7), i.e.

$$\dot{\lambda}_v = -\frac{\partial H}{\partial v} = -F + \frac{2}{J}\lambda_v bv - \lambda_s \tag{3.15}$$

$$\dot{\lambda}_s = -\frac{\partial H}{\partial s} = \frac{1}{J}\lambda_v c\cos\alpha(s)\frac{d\alpha}{ds} \tag{3.16}$$

with $\lambda_v(t_f) = \lambda_s(t_f) = 0$. The optimal propulsive force is found by minimizing the Hamiltonian with respect to the control u. Since the Hamiltonian is linearly dependent on F, the result obtained by using (3.9),

$$\frac{\partial H}{\partial u} = v + \frac{\lambda_v}{J} \tag{3.17}$$

does not give the optimal control directly. However, this function plays an important role and will be referred to as the control switching function. Using the maximum principle (3.10) it is seen that when the control switching function is negative maximum propulsive force is used and when the control switching function is positive minimum propulsive force is used. When

$$\frac{\partial H}{\partial u} = v + \frac{\lambda_v}{J} = 0 \tag{3.18}$$

for finite periods of time further reasoning needs to be done in order to find the optimal control.

Another way of approaching the problem is as follows. Since road slope α is a function of position it is convenient to change independent variable according to

$$\frac{d}{ds} = \frac{1}{v}\frac{d}{dt} \tag{3.19}$$

The natural choice of states are then vehicle speed v and traveled time T, and the system dynamics is

$$\frac{dv}{ds} = \frac{1}{Jv}\left(F - a - bv^2 - c\sin\alpha(s)\right) \tag{3.20}$$

$$\frac{dT}{ds} = \frac{1}{v} \tag{3.21}$$

The objective function is then

$$\min \int_0^{s_f} F\,ds \tag{3.22}$$

i.e. $L = F$, and the Hamiltonian is

$$H = F + \lambda_v \frac{1}{Jv}(F - a - bv^2 - c\sin\alpha(s)) + \lambda_T \frac{1}{v} \tag{3.23}$$

The adjoint dynamics becomes

$$\frac{d\lambda_v}{ds} = -\frac{\partial H}{\partial v} = \frac{\lambda_v}{Jv^2}\left(F - a + bv^2 - c\sin\alpha(s)\right) + \frac{\lambda_T}{v^2} \tag{3.24}$$

$$\frac{d\lambda_T}{ds} = -\frac{\partial H}{\partial T} = 0 \tag{3.25}$$

Note that the second adjoint variable λ_T now is constant.

3.2.1 Optimal control with specified final states

Now, consider the optimization problem studied above but with some of the states specified at the final time t_f. If x_i is specified at the terminal time the boundary condition $\frac{\partial\varphi}{\partial x_i(t_f)} = \lambda_i(t_f)$ is exchanged to $x_i(t_f) = x_{i,f}$. If a system with n states has states $j = 1,\ldots,q$ specified at the final time, see Chapter 2.4 in [4], the constraint (3.8) is exchanged to the following, where ϑ_j are associated multipliers to be decided by the problem

$$\lambda_j(t_f) = \begin{cases} \vartheta_j, & j = 1,\ldots,q \\ \frac{\partial\varphi}{\partial x_j(t_f)} & j = q+1,\ldots,n \end{cases} \tag{3.26}$$

Example 3.2

Consider again Example 3.1. For that problem to be of any interest a constraint on the traveled distance at the time t_f has to be imposed. For the formulation using time as independent variable this means that $\lambda_s(t_f)$ no longer is zero, but instead that value has to be chosen such that the optimality conditions are satisfied. If also $v(t_f)$ is specified, λ_v is treated similarly. If s is the independent variable instead of time, the same reasoning is applied to $\lambda_T(s_f)$ and $\lambda_v(s_f)$.

3.2.2 Restrictions on control variables and states

In some problems it is interesting to study optimal solutions under constraints on functions of the control and state variables. Such a constraint is written

$$C(x,u,t) \leq 0 \tag{3.27}$$

This problem is handled by adjoining the constraint to the Hamiltonian with a multiplier μ

$$H = L + \lambda^T f + \mu C \tag{3.28}$$

where

$$\mu\begin{cases} > 0, & C = 0 \\ = 0, & C < 0 \end{cases} \tag{3.29}$$

Necessary optimality conditions are discussed in Chapter 3.10 in [4], and is as follows: The adjoint dynamics is

$$\dot{\lambda}^T = -H_x = \begin{cases} -L_x - \lambda^T f_x - \mu C_x, & C = 0 \\ -L_x - \lambda^T f_x, & C < 0 \end{cases} \tag{3.30}$$

and the optimal control is found from

$$H_u = L_u + \lambda^T f_u + \mu C_u = 0 \tag{3.31}$$

When $C = 0$, i.e. $\mu \neq 0$, (3.27) and (3.31) together determine $u(t)$ and $\mu(t)$.

3.2.3 Singular solutions

In many applications the system is in the form

$$\dot{x} = f(x) + g(x)u \tag{3.32}$$

Also assume that L is linearly dependent on u, i.e.

$$L = l(x)u \tag{3.33}$$

The Hamiltonian is then

$$H = l(x)u + \lambda^T(f(x) + g(x)u) \tag{3.34}$$

and

$$\dot{\lambda}^T = -l_x u - \lambda^T(f_x + g_x u) \tag{3.35}$$

If u is bounded the minimum of H may occur on the boundary of the set of all u. It is however possible that there are intervals where a function $u(t)$ will yield $x(t)$ and $\lambda(t)$ such that

$$H_u = l(x) + \lambda^T g(x) = 0 \tag{3.36}$$

A convexity condition for a local minimum is $H_{uu} \geq 0$. When (3.36) is fulfilled $H_{uu} = 0$ and such solutions are referred to as singular solutions. For such sections (3.36) does not directly determine $u(t)$, but it must also hold that

$$\frac{d}{dt}H_u = l_x\dot{x} + \dot{\lambda}^T g + \lambda^T g_x \dot{x} = 0 \tag{3.37}$$

Using (3.32) and (3.35) in (3.37) gives

$$\frac{d}{dt}H_u = l_x(f + gu) - (l_x u + \lambda^T(f_x + g_x u))g + \lambda^T g_x(f + gu) = 0 \tag{3.38}$$

Note that the terms in the control variable u cancels out in this expression. Equation (3.38) hence does not help directly in finding u, but it may give valuable insight in the dependence between λ and x, which in turn can give information about u. This method will be used later in paper F. In Chapter 8.3 in [4] Equation (3.38) is differentiated once again with respect to time to get an expression that determines u.

Example 3.3

Consider again the problem of Examples 3.1 and 3.2 formulated with position as independent variable. With $u = F$ the partial derivative of the Hamiltonian (3.23) with respect to the control is

$$\frac{\partial H}{\partial F} = 1 + \frac{\lambda_v}{Jv} \tag{3.39}$$

and

$$\frac{d}{ds}\frac{\partial H}{\partial F} = \frac{1}{Jv}\frac{d\lambda_v}{ds} - \frac{\lambda_v}{Jv^2}\frac{dv}{ds} = \frac{2\lambda_v b}{J^2 v} + \frac{\lambda_T}{Jv^3} \tag{3.40}$$

For singular arcs $\frac{\partial H}{\partial F} = 0$ for finite distances which from (3.39) means that $\lambda_v = -Jv$. Using this the following dependency between v and λ_T is obtained

$$\frac{d}{ds}\frac{\partial H}{\partial F} = \frac{\lambda_T}{Jv^3} - \frac{2b}{J} = 0 \tag{3.41}$$

Since λ_T is constant v is also constant during singular arcs. From that information the optimal control is found from the vehicle dynamics.

3.3 Dynamic programming

Dynamic programming became popular after the works [1, 2]. There is also a presentation given in [4], and a more recent textbook on the subject is [3]. In the previous section optimal control was discussed given an initial state and time. In control applications it is often desired to know optimal control solutions from many initial states and times in order to implement feedback control. In [4] it is discussed how this is treated for continuous time problems, and a short review will be given here.

Typically, only one optimal path passes through a point $(x(t),t)$ which means that a unique optimal control u° is associated with it. An optimal feedback control law can then be expressed,

$$u^\circ = u^\circ(x,t) \tag{3.42}$$

Also, for each point $(x(t),t)$, following the optimal path to the surface of the terminal boundary, there is a unique optimal value of the performance index, J°. Hence, J° can be regarded as a function of the starting point, i.e.

$$J^\circ = J^\circ(x,t) \tag{3.43}$$

This is referred to as the optimal return function.

For an arbitrary initial point (x,t) the performance index is

$$J = \varphi(x(t_f),t_f) + \int_t^{t_f} L(x(\tau),u(\tau),\tau)d\tau \tag{3.44}$$

with terminal conditions $\psi(x(t_f),t_f)=0$. The optimal return function (3.43) is then

$$J^{\circ}(x,t)=\min_{u(t)}\{\varphi(x(t_f),t_f)+\int_t^{t_f}L(x(\tau),u(\tau),\tau)d\tau\} \tag{3.45}$$

with boundary condition that $J^{\circ}(x,t)=\varphi(x,t)$ on the hypersurface $\psi(x,t)=0$. In [3] there is a thorough description how this problem is solved iteratively by discretizing time. There, time is divided in $N+1$ stages and the system is described as

$$x_{k+1}=f(x_k,u_k) \tag{3.46}$$

The return function, or cost-to-go as it is called by Bertsekas [3], in the last stage is

$$J_N(x_N)=g_N(x_N) \tag{3.47}$$

where g_N is the same function as φ used in [4], see (3.4). Now, let the cost at time instant k be $g_k(x_k,u_k)$. Then, from the value of the end cost, (3.47), the optimal control policy is found by iterating backward in time according to

$$J_k(x_k)=\min_{u_k}\{g_k(x_k,u_k)+J_{k+1}(f_k(x_k,u_k))\},\ k=0,1,\ldots,N-1 \tag{3.48}$$

Let the optimal value of the cost-to-go function at stage k be $J_k^*(x_k)$.
Let $\pi^k=\{\mu_k,\mu_{k+1},\ldots,\mu_{N-1}\}$. Then the optimal value of the cost to go function is

$$J_k^*(x_k)=\min_{\pi^k}\{g_N(x_N)+\sum_{i=k}^{N-1}g_i(x_i,\mu_i(x_i))\} \tag{3.49}$$

This expression can be compared to (3.45). In [3] it is shown that the function $J_k^*(x_k)$ are equal to the functions $J_k(x_k)$ generated by the dynamic programming algorithm (3.48).

When solving an optimal control problem it is also practical to discretize the state-space. The dynamic programming problem can then be described by a transition graph. In a deterministic graph the same optimal solution is found independent if the algorithm is run backward or forward in the graph.

Example 3.4

Consider again example 3.1 but now to be solved with the discrete dynamic programming algorithm. The vehicle dynamics using the Euler approximation with step length h is

$$v_{k+1}=f(v_k,F_k)=\frac{h}{J}\left(F_k-a-bv_k^2-c\sin\alpha(s)\right)+v_k \tag{3.50}$$

Let the final state cost be $g_N(v_N)=0$ and the cost for a transition from state v_i to v_{i+1} be the propulsive work hF_i. Then the state transition cost is

$$g_k(v_k,F_k)=hF_k,\ k=0,\ldots,N-1 \tag{3.51}$$

The optimal control is then found from the backward iteration, with $J_N=0$,

$$J_k(x_k)=min_{F_k}\left\{g_k(v_k,F_k)+J_{k+1}(f_k(v_k,F_k))\right\},\ k=0,\ldots,N-1 \tag{3.52}$$

The dynamic programming method described is used in Paper C and D. An example simulation is seen in Figure 3.2, which also will be the starting point of the next section.

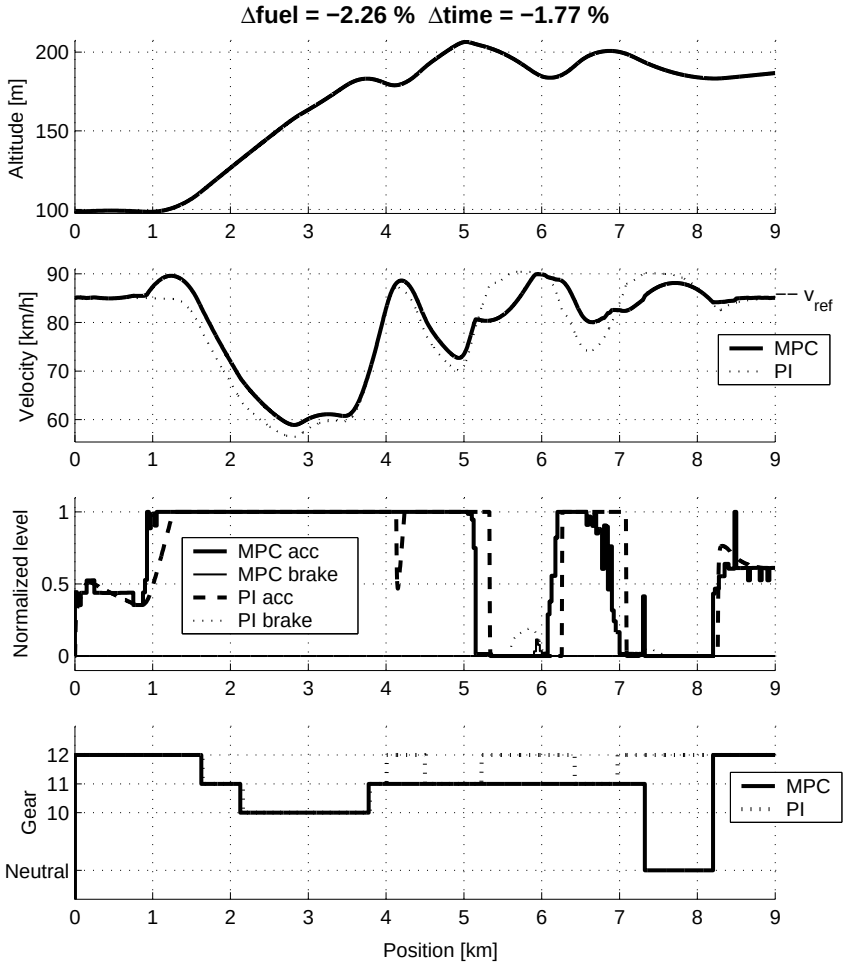

Figure 3.2: *A simulation example of an authentic road from Paper D. Two simulations are depicted, one using a standard cruise controller (PI) and one with a predictive controller using dynamic programming (MPC). The top plot shows the road topography, the second vehicle velocity, the third normalized accelerator and brake levels, and the fourth gear selection.*

3.4 Towards practical rule based control

In Figure 3.2, part of an example simulation from Paper D is presented. In that case the dynamic programming algorithm has been used in each sample to calculate the optimal accelerator level, i.e. fueling, optimal brake level, and optimal gear choice. Some typical behavior can be observed in the figure, e.g., prior to a significant incline the vehicle is accelerated which can be seen at 1, 4 and 6 km, and prior to a decline the vehicle is retarded which can be seen at 5 and 7 km. Inspired by such observations it is interesting to see if simple rules can be found that can be used in an intuitive and more computationally efficient control system, and to what extent such a controller is able to save fuel.

To quantify when and how to take actions such as acceleration before inclines and retardation before declines, the optimality conditions from Section 3.2 can be used.

Example 3.5

Again consider Example 3.1. Recall the control switching function (3.17), and that if $\frac{\partial H}{\partial u} > 0$ minimum tractive force is used, and that if $\frac{\partial H}{\partial u} < 0$ maximum tractive force is used. It is seen that vehicle inertia, which mostly depends on vehicle mass, is a decisive parameter for the optimal control, but also that the relation between vehicle speed v and the adjoint variable λ_v is important.

Those equations also gives a possibility to find the decisive parameters for the optimal control. It is natural that for example engine torque, vehicle mass, and road inclination are decisive but it is not clear in what relation they will enter into practical rules. By using simple yet descriptive models and formulating the analytical optimality conditions a lot of insight can be obtained. The results point toward a practical rule-based controller as is described in Paper F.

3.5 Overview and contributions of the papers

A brief overview of the papers will here be given and the contributions will be stated.

Controlling Gear Engagement and disengagement on heavy trucks for minimization of fuel consumption, Anders Fröberg, Lars Nielsen, Lars-Gunnar Hedström, and Magnus Pettersson, IFAC World Congress 2005. In steep downhill slopes a heavy truck will accelerate even though there is no fuel injected to the engine, i.e. the engine produces negative work due to friction. A possibility to reduce the total powertrain friction is to engage neutral gear. This will increase the vehicle acceleration and the gain in kinetic energy will increase. However, to drive systems like power steering etc, the engine has to be run in idle conditions and thus consuming some amount of fuel. The contribution of this paper is to show the magnitude of possible fuel savings by making the correct decision in significant downhill slopes whether to disengage the gear or to cut the fuel injection.

A Real-Time Fuel-Optimal Cruise Controller for Heavy Trucks using Road Topography Information, Erik Hellström, Anders Fröberg, and Lars Nielsen, SAE World Congress 2006. If knowledge of road profile ahead of the vehicle is known that information can be used to control engine fueling and gear choice in a fuel optimal way. This paper shows how a predictive cruise controller with real time performance can be designed using dynamic programming, and the magnitude of possible fuel savings is demonstrated through

simulations on authentic road profiles. This work is based on the master thesis by Erik Hellström [6] which was supervised by Anders Fröberg.

Explicit Fuel Optimal Speed Profiles for Heavy Trucks on a Set of Topograhic Road Profiles, Anders Fröberg, Erik Hellström, and Lars Nielsen, SAE World Congress 2006. To gain knowledge of decisive parameters affecting fuel consumption fueling control is here studied on constructed road profiles. The simple test cases together with analytical solutions to vehicle motion gives valuable insight into the properties of the optimal control. The results can also be used to validate the behavior of numerical predictive controllers such as presented in Paper D.

Optimal Control Utilizing Analytical Solutions for Heavy Truck Cruise Control, Anders Fröberg and Lars Nielsen, technical report that is an extended version of the paper [5], *Optimal fuel and gear ratio control for heavy trucks with piece wise affine engine characteristics.* Again solutions on constructed road profiles are studied, but now by solving the optimal control problem in more detail. The analytical expressions that are derived for the necessary optimality conditions provide insight in how each parameter affects the optimal solution.

Optimal control solutions for affine engine torque modeling are compared to solutions for piece-wise affine models, and it is shown that even small non-linearities have significant effect on optimal control switch points. Solutions on optimal gear ratio control for both a continuous variable transmission and a discrete stepped transmission show that the maximum fueling function and the gear shifting losses are important for the optimal control behavior.

The theoretical results are used in a simple rule based predictive cruise controller and the possible fuel savings for that method is demonstrated in simulations on authentic road profiles showing promising results.

Bibliography

[1] Richard Bellman. *Dynamic Programming.* Princeton University Press, 1957.

[2] Richard Bellman and Stuart E. Dreyfus. *Applied Dynamic Programming.* Princeton University Press, 1962.

[3] Dimitri P. Bertsekas. *Dynamic Programming and Optimal Control.* Athena Scientific, 2000.

[4] Arthur E. Bryson and Yu-Chi Ho. *Applied optimal control.* Taylor and Francis, 1975.

[5] Anders Fröberg and Lars Nielsen. Optimal fuel and gear ratio control for heavy trucks with piece wise affine engine characteristics. Fifth IFAC symposium on advances in automotive control, Monterey Coast, California, 2007.

[6] Erik Hellström. *Explicit use of road topography for model predictive cruise control in heavy trucks.* Masters thesis, LiTH-ISY-EX-05/3660-SE, Linköping Institute of Technology, Linköping, 2005.

[7] George Leitmann. *The calculus of variations and optimal control.* Plenum press, 1981.

Paper C

CONTROLLING GEAR ENGAGEMENT AND DISENGAGEMENT ON HEAVY TRUCKS FOR MINIMIZATION OF FUEL CONSUMPTION[1]

Anders Fröberg[⋆], Lars Nielsen[⋆], Lars-Gunnar Hedström[†], Magnus Pettersson[†]

[⋆]*Dep. of Electrical Engineering, Linköpings universitet,*
SE-*581 83 Linköping, Sweden.* {froberg, lars}@isy.liu.se.
[†]*Scania, SE-151 87 Södertälje, Sweden*

Abstract

There is a potential to save fuel for heavy trucks by storing kinetic energy in the vehicle when driving downhill, because the speed adds kinetic energy to the vehicle which can be used after the downhill slope to propell the vehicle. This behavior can be even more utilized by disengaging the gear to reduce the friction in the driveline and thus increase the speed even more. Two different control strategies to choose when to disengage the gear is presented: One that uses instantaneous inclination and one predictive control scheme that uses look ahead information of the road topology. Simulation results show that gear disengagement in downhills can reduce the fuel consumption about 3% on specialized constructed road profiles, but only about one tenth of that on an authentic road profile.

[1]This is an edited version of [3], Controlling gear engagement and disengagement on heavy trucks for minimization of fuel consumption, published in the preprints of the IFAC world congress 2005.

1 Introduction

In order to save fuel it can be beneficial to increase speed when driving downhill to build up kinetic energy that can be used driving uphill. Typical cruise controllers used in heavy trucks allow the speed to vary between specified limits such that the speed is high in hollows and low on crests. If the slope is high when driving downhill the fuel injection can be cut off and no fuel is consumed. However, for small slopes the engine friction can be so high such that the speed is decreased when going into fuel cut-off mode. In these cases some fuel has to be injected to overcome the engine friction. Then it can be beneficial to disengage the gear so that the powertrain friction is reduced and the speed can be increased or maintained with only idle fuel flow. Further, if the road profile ahead is known, using e.g. GPS or collected data, then further improvements can be done. Here dynamic programming is used to make the trade off between going into fuel cut off and disengaging the gear. In this paper, two strategies will be developed, simulated, and evaluated to explore the potential fuel savings.

2 Truck model

The truck is modeled with standard equations for a stiff driveline [5, 6] as summarized here. See Section 6 for notations.

The dynamics of the engine inertia is modeled as

$$J_e\dot{\omega}_e = T_e - T_t \tag{1}$$

where T_e is the engine torque, which includes negative values representing e.g. negative torque during fuel cut off or if present an exhaust brake. Transmission and final drive are modeled as stiff rotational components with constant efficiencies.

$$\omega_e = i_t i_f \omega_w \tag{2}$$

$$T_t i_t \eta_t i_f \eta_f = T_w \tag{3}$$

The wheels are modeled as rolling wheels with brakes

$$J_w\dot{\omega}_w = T_w - Fr_w - T_b \tag{4}$$

$$v = r_w\omega_w \tag{5}$$

The vehicle motion is described by

$$F = m\dot{v} + F_{air} + F_r + mg\sin(\alpha) \tag{6}$$

where the air and rolling resistance is

$$F_{air} = \frac{1}{2}c_d A\rho v^2 \tag{7}$$

$$F_r = mgc_r\cos(\alpha) \tag{8}$$

Negative values of α indicates a downhill slope and positive values indicates an uphill slope. If Equations (1)-(8) are combined the result is

$$c_1\dot{v} = c_2 T_e + c_3 T_b + c_4 v^2 + c_5 \cos(\alpha) + c_6 \sin(\alpha) \tag{9}$$

where c_i are lumped model parameters.

The control input to the engine is the injected amount of fuel per engine stroke δ. The resulting engine torque is mapped as a function of δ and engine speed ω_e.

$$T_e = T_e(\delta, \omega_e) \tag{10}$$

The fuel consumption is computed as

$$m_f(\delta(t), \omega_e(t)) = \int \delta(t) \frac{\omega_e(t)}{2\pi} \frac{n_{cyl}}{n_r} dt \tag{11}$$

3 Control strategies

Cruise controllers in heavy trucks normally allow the speed to increase some above the setpoint when driving downhill [8]. If the speed increases even though the engine does not deliver any torque, the brakes are not applied until a speed limit defined by the cruise controller is reached. The typical speed interval allowed is 5-10 km/h. In this work, the cruise controller is implemented as two PI-controllers, one controlling the fueling and one controlling the brakes.

Two strategies will be developed in the following: one instantaneous strategy in Section 3.1, and one strategy with look ahead in Sections 3.2-3.5.

3.1 Using instantaneous inclination, II-strategy

As mentioned above, there are possibilities to enhance the cruise controller to save fuel. For example a gyro, an accelerometer, or a GPS and 3D map can be used to obtain information about the inclination. This instantaneous inclination can be utilized, and the rationale behind the algorithm below is as follows: Consider driving downhill with the gear engaged in such a small slope that the engine has to deliver some torque for the vehicle to maintain speed. In such a slope it can be possible to disengage the gear, and thereby lowering the driveline friction sufficiently much, such that the speed can be maintained or even increased. The increase in kinetic energy that is stored in the vehicle leads to lower fueling some distance after the downhill slope and thereby the overall fuel consumption can be reduced. When the gear is disengaged the engine has to be run in idle mode to deliver power supply to auxiliary systems such as power steering, and hence consumes a certain amount of fuel. In downhills with inclination so high that the engine does not has to deliver any torque to maintain speed it is always beneficial to go into fuel cut-off mode.

Following this idea, the model presented in Section 2 is used to derive the inclination angles for when it is beneficial to disengage the gear. When the gear is disengaged it is seen from Equation (9), setting $T_e = 0$, $T_b = 0$, that for inclination angles

$$\tilde{\beta} \in \{\tilde{\beta} : c_4 v^2 + c_5 \cos(\tilde{\beta}) + c_6 \sin(\tilde{\beta}) \geq 0\} \tag{12}$$

the speed will be maintained or increased. The boundary for the set (12) (using equality in (12), then becomes

$$\beta = \arcsin\left(\frac{c_4 v^2}{\sqrt{c_5^2 + c_6^2}}\right) - \arctan\frac{c_5}{c_6} \tag{13}$$

On the other hand, if the inclination is too high it was earlier stated that fuel cut off was beneficial. The following model for the engine friction when it is being dragged

$$T_{ed} = d_1\omega_e + d_2 \tag{14}$$

with both $d_i < 0$, is used. Together with Equation (9) it is seen that for inclination angles

$$\tilde{\gamma} \in \{\tilde{\gamma} : c_2(d_1\omega_e + d_2) + c_4 v^2 + c_5\cos(\tilde{\gamma}) + c_6\sin(\tilde{\gamma}) \geq 0\} \tag{15}$$

the speed will be maintained or increased even when the gear is engaged. The boundary for the set (15) can be expressed as

$$\gamma = \arcsin\left(\frac{c_2(d_1\omega_e + d_2) + c_4 v^2}{\sqrt{c_5^2 + c_6^2}}\right) - \arctan\left(\frac{c_5}{c_6}\right) \tag{16}$$

3.2 Lookahead

As stated above it is possible to have knowledge about the upcoming road profile. This can be used to make a more intelligent choice, than the method described in Section 3.1, on when to disengage the gear. To use the extra information about the upcoming road profile and find the optimal control strategy a model predictive control scheme is used [1, 9].

3.3 Formulation of the optimization problem

Since the altitude information of the road profile is given as a function of position, the model (9) is reformulated with a change of variables from time to position according to

$$\frac{dv}{dt} = \frac{dv}{ds}\frac{ds}{dt} = v\frac{dv}{ds} \tag{17}$$

which introduced in (9) gives

$$c_1\frac{dv}{ds} = \frac{1}{v}(c_2 T_e + c_3 T_b + c_4 v^2 + c_5\cos(\alpha) + c_6\sin(\alpha)) \tag{18}$$

Using this model the choices of whether to disengage the gear or not can be represented by a transition graph as depicted in Figure 1. The sample distance Δ was chosen to the same as the distance between the samples of the altitude. The cost for a transition between state v_k to state v_{k+1} is computed as

$$g_k(v_k, (\delta_k, u_k)) = \begin{cases} m_f(\delta_k, \omega_e), & u_k = 1 \\ m_{f,idle} & u_k = 0 \end{cases} \tag{19}$$

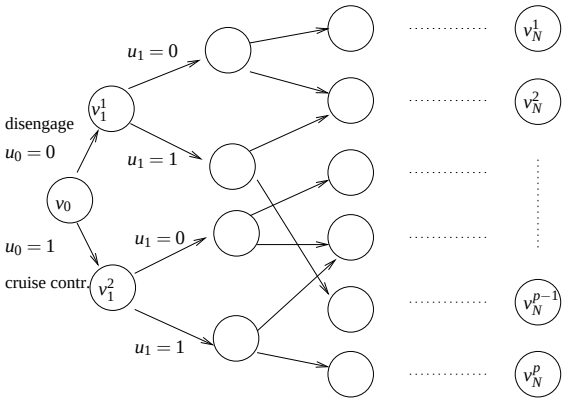

Figure 1: *An example of a dynamic programming transition graph for a prediction horizon of N samples. From each state there are two choices, either disengage the gear or use the cruise controller over the next sample interval. The cost for each transition is the amount of fuel that is needed to go between the corresponding states, i.e. change the speed from v_i^l to v_{i+1}^m on the length of one sample interval.*

where $u_k = 1$ denotes that the gear is engaged and $u_k = 0$ denotes that the gear is disengaged. Fueling δ_k and engine speed ω_e is computed from a simulation of the model using the standard cruise controller, and m_f is computed from Equation (11). The fuel consumption at idle is $m_{f,idle}$.

The following optimization problem is general, but since the aim is dynamic programming the notation from [2] is used. Let $\mu_k(v_k) = (\delta_k, u_k)$. Consider the class of all admissible control laws

$$\pi = \{\mu_0, \ldots, \mu_{N-1}\} \tag{20}$$

that maps states v_k into controls. Given an initial state v_0 and an admissible control law, the states v_k are defined by the equation

$$v_{k+1} = f_k(v_k, \mu_k(v_k)) \tag{21}$$

where $f_k(\cdot)$ is defined by a discrete approximation method of (18), e.g. Eulers method or a Runge-Kutta method, see [4]. If the cost for an end state is $g_N(v_N)$ the total cost for π starting at v_0 is

$$J_\pi(v_0) = g_N(v_N) + \sum_{k=0}^{N-1} g_k(v_k, \mu_k(v_k)) \tag{22}$$

The optimal control strategy to drive the distance corresponding to N samples is to find the way, π^*, through the transition graph with the lowest cost, which is given by

$$J_{\pi^*}(v_0) = \min_\pi J_\pi(v_0) \tag{23}$$

3.4 Design considerations

The design criterion (22) is defined by the fuel consumption (19), but the final cost $g_N(v_N)$ remains to be designed. Sometimes this may need consideration. If all end states are

assigned the same cost it is in most cases optimal to end up in the state with lowest velocity, because the fuel required to reach that state is lower than for all other states (of course except if braking is considered). However, if the end state is in a downhill slope, it can be beneficial for the total cost of the whole driving scenario if the end state for the current optimization has a higher velocity. The fuel consumption for reaching such an end state has to be compared to the velocity of that state in some way, and here the idea is that the final states are assigned a cost corresponding to a fuel equivalent of the higher kinetic energy they corresponds to. This comparison is made with an efficiency model of the truck.

3.5 Determining the reachable state space

Using dynamic programming to optimize (22) means backward calculation in a transition graph, and here this graph has the following characteristics. In the problem considered, there are natural bounds on the velocity. Too high speed can not be accepted for, e.g., safety or regulation reasons. The driver will probably not allow the speed to decrease below a certain limit. To find the upper limit for the speed the truck model is simulated with maximum fueling which results in a speed sequence $(v_{sf}^0, \ldots, v_{sf}^N)$. The upper limit is then taken as $\min(v_{sf}, v_{max})$, where v_{max} is the highest speed allowed. As lower limit $v_{min} = \min(v_c, v_{set})$ is chosen, where $(v_c^0, \ldots, v_c^N)$ is the speed sequence obtained with a standard cruise controller and v_{set} is a set-point speed chosen by the driver.

Even though the state space is restricted with an upper and lower bound one can have infinitely many states in between. Therefor an approximation is done such that if two states are very close to each other, $|v_1 - v_2| < \varepsilon$ for some small positive value ε, they are approximated to the same state. Following this procedure the problem grows linearly with prediction horizon, and the maximum number of states in each stage in the transition graph in Figure 1 is $(v_{max} - v_{min})/\varepsilon$.

4 Simulation results

To evaluate the control strategies described in Section 3 the truck model presented in Section 2 has been simulated with different road topologies. Both constructed test topologies as well as actual topologies from the highway E4 outside Linköping, Sweden have been used, see Figures 2- 7. The constructed road topologies have been chosen such that they should show interesting properties of, and differences between, the two proposed control strategies and an ordinary cruise controller.

The standard cruise controller and the controller using instantaneous inclination, II-strategy, were sampled with 10 Hz. The look ahead controller was sampled each 25 meters, and the prediction horizon was 10 samples corresponding to 250 meters.

The gap between β and γ defined by Equations (13) and (16) is narrow, typically in the order of 0.1 degree for trucks weighing around 20-60 tons and speeds around 85 km/h. In Figure 2 the inclination is between β and γ. The II-strategy disengages the gear in the downhill which can be seen in the second subplot from above, where 0 means disengaged gear. There is thus two periods around position $s = 600$ and $s = 800$ where this happens. Thereby the speed increases, as can be seen in the lowest subplot as the

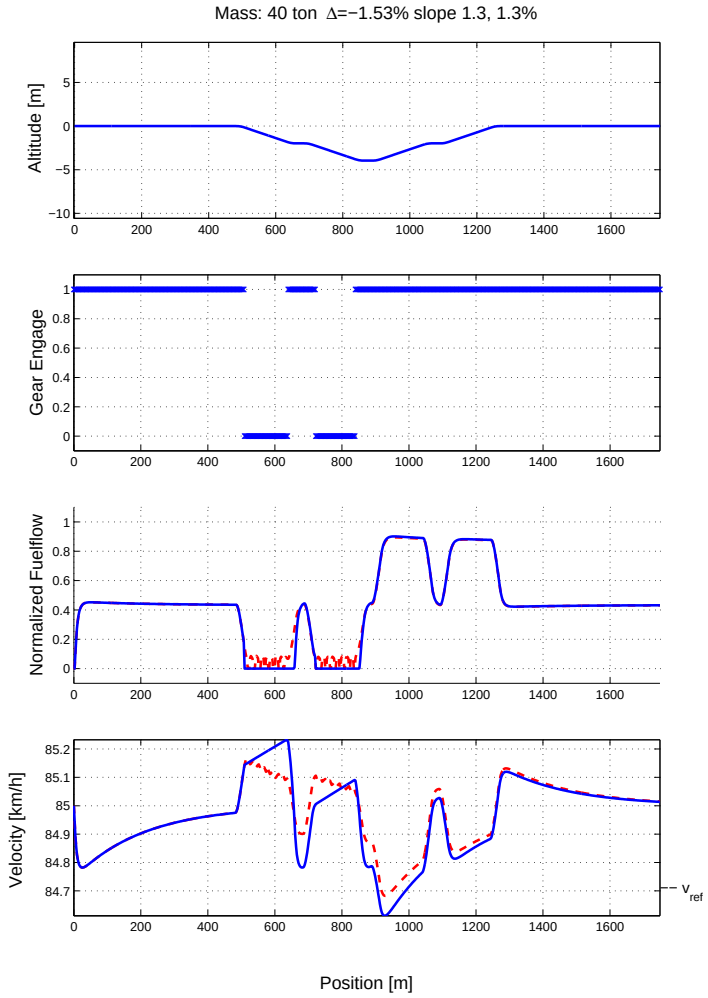

Figure 2: *Simulations of a 40 ton truck. The dashed line represents a standard cruise controller and the solid line the II-strategy. The inclination in the slopes is* $\mp 1.3\%$ *and the fuel saving is 1.53%.*

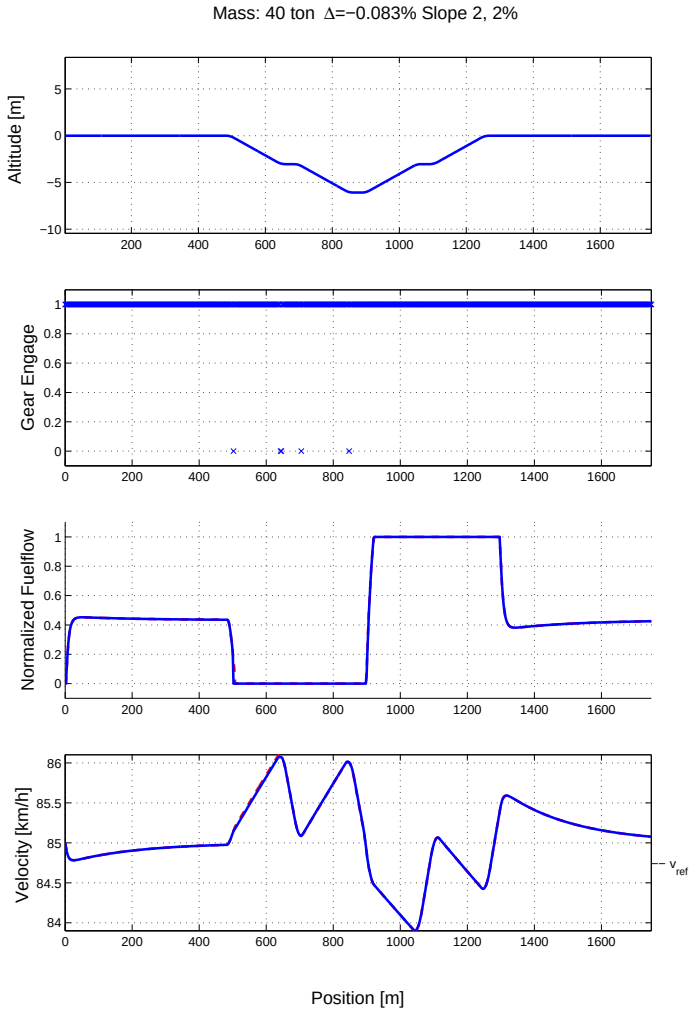

Figure 3: *Simulations of a 40 ton truck. The dashed line represents a standard cruise controller and the solid line the II-strategy. The inclination in the slopes is* $\mp 2\%$ *and the fuel saving is 0.083%.*

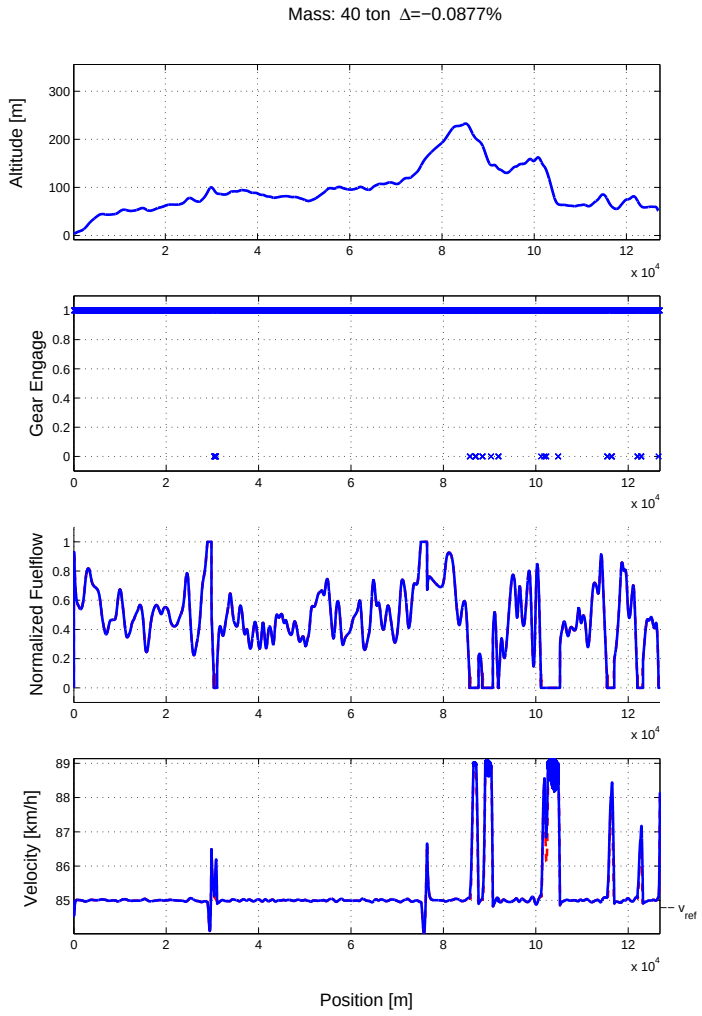

Figure 4: *Simulations of a 40 ton truck. The dashed line represents a standard cruise controller and the solid line the II-strategy. The road data comes from the highway E4 outside Linköping and the fuel saving is 0.088%.*

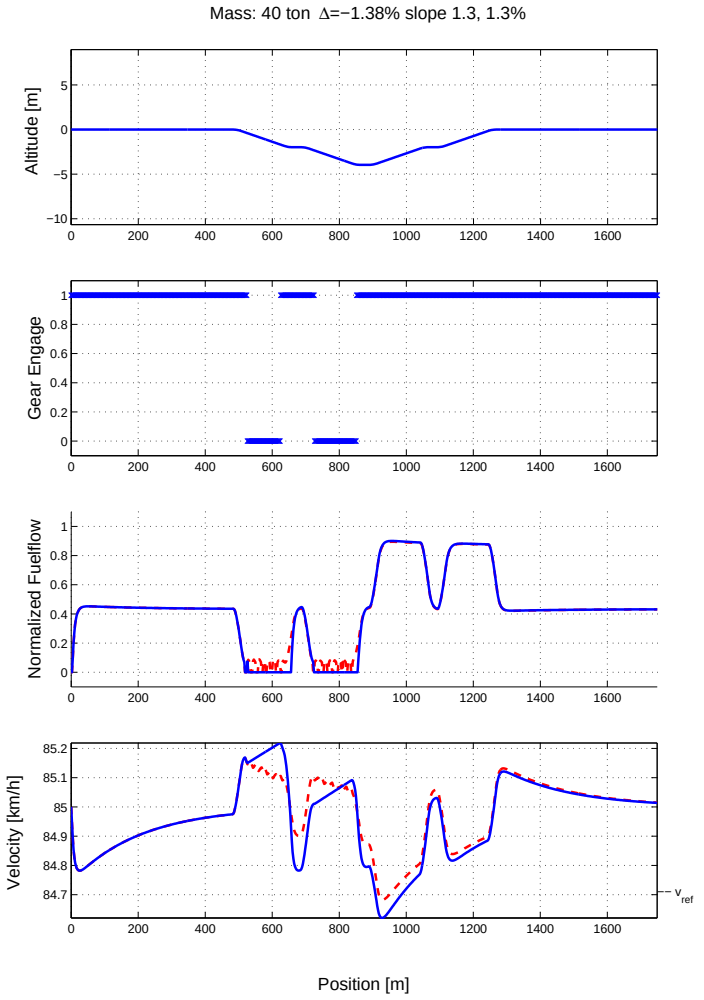

Figure 5: *Simulations of a 40 ton truck. The dashed line represents a standard cruise controller and the solid line the look ahead strategy. The inclination in the slopes is* $\mp 1.3\%$ *and the fuel saving is 1.38%.*

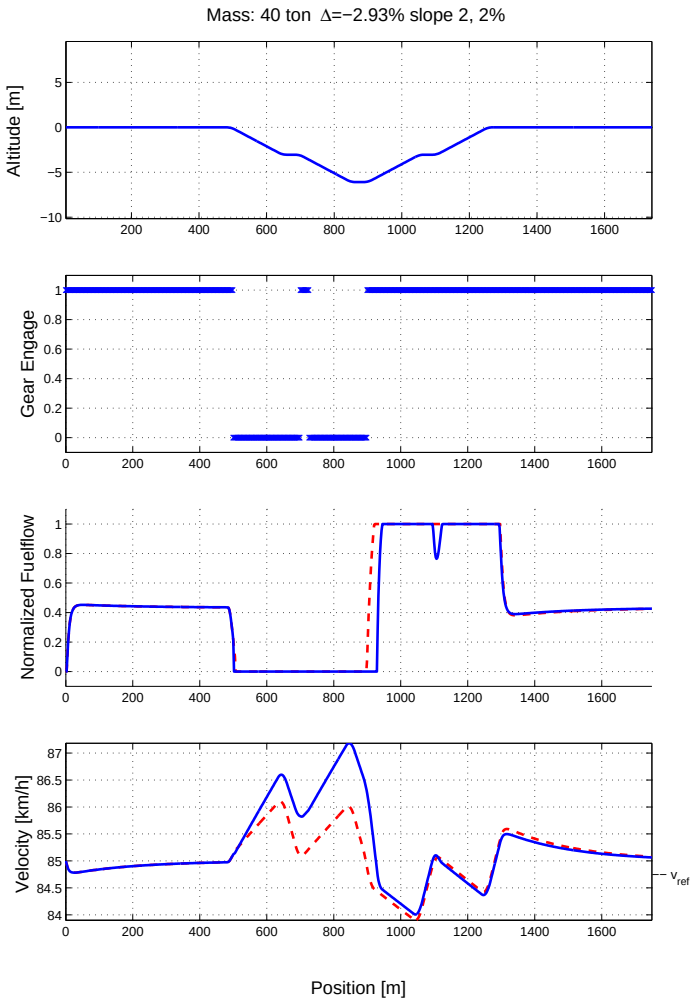

Figure 6: *Simulations of a 40 ton truck. The dashed line represents a standard cruise controller and the solid line the look ahead strategy. The inclination in the slopes is* $\mp 2\%$ *and the fuel saving is 2.93%.*

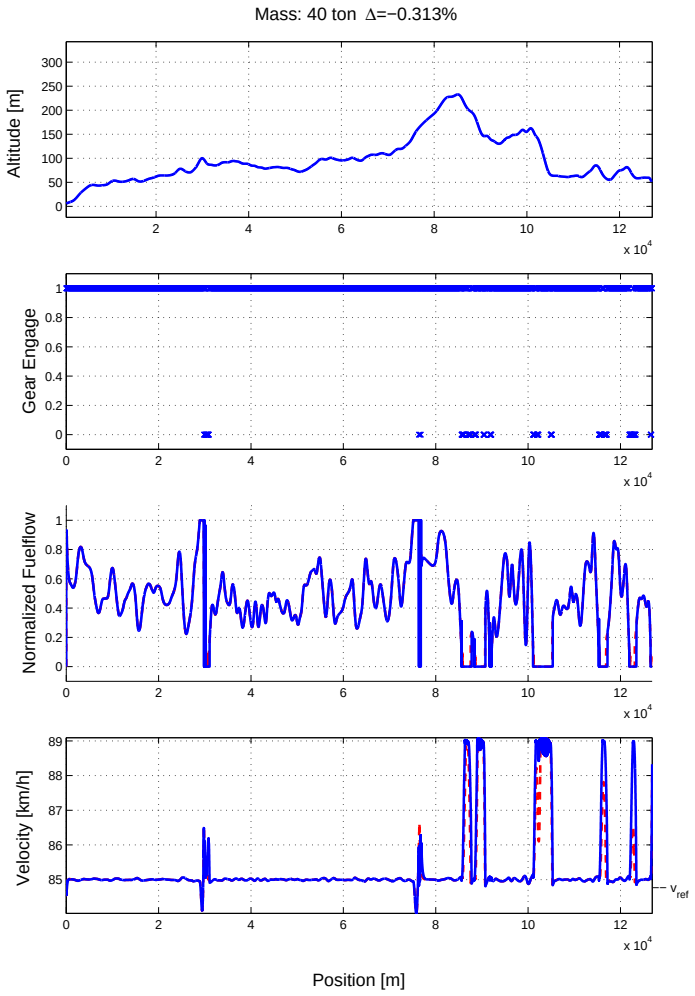

Figure 7: *Simulations of a 40 ton truck. The dashed line represents a standard cruise controller and the solid line the look ahead strategy. The road data comes from the highway E4 outside Linköping and the fuel saving is 0.31%.*

solid line. The behavior of the standard cruise controller is seen in the same subplot as dashed line. It does not disengage so the speed is in these periods (around $s = 600$ and $s = 800$) decreasing instead of increasing as for the II-strategy. In subplot 3 from above the fuel savings, about 1.5 %, for the II-strategy, is seen as the difference between the curves in the same period ($s = 600$, $s = 800$).

In Figure 3 the inclination is outside the operating range of the II-strategy and it gives the same result as the standard cruise controller. If the plot of gear engagement and disengagement is studied closely it is seen that the II-strategy does in fact disengage the gear at 4 positions even though the inclination is outside the range $[\beta, \gamma]$. This is because the algorithm calculates the instantaneous inclination as an interpolation between two consecutive samples. In Figure 4 the II-strategy is illustrated on a real road profile, and subplot 2 shows that the gear is seldom disengaged. Only in the last third of the driving scenario there are downhill slopes where the strategy can be used and the total reduction of fuel consumption is small. In Figure 5 it is seen, for this road profile, that the look ahead strategy works almost as the II-strategy in Figure 2. It would however be expected that the look ahead strategy should give a lower or at least equal fuel consumption as the II-strategy, and the reason for not being so is that the look ahead strategy only changes its control signal each 25 m. Driving in 85 km/h this is roughly 0.1 times the sampling frequency of the II-strategy. On the other hand, for the test profile in Figure 6 it is seen that the look ahead strategy disengages the gear not only in the downhill slopes but also in the flat sections between and after the downhill. Compared to the standard cruise controller the kinetic energy is increased in the downhill. Because of this the look ahead strategy can start to inject fuel later after the downhill, (subplot 2 around position $s = 900$ m), and still keeps the same speed as the standard cruise controller. The reduction of fuel consumption is almost 3 %. In Figure 7 it is seen that the look ahead strategy disengages the gear in the downhills of the third part of the driving scenario. Compared to the II-strategy in Figure 4, for the same real road profile, the gear is, in the look ahead case, disengaged during approximately three times as long. The reduction of fuel consumption is higher than for the II-strategy, but is still modest over the total distance.

5 Conclusions

Simulations shows that fuel consumption can be decreased with up to approximately 3% for some driving scenarios by disengaging the gear when driving downhill, and thereby increasing the vehicle's kinetic energy. This increase leads to lower fueling directly after the downhill. As mentioned in Section 3.5 the size of the optimization problem is linear in prediction horizon, and the case presented can easily be run well under real time.

If the vehicle is equipped with an automated manual transmission, see e.g. [7], or an automatic clutch, no extra hardware in the powertrain is needed to implement the control strategies presented. Since only the control software has to be changed the implementation cost is expected to be reasonably low.

Acknowledgments

The Swedish Energy Agency and the Swedish Foundation for Strategic Research are gratefully acknowledged for their funding. This project started with an initial study in an undergraduate course, and this work is a continuation of those efforts. The students are gratefully acknowledged for their work with the simulation environment.

6 Nomenclature

A	Vehicle cross sectional area
c_d	Air drag coefficient
c_i	Lumped vehicle model parameters
c_r	Rolling resistance coefficient
d_i	Engine drag torque parameters
F	Vehicle Forces
g	Gravitational acceleration
i	Gear ratio
J	Inertia
m	Vehicle mass
m_f	Fuel mass
n_{cyl}	Number of cylinders
n_r	Revolutions per engine cycle
q_{hv}	Fuel heating value
r_w	Wheel radius
T	Torque
v	Vehicle speed
α	Inclination
η	Efficiencies
Δ	Sample distance
δ	Injected amount of fuel per engine stroke
ρ	Air density
ω	Rotational speed

Bibliography

[1] M. Back, S. Terwen, and V Krebs. Predictive powertrain control for hybrid electric vehicles. *First IFAC Symposium on Advances in Automotive Control*, 2004.

[2] Dimitri P. Bertsekas. *Dynamic Programming and Optimal Control.* Athena Scientific, 2000.

[3] A. Fröberg, L. Nielsen, L-G. Hedström, and M. Pettersson. Controlling gear engagement and disengagement on heavy trucks for minimization of fuel consumption. *IFAC World Congress. Prague, Czech Republic*, 2005.

[4] E. Hairer, S.P. Nørsett, and G. Wanner. *Solving Ordinary Differential Equations 1.* Springer, 2000.

[5] U. Kiencke and L. Nielsen. *Automotive Control Systems, 2nd ed.* Springer-Verlag, 2005.

[6] Hans B. Pacejka. *Tire and Vehicle Dynamics.* SAE, 2002.

[7] Magnus Pettersson and Lars Nielsen. Gear shifting by engine control. *IEEE Transactions Control Systems Technology*, Volume 8(No. 3):pp. 495–507, May 2000.

[8] Tony Sandberg. *Heavy Truck Modeling for Fuel Consumption Simulations and Measurments.* Licentiate thesis, LiU-TEK-LIC-2001:61, Linköping Institute of Technology, Linköping, 2001.

[9] S. Terwen, M. Back, and V Krebs. Predictive powertrain control for heavy duty trucks. *First IFAC Symposium on Advances in Automotive Control*, 2004.

Paper D

A REAL-TIME FUEL-OPTIMAL CRUISE CONTROLLER FOR HEAVY TRUCKS USING ROAD TOPOGRAPHY INFORMATION[1]

Erik Hellström[⋆], Anders Fröberg[⋆], Lars Nielsen[⋆]

[⋆] *Dep. of Electrical Engineering, Linköpings universitet,*
SE-*581 83 Linköping, Sweden.* {hellstrom,froberg,lars}@isy.liu.se.

Abstract

New and exciting possibilities in vehicle control are revealed by the consideration of topography, for example through the combination of GPS and three dimensional road maps. How information about future road slopes can be utilized in a heavy truck is explored. The aim is set at reducing the fuel consumption over a route without increasing the total travel time.

A model predictive control (MPC) scheme is used to control the longitudinal behavior of the vehicle, which entails determining accelerator and brake levels and also which gear to engage. The optimization is accomplished through discrete dynamic programming. A cost function that weighs fuel use, negative deviations from the reference velocity, velocity changes, gear shifts and brake use is used to define the optimization criterion.

Computer simulations back and forth on 127 km of a typical highway route in Sweden, show that the fuel consumption in a heavy truck can be reduced with 2.5% with a negligible change in travel time.

[1]This is an edited version of [4], A real-time fuel-optimal cruise controller for heavy trucks using road topography information, published in the preprints of the SAE World Congress 2006.

1 Introduction

Fuel cost is a major part of the life cycle cost of a truck. Reducing fuel consumption is therefore attractive to the the owner as well as a gain for the environment.

In [3] the use of neutral gear and look ahead information for fuel savings were explored. The present paper is a continuation where the derived controller also determines fueling, braking and gear shifts. The paper [7] also describes such a predictive algorithm which uses topography information. Compared to that, here conclusions are also drawn regarding optimal length of the prediction horizon and the potential fuel savings of using the neutral gear.

When reporting effects on the fuel consumption from new controller strategies it is important to study the effects on travel time. To get a fair assessment of controller performance, it is preferable with controller configurations and road sections where the relative difference in travel time compared to the reference model is negative or close to zero. This paper presents some results from short illustrative test profiles with the aim of showing controller behavior in detail. To assess fuel saving potential, longer and authentic road measurements are used.

The main objectives of the present paper are therefore to devise a control criterion for a sufficiently complex truck model and drive mission on a realistic road profile, and further, to study the interplay between model, criterion, and dynamic programming with its tuning parameters, and to interpret the resulting optimal strategies obtained in the simulations. Some of the observations are under simplifying assumptions given analytic interpretations in [2]. The presentation is organized so that the following two sections describe the truck model and the dynamic programming algorithm which is used for optimization in an MPC controller. In the final sections simulation results are presented and conclusions are drawn.

2 Truck model

In the following section, a model for the longitudinal dynamics of a truck is formulated. The foundation for this model is found in [6].

The engine torque T_e is modeled as

$$T_e = f_e(\omega_e, \delta) \tag{1}$$

where ω_e is engine speed [rpm] and δ is the fueling [mg/stroke]. The function f_e is approximated with polynomial functions which are fitted to data from steady state measurements.

The engine transmits a torque T_c to the clutch through

$$J_e\dot{\omega}_e = T_e - T_c \tag{2}$$

where J_e is the engine inertia. The inertia of the transmission and final drive is neglected. The resulting conversion ratio is i and energy losses are modeled with an efficiency η.

Force	Explanation	Expression
$F_a(v)$	Air drag	$\frac{1}{2}c_w A_a \rho_a v^2$
$F_r(\alpha)$	Rolling resistance	$mgc_r \cos\alpha$
$F_g(\alpha)$	Gravitational force	$mg\sin\alpha$

Table 1: *Longitudinal forces. α is the road slope [rad] and c_r is the rolling resistance coefficient [-]*

The clutch, propeller shafts and drive shafts are further assumed stiff. This gives

$$\begin{aligned} \omega_e &= i\omega_w \\ T_c &= \frac{1}{i\eta}T_w \\ J_w\dot{\omega}_w &= T_w - T_b - r_w F_w \end{aligned} \tag{3}$$

where T_w is the torque transmitted to the wheel, J_w is the wheel inertia, T_b is the braking torque and r_w is the wheel radius. F_w is the resulting friction force at the wheel.

The motion of the truck is governed by

$$m\dot{v} = F_w - F_a - F_r - F_g \tag{4}$$

The longitudinal forces are explained in Table 1. Assuming no slip, the vehicle velocity v is

$$v = r_w\omega_w$$

Equation (2) to (4) can then be combined to yield

$$\dot{v} = \frac{r_w}{J_w + mr_w^2 + \eta i^2 J_e}\Big(i\eta T_e(v,\delta) - T_b - r_w\left(F_a(v) + F_r(\alpha) + F_g(\alpha)\right)\Big) \tag{5}$$

The mass flow of fuel $\dot{m}_f$ [g/s] is determined by the fueling δ [mg/stroke] and the engine speed. Assuming zero slip the velocity is $v = \frac{r}{i}\omega_e$. The mass flow in [g/s] is then

$$\begin{aligned} \dot{m}_f(v,\delta) &= c_f v\delta \\ \text{where } c_f(i) &= \frac{1}{2\pi\cdot 10^3}\frac{n_{cyl}}{n_r}\frac{i}{r} \end{aligned} \tag{6}$$

where n_{cyl} is the number of cylinders and n_r is the number of crankshaft revolutions per stroke.

3 Look ahead control

An MPC controller has been developed to control the vehicle. This section describes the shortest path Dynamic Programming (DP) algorithm which is used for the optimization in an MPC scheme [5]. The control objectives are first identified and based on these, the cost function is chosen. The problem is then presented in a form suitable for implementation. Lastly, the DP algorithm is described and the algorithm complexity is discussed.

3.1 Objective

The main objective is to keep the vehicle in an allowed range of velocities with a minimum use of fuel. Denote the reference velocity v_{ref} [km/h]. The vehicle velocity is allowed to decrease with v_{dec} and increase with v_{inc} from v_{ref}. The brake system is assumed to be effective enough for the road ahead and thus the upper bound $(v_{ref}+v_{inc})$ never needs to be violated. It is however not sure that a heavy truck can keep the lower bound $(v_{ref}-v_{dec})$ on all road profiles. This bound is therefore lowered if the maximum torque possible which the vehicle can produce is not enough to keep the bound. It is assumed though, that it is possible to keep a velocity greater than zero at all time. Denote the velocity achieved when applying maximum torque v_{Tlim}. The constraint on the vehicle speed v can then be expressed as

$$0 < \min\left\{v_{ref}-v_{dec}, v_{Tlim}\right\} \leq v \leq v_{ref}+v_{inc} \tag{7}$$

3.2 Cost function

The cost function is

$$J = \zeta_N + \sum_{k=0}^{N-1} \zeta_k \tag{8}$$

where k is the stage number. The weighting functions ζ is, with basis of the objectives, chosen as

$$\begin{aligned} \zeta_k &= Q \begin{bmatrix} m_{f,k} \\ \kappa(e_k){e_k}^2 \\ |v_k - v_{k+1}| \\ \kappa(|g_k - g_{k+1}|) \\ T_b \end{bmatrix} \quad k = 0,1,\ldots,N-1 \\ \zeta_N &= 0 \end{aligned} \tag{9}$$

where $e_k = v_{ref} - v_k$, Q is a vector with five scalar penalty factors, $Q_i,\ i = 1,2,3,4,5$, and κ is a step function

$$\kappa(t) = \begin{cases} 1 & , \quad t > 0 \\ 0 & , \quad t \leq 0 \end{cases} \tag{10}$$

The required fuel mass $m_{f,k}$ for a state transition is weighed with Q_1. In order to limit the state space, the state vector will not be expanded to include any cumulative information of the state history. This leads to that it is not possible to penalize the mean velocity (with a terminal constraint on such a state). Therefore, the factor Q_2 is included which adds a cost on velocities below the reference speed. A smoother control is received through Q_3 which penalizes velocity changes. Gear shifts are penalized with Q_4. A cost is finally added that is proportional, with the constant Q_5, to the braking torque T_b. Intuitively one may perhaps conclude that because of the fact that braking converts kinetic energy into heat, it is a waste and hence it can not be fuel optimal. However, because of the factor Q_2 it can for example be advantageous to penalize braking to favor a solution where the speed is lowered at one point to lessen brake usage at a later point. One example of this can be seen in the next section, in Figure 4. The terminal cost ζ_N

is set to zero. One obvious possibility is to penalize the velocity in the end stage with ζ_N. The state velocities will however be limited, as described later in this section, to only contain desired velocities.

3.3 Problem presentation

The vehicle is modeled by (5) and the fuel consumption according to (6). This gives a state description with vehicle velocity as the only state and the slope α as a measurable disturbance. The vehicle velocity and the fuel flow are viewed as the output signals. Let a signal g denote a gear number that maps to a conversion ratio i and an efficiency η. The control signals are then the fueling δ, the gear number g and the brake torque T_b.

$$\begin{aligned}\dot{v} &= f_v(v,\delta,T_b,g,\alpha) = \frac{r_w}{J_w + m r_w^2 + \eta i^2 J_e}\Big(i\eta T_e(v,\delta) - T_b - r_w\left(F_a(v) + F_r(\alpha) + F_g(\alpha)\right)\Big)\\ y_1 &= v\\ y_2 &= f_f(v,\delta,g) = c_f(g)v\delta\end{aligned} \tag{11}$$

The road slope is position dependent rather than time dependent, as is the vehicle model. This is handled by transforming the latter to a position dependent model by the following simple rewrite.

$$\frac{dv}{dt} = \frac{dv}{ds}\frac{ds}{dt} = \frac{dv}{ds}v \Rightarrow \frac{dv}{ds} = \frac{1}{v}\frac{dv}{dt},\ v \neq 0 \tag{12}$$

It is assumed that it is possible to keep a velocity v greater than zero at all time.

3.4 Problem reformulation

The system defined by Equation (11) is deterministic because all unknown disturbances are neglected.

If the state space is discretized, it becomes finite due the velocity constraints in (7). The evolution of this system under the influence of different control signals can then be represented in a directed graph. An arc represents a transition between states in successive stages and is associated with a cost for this transition. The cost of an arc can be viewed as the length of that arc. Through this, the problem is a shortest path problem in a graph [1].

The optimization problem at hand is to be solved numerically by means of dynamic programming (DP). A discrete model is therefore needed. The stage grid in DP is noted S [m]. Denote

$$\begin{aligned}v_k &= v(kS)\\ m_{f,k} &= m_f(kS)\end{aligned}$$

It is assumed that the inputs and the disturbance is constant during S, that is

$$\begin{aligned}u(s) &\equiv u_k\\ \alpha(s) &\equiv \alpha_k\end{aligned} \quad \forall s \in [kS,(k+1)S[\tag{13}$$

Euler's method with step length h and the velocity assumption then gives

$$v_{k+1} = v_k + \frac{h}{v_k} f_v \tag{14}$$

To determine the fuel mass consumed the output signal y_2 is integrated. Applying Euler's method again with the step length h yields

$$m_{f,k+1} = m_{f,k} + \frac{h}{v_k} f_f \tag{15}$$

3.5 Reducing the search space

The aim is a real-time algorithm, and therefore the search space which is considered by the algorithm should be small enough to enable fast calculation of the optimal trajectory and at the same time accurate enough to receive satisfactory solutions. In order to reduce the search space, states that do not meet the constraints or can not be reached because of various physical limitations in the system, are removed. To balance grid size and accuracy, the state and control spaces are not straightforwardly discretized. Instead, the state space is discretized and the control signals that transforms the system to these states are calculated by an inverse simulation of the system equations. This avoids discretizing the control signals which will lead to inevitable rounding errors in the state-space grid. The search-space reductions are described in more detail in the remainder of this section.

Frequent gear shifting is not desirable and therefore shifts are penalized in the cost function (9). In order to make this possible, the state vector is expanded with the gear that brought the system to the current state. With this information in a state, the search space can easily be reduced by introducing a limit on the maximum possible gear shifting frequency. The only need is a counter, for the number of stages passed since the last shift, in the state information.

The search space is a grid consisting of the states which are considered by the DP algorithm. The distance between two adjacent stages is S [m]. A grid point is made up of a velocity value, the gear number that brought the system to this state and the number of stages for which this gear has been engaged. The velocity is further equidistantly spaced with τ [km/h], see Figure 1. The control signals fueling and brake torque are not discretized. They are instead calculated by an inverse simulation of Equation (5).

With a given velocity, only a subset of the gears in the gear-box is applicable. With bounds on the engine speed $[N_{min}, N_{max}]$ it is possible to select a set of a usable gears in a state. Only gears with a ratio which give a engine speed in the allowed range are then considered. In a state with the velocity v, the set of usable gears G_v is then defined as

$$G_v = \{g \,|\, N_{min} \leq N(v,g) \leq N_{max}\} \cup \{0\} \tag{16}$$

where $N(v,g)$ is the engine speed at vehicle velocity v and gear number g with parameters $\{i, \eta\}$. The neutral gear is modeled as gear number zero with a ratio which equals zero.

In order to determine which velocities to consider, the reachable velocities from the initial state along the horizon is calculated with consideration of the allowed range. This is achieved by simulating Equation (5). This gives an interval of velocities for each stage. The lower bound in the last stage is then increased to the reference velocity v_{ref}, or set equal to the higher bound if it goes below v_{ref}. With this restriction it is possible to go through the interval backwards from the last stage and remove states from where it is not possible to reach one of the allowed velocities in the last stage. An example is shown in Figure 1. The light gray area is the part of the state space that will be considered. The

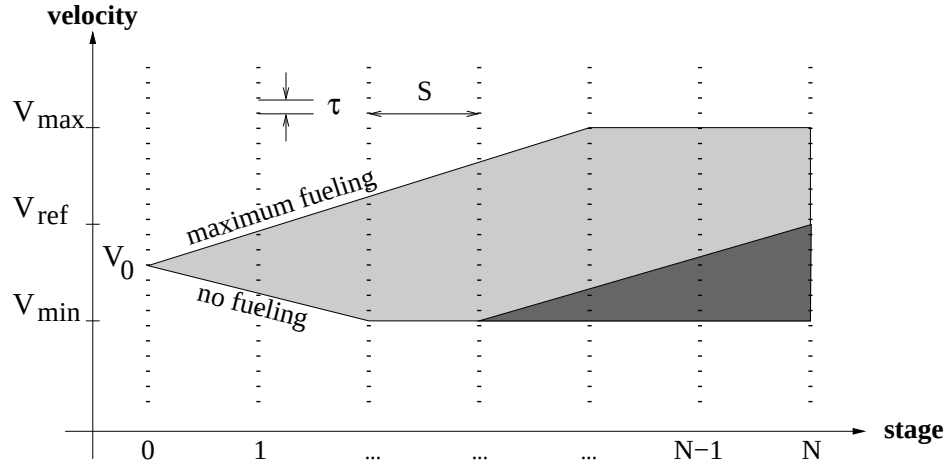

Figure 1: *The velocity state space*

darker area is the velocities that are removed when going backwards from the last stage. There is now, for each stage, a set of velocities which are to be considered, $\left[v_{low}, v_{high}\right]$. This is a subset of the reachable velocities. The set in stage k is discretized in constant steps of τ. This makes up a set V_k

$$V_k = \left\{v_{low}, v_{low}+\tau, v_{low}+2\tau, \ldots, v_{high}\right\} \tag{17}$$

3.6 DP algorithm

A state i is made up of a velocity v^i, a gear number g^i and the counter c^i. The possible states i in stage k is a set S_k and will be generated from the velocity range V_k and the set of gears G_v,

$$S_k = \left\{\{v,g,c\} \,|\, v \in V_k, g \in G_v, c \in \mathbf{Z}^+\right\} \tag{18}$$

The counters in the states of the last stage, c^j, $j \in S_N$, are set to k_{lim}. The other counters will be set in the DP algorithm. For each state in stage k, feasible control actions are sought (by an inverse simulation of the system equations) which transforms the system into the states in stage $k+1$. The feasible control action with the lowest cost is the optimal control from the current state.

The transition cost at step k from state $i \in S_k$ to state $j \in S_{k+1}$ is

$$\zeta_k^{i,j} = \zeta_k(v^i, v^j, u_k^{i,j}, \alpha_k)$$

where the control $u_k^{i,j}$ causes the transition from state i to j with a road slope of α_k.

If there is no control that transforms the system from state i to j at stage k, the cost is set to infinity [2]. The algorithm is summarily stated below.

1. Let $J_N(i) = \zeta_N = 0$.

[2] With a numerical approach, an infinite cost means a very large number.

2. Let $k = N-1$.

3. Let
$$J_k(i) = \min_{j \in S_{k+1}} \left\{ \zeta_k^{i,j} + J_{k+1}(j) \right\}, \; i \in S_k.$$
A control action $u_k^{i,j}$ that transforms the system from a state $i \in S_k$ to a state $j \in S_{k+1}$ is only allowed if $g^i = g^j$ or $c^j > k_{lim}$. The counter of state i, c^i is set to $c^j + 1$ if $g^i = g^j$ and 1 otherwise.

4. Repeat step 3 for $k = N-2, N-3, \ldots, 0$

5. The optimal cost is J_0 and the sought control is the optimal control set from the initial state.

In the simulations, the DP algorithm is used for optimization in an MPC scheme. The algorithm is issued once every S m. If the vehicle position is s, the algorithm calculates the control signals to apply when $s \in [s+S, s+2S[$. The state at $s+S$ is predicted and used as the initial state in the first stage in the algorithm. The available time for computation is thus the travel time between position s and $s+S$. Due to the fact that the algorithm is restarted every S m, there is no need to store any information about the subsequent stages when the optimal costs has been computed for all states in one stage.

3.7 Complexity

At step k in the DP algorithm, every combination of states in stage k and $k+1$ will be processed. If n_i denotes the number of states in stage i, the number of operations in this step will thus be proportional $n_k n_{k+1}$. At the next step, all combinations between states in stage $k+1$ and $k+2$ will be processed. The number of operations in this step is proportional to $n_{k+1} n_{k+2}$. Repeating this for the horizon of N steps, the total number of operations is approximately proportional to $N n_m^2$, if n_m is the maximum number of states in any stage $n_m = \max_{i=1..N} \{n_i\}$.

4 Simulations

A reference truck-model is implemented in Matlab/Simulink. As in the design of the controller, the basic Equation is (5) but measured data maps are used instead of using polynomial functions that are fitted to data. A PI cruise controller and gear switching logic are implemented to imitate driver behavior. The ability of this model to accurately predict the fuel consumption in a real truck has been shown in [9]. To assess the performance, the relative difference in the fuel consumption $\Delta fuel$ and the travel time $\Delta time$ are used. The algorithm parameters used are stated in Table 2 and the penalty factors are shown in Table 3. These factors have been adjusted in order to receive an acceptable behavior on the short test profiles and a negligible effect on the travel time when simulating longer distances with authentic road measurements. The results and the values of the penalty factors naturally depends on the vehicle parameters used. The most important parameter is the mass of the vehicle. The vehicle mass has been chosen to 40 metric tons and the reference velocity is constant 85km/h in all simulations. The gear-box is made up of twelve gears,

Parameter	Function	Value
S	Stage grid	25 m
N	Number of steps	40
$S \cdot N$	Horizon	1000 m
h	Step length	25 m
τ	Velocity discretization	0.1 km/h
v_{inc}	Max. inc. above ref.	5 km/h
v_{dec}	Min. dec. below ref.	5 km/h
k_{lim}	Min. steps before a shift	8
N_{min}	Lower engine bound	1000 rpm
N_{max}	Upper engine bound	2000 rpm

Table 2: *User parameters*

Factor	Penalizes	Value
Q_1	Fuel use	2
Q_2	Neg. dev. from ref. speed	5
Q_3	Velocity changes	15
Q_4	Gear shifts	15
Q_5	The use of brakes	0.005

Table 3: *Penalty factors*

Gear	Ratio	Gear	Ratio
No. 10	1.55	No. 12	1.00
No. 11	1.23	Final drive	3.27

Table 4: *The gear-box*

and the conversion ratio i in (3) is the product of a final drive ratio and a gear ratio. Data for the final drive and the three gears used here are given in Table 4. Disturbances from other vehicles are disregarded.

4.1 Constant slope

In Figure 2 an example incline is shown. With the acceleration before the hill(300-500m) it is possible to keep a higher velocity throughout the incline and the time required on a lower gear(700-1050m) is reduced, compared to the reference controller (700-1300m). The integral part of the PI controller is saturated after the hill which is causing the difference between 1300 and 1500m.

Examples of declines are seen in Figures 3 and 4. In the short downhill, Figure 3, neutral gear is used for about 700m(at 300-1000m). The gain in form of kinetic energy is evidently greater than the cost of the fuel used to run the engine on idle. When the engine is dragged, the fuel supply can in general be cut off. If the neutral gear was to be used in the 500m downhill, Figure 4, the maximum velocity would be reached earlier and increase the need for braking. The truck is in this case instead let to slow down before the steep decline. In both examples the brake use is lowered compared to the PI-controller. The mentioned saturation effect is evident at about 1250m in both Figure 3 and 4.

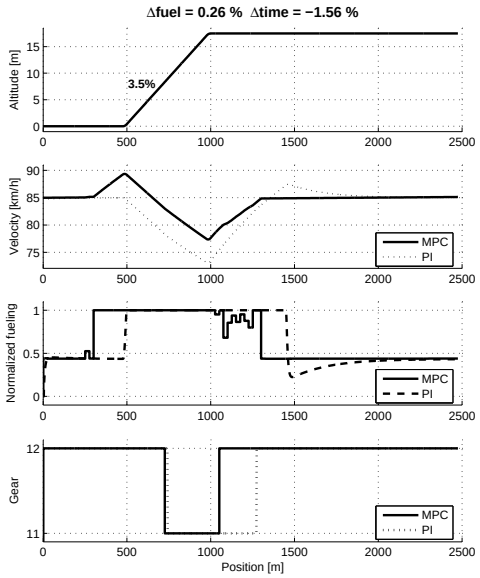

Figure 2: *A 500m incline with slope of 3.5%. The MPC controller accelerates the vehicle before the incline. No braking occurs.*

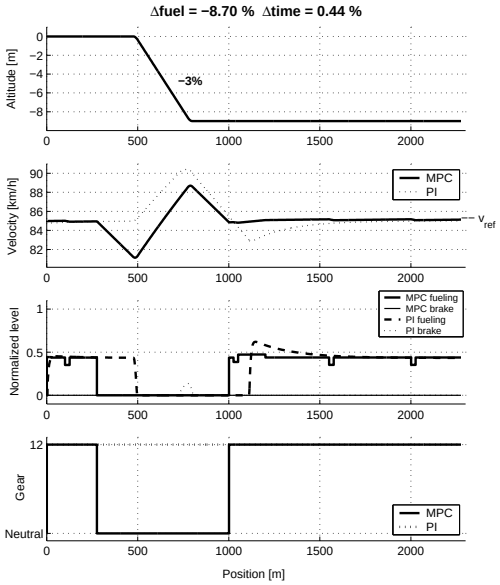

Figure 3: *A 300m decline with slope of -3%. Fuel and brake use is lowered by the MPC controller by letting the vehicle slow down before the decline.*

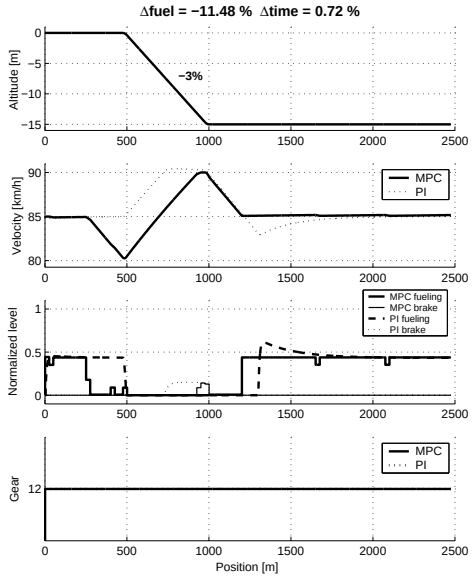

Figure 4: *A 500m decline with slope of -3%. Fuel and brake use is lowered by the MPC controller by letting the vehicle slow down before the decline.*

4.2 Hills and depressions

In Figure 5 neutral gear is used in the beginning to the bottom of the depression (500-1200m). The lessened resistance torque allows the vehicle to accelerate faster than if a gear was engaged and the engine was dragged. Owing to this acceleration, the MPC controller can increase the fueling after the PI controller (at 1150m instead of at 950m) and still keep about the same velocity later through the hill. This delay evidently saves more fuel than was used to run the engine on idle resulting in a fuel use reduction of about 2% without increasing the travel time.

A steeper depression is shown in Figure 6. In the MPC case, there is no need for braking in the downhill because the truck is let to slow down before the downhill (300-500m). In the end of the downhill part, the MPC controller increases the fueling (at 1100m) despite the fact that the velocity is well above the reference. This is due to the controllers knowledge about the steep uphill in front of the truck. This pre-acceleration makes the need for a down-shift of gear unnecessary and keeps a higher velocity through the hill. In total, both fuel(-6.97%) and time(-0.76%) can be saved.

In the hill, Figure 7, the controller accelerates the vehicle before the uphill begins (300-500m). This leads to a higher velocity from the foot to the top of the hill. Before the top is reached, the accelerator level is decreased despite that the velocity is much below the reference (at 900m). The coming downhill will accelerate the vehicle above the reference anyway and the lower velocity on the top of the hill will reduce the need for braking. The lower gear is kept throughout the hill to further reduce the need of braking. The vehicle is finally let to slow down to the reference velocity on the neutral gear (2000-2250m). Neutral gear makes the retardation slightly slower. The travel time is increased with half a percent on the section and the fuel consumption is reduced with 7.85%.

4.3 Authentic roads

In order to estimate fuel saving potential, authentic altitude measurements are used to calculate slope values. The altitude is measured once each 25m on the highway between the two cities of Linköping and Jönköping in Sweden. A portion of the road is selected [3]. Simulations are made with this section in both directions. The results are shown in Figures 8 and 9. The effects discovered in the illustrative test profiles are also found in these simulations with authentic sections.

In Figure 8, acceleration prior to a steep incline is seen at 3km. Retardation prior to a decline is seen at 2, 4 and 5km. A lower gear is used to reduce the load on the brake systems between about 6 and 8km. Brake use is however mostly lowered by the retardation before the decline. The truck is let to slow down to the reference velocity on neutral gear after a steep decline at about 8km.

In Figure 9, acceleration prior to a steep incline is seen at 1,4 and 6km. Retardation prior to a decline is seen at 5 and 7km. A lower gear is used to reduce the load on the brake systems between about 5.5 and 6km. Brake use is however mostly lowered by the retardation before the decline. Between about 7 and 8km, neutral gear is used and

[3] The selected section is 9km and begins 97km from Linköping and ends 21km from Jönköping. The route data is shown in Figure 10.

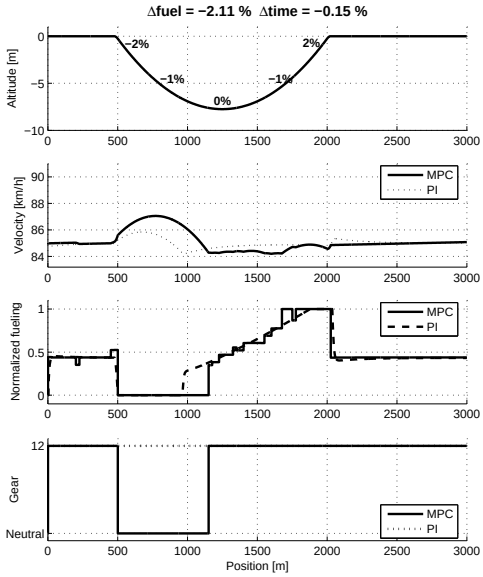

Figure 5: *A 1500m depression. The MPC controller uses neutral gear to let the truck accelerate faster than if the twelfth gear was engaged. No braking occurs.*

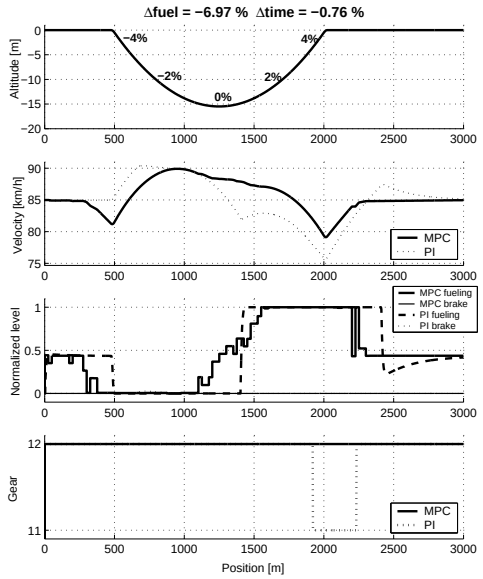

Figure 6: *A 1500m depression. The MPC controller lets the vehicle slow down before the depression and accelerates it before the uphill slope begins.*

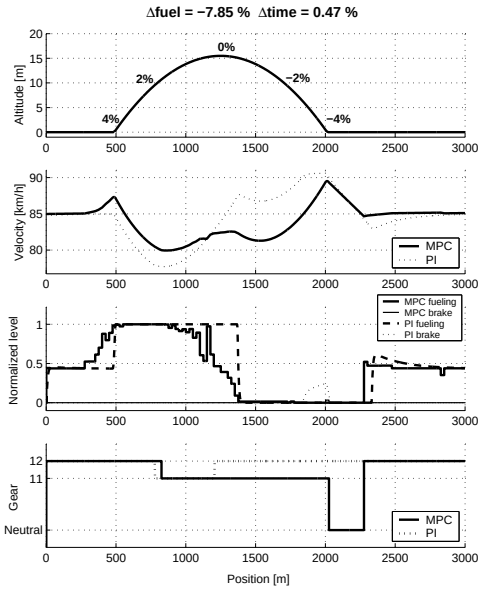

Figure 7: *A 1500m hill. The MPC controller accelerates the vehicle before the hill and lets it slow down at the top.*

the truck accelerates. When the slope lessens and the truck retards, the twelfth gear is engaged when the reference velocity is reached.

The use of fuel is greatly reduced (-12.73%) in the first section shown in Figure 8. The reduction is mainly made through the retardations before the downhill slopes at about 2, 4 and 5km. The acceleration prior to the uphill at 3km leads to that the twelfth gear is used for about 200m longer and a higher velocity is maintained throughout the hill compared to the PI-case. The higher velocity in the uphill between 3 and 4km lessens the increase of the travel time that is a result of the retardations. The change in travel time for this section then becomes negligible (+0.07%). The magnitude of the fuel consumption reduction is of course dependent on the fact that the altitude above sea level decreases with almost 100m over the 9km in Figure 8. However, when this section is used in the other direction, Figure 9 shows that a satisfactory reduction of the fuel consumption still can be achieved (-2.26%).

Figure 9 shows the section where the altitude increases with about 100m over 9km. Fuel is primarily saved through the retardations before the downhill slopes at 5 and 7km. In this case, the accelerations prior to inclines evidently increases the mean velocity more than the retardations prior to declines decreases it, resulting in a travel time reduction (-1.77%).

Simulations on the entire route, see Figure 10, are made with varying horizon length (by varying the number of steps N). The effect on fuel consumption and travel time are shown in Figure 11. The fuel consumption is at best reduced with about 2% in the direction toward Jönköping and about 3% toward Linköping. Traveling back and forth gives a reduction of about 2.5%. The travel time is moderately affected and the

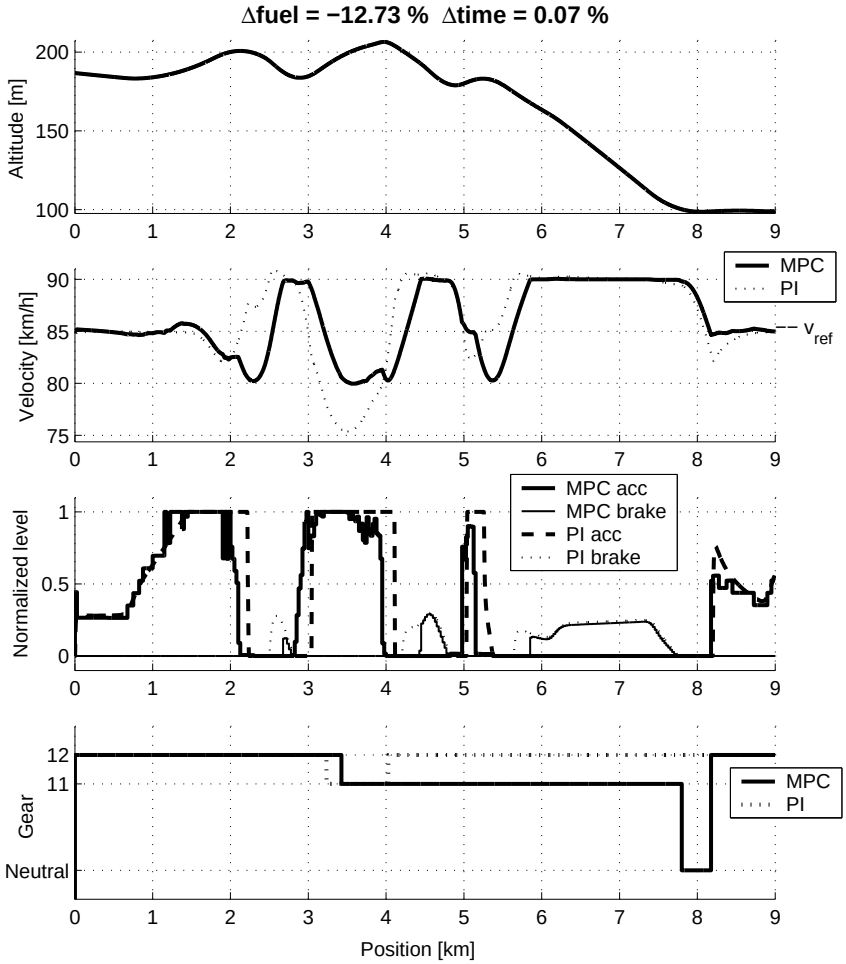

Figure 8: *A section on the road from Linköping to Jönköping. Acceleration prior to a steep incline is seen at 3km. Retardation prior to a decline is seen at 2, 4 and 5km. A lower gear is used to reduce the load on the brake systems between about 6 and 8km. Neutral gear is finally used at about 8km to slow down to the reference velocity after the steep decline.*

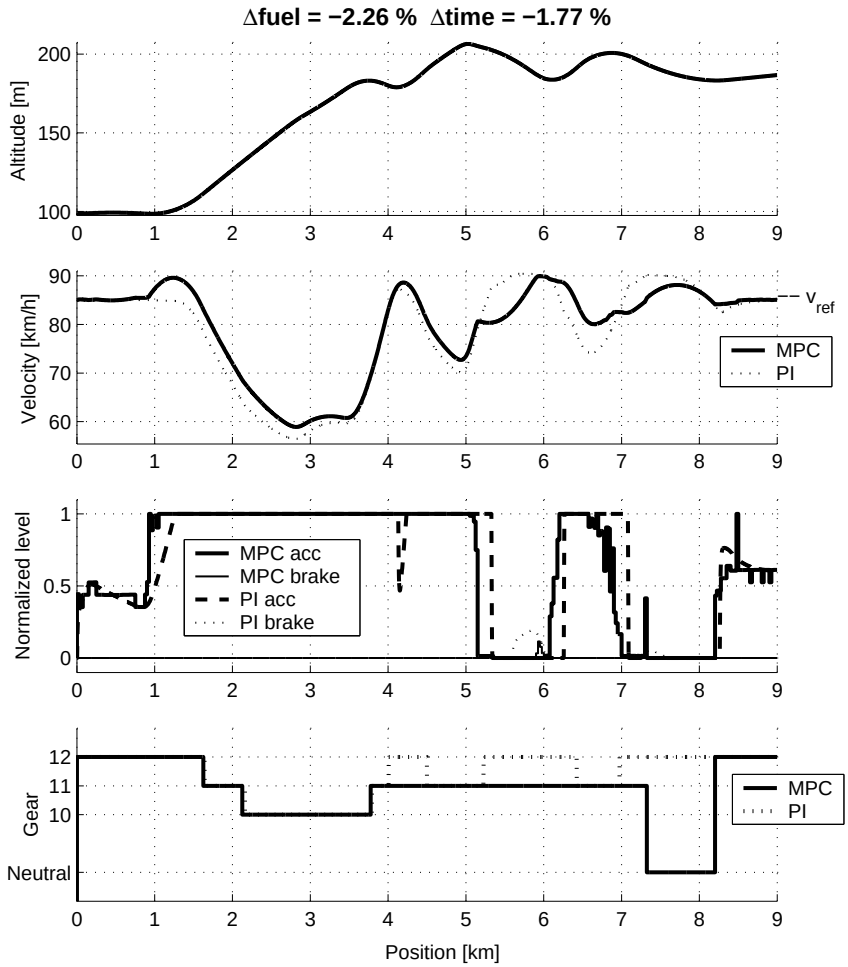

Figure 9: *A section on the road from Jönköping to Linköping. Acceleration prior to a steep incline is seen at 1,4 and 6km. Retardation prior to a decline is seen at 5 and 7km. A lower gear is used to reduce the load on the brake systems between about 5.5 and 6km. Neutral gear is used between about 7 and 8km. The truck accelerates at first and when the slope lessens and the truck retards, the twelfth gear is engaged when the reference velocity is reached.*

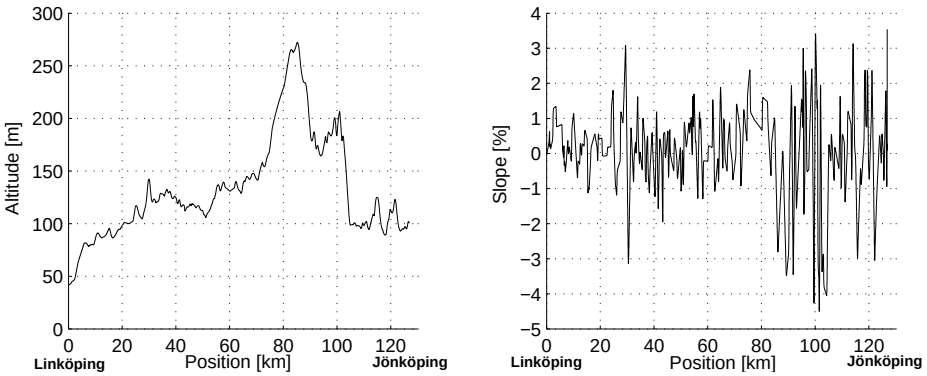

Figure 10: *The road between the cities of Linköping and Jönköping*

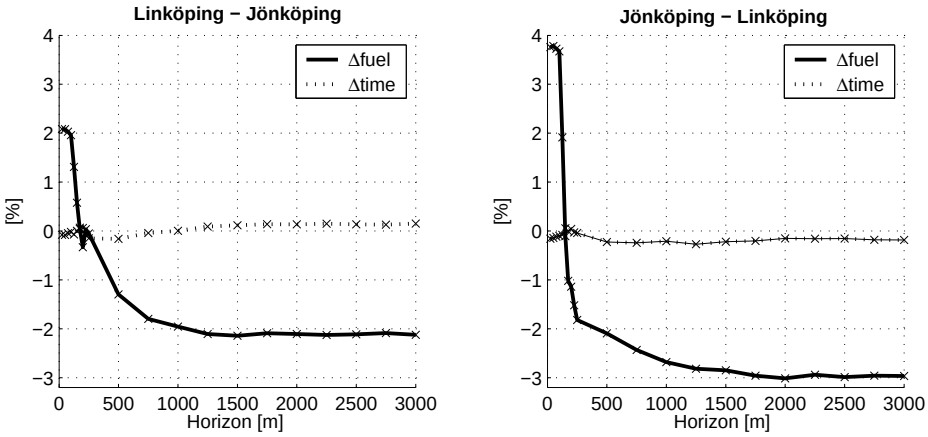

Figure 11: *The effect on fuel consumption and travel time on the road Linköping to Jönköping.*

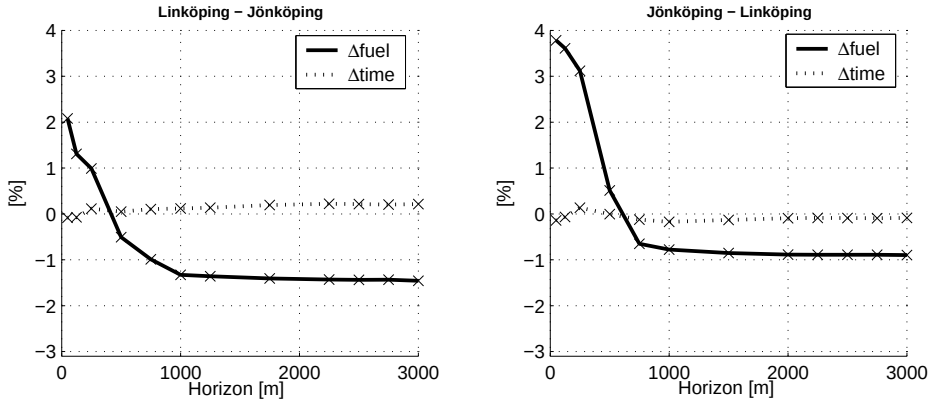

Figure 12: *The effect on fuel use and travel time on the road Linköping to Jönköping. Use of neutral gear is disallowed.*

magnitude does not vary much with the horizon according to Figure 11. The fuel use is however clearly dependent on the horizon. A horizon longer than 2000m seems absolutely superfluous and good results are achieved with about 1000m, at least for this road configuration. The simulation in Matlab/Simulink[4] runs in real time[5] up to about 750 to 1000m, depending on road configuration, if the velocity discretization is 0.1km/h. The road configuration influences the size of the search space and therefore the complexity.

4.4 Neutral gear

The use of neutral gear adds another degree of freedom in the problem. To estimate the magnitude of the gain that is achieved through this, simulations are made where neutral gear is disallowed. A comparison between Figures 11 and 12 reveals the effects. The change in travel time is similar in both directions. Traveling toward Jönköping, the fuel consumption reduction is lessened by about half a percent when neutral gear is disallowed. The most evident difference appears in the direction toward Linköping. The fuel use reduction is increased from about 1% to 3% when neutral gear is allowed. The altitude above sea level is around 60m higher in Jönköping than in Linköping, see Figure 10. Going toward Jönköping thus in general means facing more uphill than downhill slope. Neutral gear is thus, as might be expected, most useful when there is more downhill than uphill slope.

[4]The computer used was a PC with an Intel Celeron 2.6GHz processor and 480Mb of RAM running Windows XP SP2 and Matlab 6.5.1, release 13.

[5]Meaning that the time required to simulate the system is shorter than the time that is simulated.

5 Conclusions

There is an evident potential of fuel reductions by an explicit use of road topography in a cruise controller. In the reported results with authentic road maps, the travel time is only insignificantly changed which of course is important for the credibility of the fuel reduction values. Using authentic altitude measurements along a 127 km route, simulations showed that the fuel consumption traveling this road back and forth can be reduced with 2.5% without affecting the total travel time. When varying the horizon length, it appears that, at least for this road configuration, a horizon of about 1000m is sufficient. Horizon lengths longer than about 2000m do not improve the results; it only adds to the complexity.

Simulations showed that substantial reductions in fuel use can be made in a number of situations of principle interest and some of these are now summarized. When a sufficiently steep decline is ahead, the vehicle velocity can be lowered before the decline and the vehicle is then let to accelerate in the downhill slope. Slowing down before a steep decline will in general also lower the need for braking.

When there is a steep incline ahead, it may be favorable to accelerate before the uphill slope begins. A higher velocity reaching the incline can lessen the need for lower gears. This action do not decrease the use of fuel of noticeable amounts, it may even slightly increase it. Simulations did however show that the travel time can be shortened of a greater magnitude. Considering a route, the time decrease can then counterbalance the time increases introduced where the vehicle velocity is lowered prior to declines.

On a route with more downhill than uphill slope, the use of neutral gear seems to be a potent way of reducing fuel use. When going back this route and facing many inclines, a clever choice of the pedal level appear to be more important.

The control algorithm relies on topographic information. This information can be obtained with for example the combination of GPS and three dimensional road maps. Another possibility could be to record road data the first time a route is travelled, and then to use this data on later trips on that route. If the truck is equipped with an automated manual transmission, see e.g. [8], no extra hardware in the powertrain would be needed to carry out gear shifts. Hence, to realize the presented algorithm only the control software has to be altered.

The search space for dynamic programming was reduced by removing the states that can not be reached because of the various physical limitations in the system and also the states that do not meet the problem constraints. In order to balance accuracy versus grid size, the state space was discretized and the control signals were calculated by an inverse simulation. Owing to these reductions, the complexity of the algorithm, when achieving reported results, allows the simulations and thus the algorithm to run in real time on a standard PC.

6 Contact

Erik Hellström, Anders Fröberg and Professor Lars Nielsen work at the Division of Vehicular Systems, Department of Electrical Engineering, Linköpings Universitet, SE-581 83 Linköping, Sweden.

E-mail	Phone
hellstrom@isy.liu.se	+46 13 281327
froberg@isy.liu.se	+46 13 284066
lars@isy.lu.se	+46 13 281307

Bibliography

[1] Dimitri P. Bertsekas. *Dynamic Programming and Optimal Control.* Athena Scientific, 2000.

[2] A. Fröberg, E. Hellström, and L Nielsen. Explicit fuel optimal speed profiles for heavy trucks on a set of topographic road profiles. *SAE Technical Paper Series, 2006-01-1071*, 2006.

[3] A. Fröberg, L. Nielsen, L-G. Hedström, and M. Pettersson. Controlling gear engagement and disengagement on heavy trucks for minimization of fuel consumption. *IFAC World Congress. Prague, Czech Republic*, 2005.

[4] E. Hellström, A. Fröberg, and L. Nielsen. A real-time fuel-optimal cruise controller for heavy trucks using road topography information. *SAE Technical paper series*, (2006-01-0008), 2006.

[5] Erik Hellström. *Explicit use of road topography for model predictive cruise control in heavy trucks.* Masters thesis, LiTH-ISY-EX-05/3660-SE, Linköping Institute of Technology, Linköping, 2005.

[6] U. Kiencke and L. Nielsen. *Automotive Control Systems, 2nd ed.* Springer-Verlag, 2005.

[7] F. Lattemann, K. Neiss, S. Terwen, and T. Connolly. The predictive cruise control -a system to reduce fuel consumption of heavy duty trucks. *SAE Technical paper series*, (2004-01-2616), 2004.

[8] Magnus Pettersson and Lars Nielsen. Gear shifting by engine control. *IEEE Transactions Control Systems Technology*, Volume 8(No. 3):pp. 495–507, May 2000.

[9] Tony Sandberg. *Heavy Truck Modeling for Fuel Consumption Simulations and Measurments.* Licentiate thesis, LiU-TEK-LIC-2001:61, Linköping Institute of Technology, Linköping, 2001.

Paper E

EXPLICIT FUEL OPTIMAL SPEED PROFILES FOR HEAVY TRUCKS ON A SET OF TOPOGRAPHIC ROAD PROFILES[1]

Anders Fröberg[⋆]**, Erik Hellström**[⋆]**, Lars Nielsen**[⋆]

[⋆] *Dep. of Electrical Engineering, Linköpings universitet,*
SE-*581 83 Linköping, Sweden.* {froberg,hellstrom,lars}@isy.liu.se.

Abstract

The problem addressed is how to drive a heavy truck over various road topographies such that the fuel consumption is minimized. Using a realistic model of a truck powertrain, an optimization problem for minimization of fuel consumption is formulated. Through the solutions of this problem optimal speed profiles are found. An advantage here is that explicit analytical solutions can be found, and this is done for a few constructed test roads. The test roads are constructed to be easy enough to enable analytical solutions but still capture the important properties of real roads. In this way the obtained solutions provide explanations to some behaviour obtained by ourselves and others using more elaborate modeling and numeric optimization like dynamic programming. The results show that for level road and in small gradients the optimal solution is to drive with constant speed. For large gradients in downhill slopes it is optimal to utilize the kinetic energy of the vehicle to accelerate in order to gain speed. This speed increase is used to lower the speed on other road sections such that the total average speed is kept. Taking account for limitations of top speed the optimal speed profile changes to a strategy that minimizes brake usage. This is done by e.g. slowing down before steep down gradients were the truck will accelerate even though the engine does not produce any torque.

[1]This paper is an edited version of [3], Explicit Fuel optimal speed profiles for heavy trucks on a set of topographic road profiles, published in the preprints of the SAE World Congress 2006.

1 Introduction

For heavy trucks fuel is a large part of the operating cost. A good driver has an intuition of how to drive in a fuel optimal way. The problem of finding a fuel optimal way of driving has been studied for different kinds of vehicles. Earlier work in this subject have either been using simpler models [2], or they have been using an optimal control theory approach with approximate solutions using for example dynamic programming [8, 9, 11, 13]. In these types of simulations many interesting behaviors are observed. For example, it is sometimes observed that it is optimal to slow down before a downhill whereas sometimes it is not. This may depend on a change of parameters like vehicle mass or road inclination. One objective of this paper is to get insight to these observations by formulating a problem allowing analytical solutions.

The analytical derivation of fuel efficient driving behavior is presented using a physical model of a heavy truck that gives fuel consumption prediction, but still being of manageable complexity. The optimal solutions of the constructed test roads are important for the understanding of the energy usage of a heavy truck. The purpose of this study is to provide insight as mentioned before, but also to give proper strategies for standard cases such as up- and downhill slopes, hills and depressions. A complete optimal strategy will then be a continuous chain of such standard cases where the parameter dependence will be explicit. Moreover, the optimal solutions presented are usable in e.g. validation of suboptimal real time model predictive cruise controllers, or to teach drivers how to drive more efficiently.

2 Truck model

The model structure that will be used here has been verified to predict fuel consumption to within a few percent [12], but is still of such a simple character that it can be used for analytical studies of fuel consumption.

The model consists of the following components: Engine, transmission, final gear, wheels and chassis, which are all modeled as in [10]. The engine is modeled as

$$T_e = f_e(\delta, \omega_e) \tag{1}$$

where δ is engine fueling in mg/stroke, ω_e is engine speed, and the function $f_e(\delta, \omega_e)$ is mapped from measured data. For a typical diesel engine an affine model of the engine torque is a reasonable approximation, and can be written as

$$T_e = c_{e\delta}\delta + c_{e\omega}\omega_e + c_{ec} \tag{2}$$

This affine model will be used later in the optimization of fuel consumption.

The flywheel and the other rotating parts of the engine are modeled as

$$T_e - T_{fw} = J_e\dot{\omega}_e \tag{3}$$

where T_{fw} is the flywheel torque.

The transmission and final gear are modeled as a lumped component with gear ratio i and efficiency η as

$$\begin{aligned} \omega_e &= i\omega_w \\ T_{fw} i\eta - T_w &= J\dot{\omega}_w \end{aligned} \tag{4}$$

where ω_w is wheel speed, J is the lumped inertia of the driveline, and T_w is wheel torque. The wheels are modeled as rolling wheels without slip as

$$\begin{aligned} r\omega_w &= v \\ T_w &= F_w r \end{aligned} \tag{5}$$

where r is wheel radius, v vehicle speed, and F_w is wheel force. The motion of the truck is modeled as

$$m\dot{v} = F_w - F_{air} - F_{roll} - F_{inc} \tag{6}$$

where m is vehicle mass and the right hand side is wheel force, air drag resistance, rolling resistance, and normal force respectively. The resistance forces are

$$\begin{aligned} F_{air} &= \tfrac{1}{2}\rho c_d A v^2 \\ F_{roll} &= mg(c_{r1} + c_{r2}v + c_{r3}v^2) \\ F_{inc} &= mg\sin\alpha \end{aligned} \tag{7}$$

where the latter force depends on the road slope α.

If all equations are combined the result is

$$\dot{v}\left(m + J_e i^2 \eta \frac{1}{r^2} + \frac{J}{r^2}\right) = \frac{1}{r}\left(c_{e\delta}\delta + c_{e\omega}\omega_e + c_{ec}\right) i\eta - \frac{1}{2}\rho c_d A v^2 - mg\left(c_{r1} + c_{r2}v + c_{r3}v^2\right) - mg\sin\alpha \tag{8}$$

To summarize, the model can be written in the form

$$\begin{aligned} \dot{v}(t) &= f(v(t), \delta(t), \alpha(s(t))) \\ \dot{s}(t) &= v(t) \end{aligned} \tag{9}$$

where s is the distance traveled.

3 Optimal speed on level road

The model presented in the previous section is of a similar structure as the one used in [2]. Here that model structure is extended with more detailed models of the engine and the rolling resistance. In [2] it is shown that the optimal speed profile on level road is constant speed. The assumption for the engine model used there is that the fuel consumption is proportional to the produced work. It will now be shown that constant speed also is optimal when the model from [2] is extended with a more detailed engine model as described by Equation (2). The model that is studied firstly is then given by Equations (1) - (9). The model can be written as

$$\dot{v}(t) = c_\delta \delta(t) + c_\omega \omega_e(t) + c_v v(t) + c_c(\alpha) + c_{v2} v^2(t) \tag{10}$$

where c_i is the lumped model constants from Equation (8). Driving at constant speed, i.e. $\dot{v} = 0$, with fixed gear, i.e. $\omega_e = iv/r$, the fuel consumption over the distance s is proportional to

$$z = \delta s = (\tilde{c}_c + \tilde{c}_v v + \tilde{c}_{v2} v^2) s \tag{11}$$

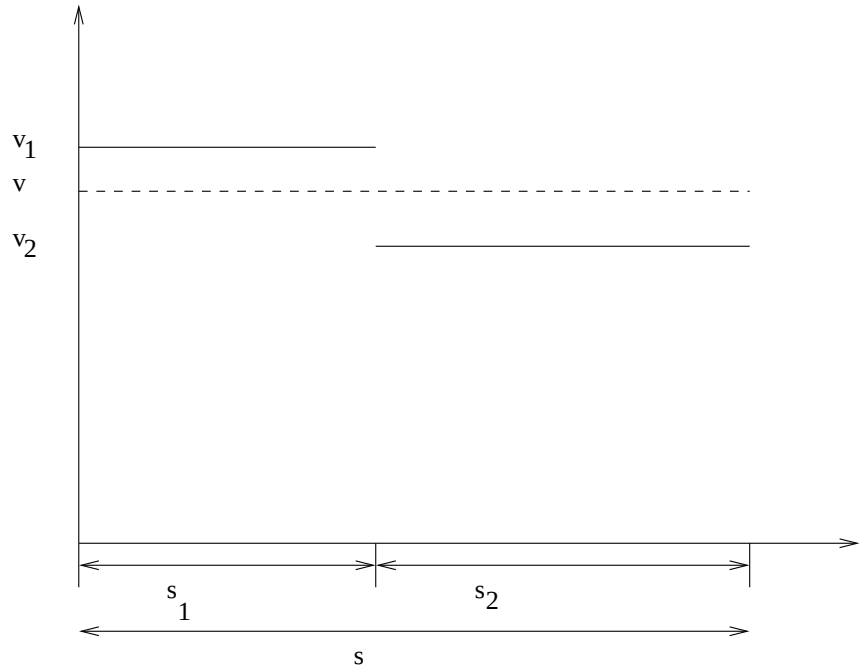

Figure 1: *Driving the distance s with average speed v, and the subdistances s_1 and s_2 with the speeds v_1 and v_2 respectively.*

where $\tilde{c}_c = -c_c/c_\delta$, $\tilde{c}_v = -c_\omega i/(c_\delta r) - c_v/c_\delta$, and $\tilde{c}_{v2} = -c_{v2}/c_\delta$. Let the distance s be partitioned in two parts as

$$s = s_1 + s_2 \tag{12}$$

and assume that the vehicle is driving the distances with the constant speeds v_1 and v_2 respectively, see Figure 1. The total consumption can then be written as

$$z = (\tilde{c}_c + \tilde{c}_v v_1 + \tilde{c}_{v2} v_1^2)s_1 + (\tilde{c}_c + \tilde{c}_v v_2 + \tilde{c}_{v2} v_2^2)s_2 \tag{13}$$

The problem studied here is how to choose v_1 and v_2 such that the fuel consumption (13) is minimized and that the distances s_1 and s_2 is traveled over the time

$$t = t_1 + t_2 = \frac{s_1}{v_1} + \frac{s_2}{v_2} = \frac{s}{v} \tag{14}$$

where v is the total average speed. The optimization problem is to minimize (13) subject to the constraint (14). The objective function is augmented with the constraint using Lagrange methods resulting in

$$L(v_1, v_2, \lambda) = (\tilde{c}_c + \tilde{c}_v v_1 + \tilde{c}_{v2} v_1^2)s_1 + (\tilde{c}_c + \tilde{c}_v v_2 + \tilde{c}_{v2} v_2^2)s_2 + \lambda(\frac{s_1}{v_1} + \frac{s_2}{v_2} - t) \tag{15}$$

where λ is a constant Lagrange multiplier. The minimum is found by solving the equations defined by setting the partial derivatives of the Lagrange function to zero

$$\frac{\partial L}{\partial v_1} = \tilde{c}_v s_1 + 2\tilde{c}_{v2} v_1 s_1 - \lambda s_1 v_1^{-2} = 0 \tag{16}$$

$$\frac{\partial L}{\partial v_2} = \tilde{c}_v s_2 + 2\tilde{c}_{v2} v_2 s_2 - \lambda s_2 v_2^{-2} = 0 \tag{17}$$

$$\frac{\partial L}{\partial \lambda} = \frac{s_1}{v_1} + \frac{s_2}{v_2} - t = 0 \tag{18}$$

Multiplying (16) with v_1^2/s_1, (17) with v_2^2/s_2, and eliminating λ gives

$$\tilde{c}_v v_1^2 + 2\tilde{c}_{v2} v_1^3 = \tilde{c}_v v_2^2 + 2\tilde{c}_{v2} v_2^3 \tag{19}$$

which can be rearranged to

$$\frac{2\tilde{c}_{v2}}{\tilde{c}_v} = \frac{v_2^2 - v_1^2}{v_1^3 - v_2^3} \tag{20}$$

For physically realistic values on $\tilde{c}_v$, $\tilde{c}_{v2}$, the only solution to this equation is that $v_1 = v_2$. Using the constraint on total travel time (18) it is seen that this speed is also the specified average speed for the distance

$$v = s/t = v_1 = v_2 \tag{21}$$

If the second partial derivatives of the Lagrangian is computed it is seen that this point is also a minimum.

In [2] it is shown that taking account for acceleration and deceleration between the speeds v_1 and v_2 does not change the solution that the speeds must be equal. At best, in the ideal case the extra energy it takes to accelerate from v to v_1, see Figure 1, will be recovered when decelerating from v_1 to v so that the effect in energy consumption of accelerating and decelerating will be zero. This fact is also easily shown with the theory of calculus of variations. Taking account for accelerations, the problem of finding the speed trajectory from point a to point b that has a given average speed and minimizes the fuel consumption can, using Equation (10), be written as

$$\min \int_{t_a}^{t_b} \delta(t) v(t) dt = \min \int_{t_a}^{t_b} (\tilde{c}_{\dot{v}} \dot{v}(t) + \tilde{c}_c + \tilde{c}_v v(t) + \tilde{c}_{v2} v^2(t)) v(t) dt \tag{22}$$

subject to the constraint of a given average speed, i.e.

$$\frac{1}{t_b - t_a} \int_{t_a}^{t_b} v(t) dt = v_{ref}(t) \tag{23}$$

where v_{ref} is the specified average speed. This problem is in the form of

$$\min \int_{t_a}^{t_b} F(t, v, \dot{v}) dt \tag{24}$$

subject to

$$\int_{t_a}^{t_b} G(t, v, \dot{v}) dt = v_{ref} \tag{25}$$

A necessary condition for $v(t)$ to be an optimum is that it fulfills the differential equation [5]

$$\frac{\partial F}{\partial v} - \frac{d}{dt}\frac{\partial F}{\partial \dot{v}} + \lambda\left(\frac{\partial G}{\partial v} - \frac{d}{dt}\frac{\partial G}{\partial \dot{v}}\right) = 0 \tag{26}$$

where λ is a constant Lagrange multiplier. In the case of (22) and (23) this becomes

$$\tilde{c}_c + 2\tilde{c}_v v(t) + 3\tilde{c}_{v2} v^2(t) + \lambda = 0 \tag{27}$$

i.e., even if accelerations and decelerations are taken account for, the optimal speed profile is constant speed.

4 Optimal speed on small gradients

In [2] it is shown that for small gradients it is optimal with constant speed. It will be shown that this is true also for the model (10)-(11). First small gradients will be defined in terms of inclination angles, [4].

Consider the model (8). Let the acceleration $\dot{v}(t)$ and the fueling $\delta(t)$ be zero. Then it is seen that for all inclination angles

$$\tilde{\gamma}_d \in \{\tilde{\gamma}_d : \frac{1}{r}\left(c_{e\omega}\omega_e + c_{ec}\right) i\eta - \frac{1}{2}\rho c_d A v^2 - mg(c_{r1} + c_{r2}v + c_{r3}v^2) - mg\sin\tilde{\gamma}_d > 0\} \tag{28}$$

the vehicle will accelerate even though the engine does not produce any work. The limit for the set $\tilde{\gamma}_d$ is found by setting equality in (28) resulting in

$$\gamma_d = \arcsin\frac{\left(c_{e\omega}\omega_e + c_{ec}\right)\frac{i\eta}{r} - \frac{\rho}{2}c_d A v^2 - mg(c_{r1} + c_{r2}v + c_{r3}v^2)}{mg} \tag{29}$$

See Figure 2 for the characteristics of the limit angle. For uphill slopes the angles are defined using maximum fueling $\delta_{max}(\omega_e)$ as

$$\begin{aligned}\tilde{\gamma}_u \in \{\tilde{\gamma}_u : &\tfrac{1}{r}\left(c_{e\delta}\delta_{\max} + c_{e\omega}\omega_e + c_{ec}\right) i\eta - \tfrac{1}{2}\rho c_d A v^2 \\ &- mg(c_{r1} + c_{r2}v + c_{r3}v^2) - mg\sin\tilde{\gamma}_u > 0\}\end{aligned} \tag{30}$$

i.e. the angles for which the engine is powerful enough to accelerate. The limit angle is then

$$\gamma_u = \arcsin\frac{\left(c_{e\delta}\delta_{\max} + c_{e\omega}\omega_e + c_{ec}\right)\frac{i\eta}{r} - \frac{\rho}{2}c_d A v^2 - mg(c_{r1} + c_{r2}v + c_{r3}v^2)}{mg} \tag{31}$$

The maximum fuel injection δ_{max} is here modeled as a second order polynomial in engine speed. See Figure 3 for the characteristics of the limit angle.

The definition of small gradients can now be made.

Definition 1: Small gradients are all gradients with inclinations α such that

$$\gamma_d < \alpha < \gamma_u \tag{32}$$

Note that γ_d takes a negative value while γ_u is positive.

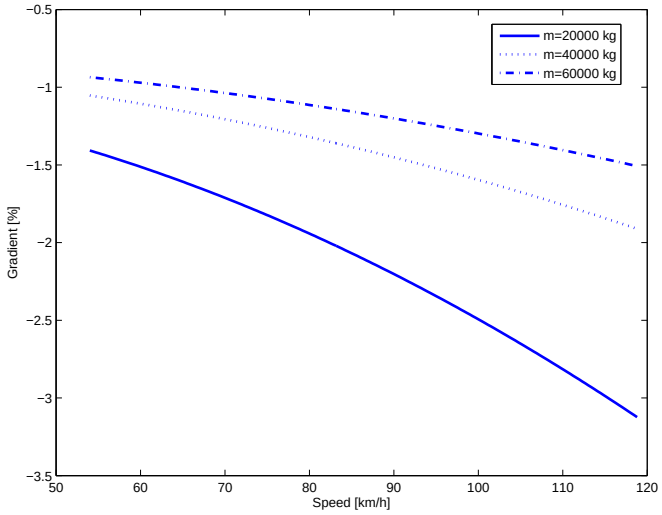

Figure 2: *The limit angle in downhill slopes as a function of vehicle speed for different vehicle masses and highest gear.*

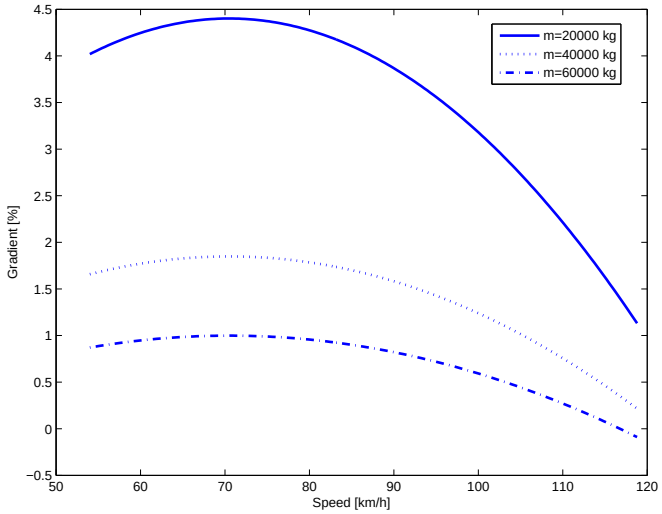

Figure 3: *The limit angle in uphill slopes as a function of vehicle speed for different vehicle masses.*

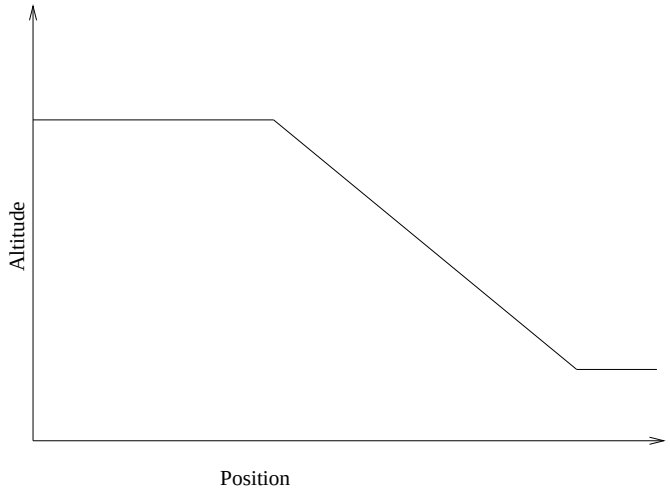

Figure 4: *A constructed road profile that captures important behavior of a truck traveling in a downhill slope with large gradient. The gradient is such that the vehicle will accelerate in the slope even though the engine does not produce any work.*

Now with a definition of small gradients, optimal solutions for roads with level sections and sections with small gradients can be calculated. For a road section with a small gradient with constant inclination the fuel consumption (11) is written

$$z = \delta s = (\tilde{c}_c + \tilde{c}_v v + \tilde{c}_{v2} v^2 + c_{inc}) s \tag{33}$$

where c_{inc} is the additional cost due to road inclination. Combining one level tangent section with one of small gradient the total fuel consumption (13) is now

$$z = (\tilde{c}_c + \tilde{c}_v v_1 + \tilde{c}_{v2} v_1^2) s_1 + (\tilde{c}_c + \tilde{c}_v v_2 + \tilde{c}_{v2} v_2^2 + c_{inc}) s_2 \tag{34}$$

The Lagrangian (15) becomes

$$L(v_1, v_2, \lambda) = (\tilde{c}_c + \tilde{c}_v v_1 + \tilde{c}_{v2} v_1^2) s_1 + (\tilde{c}_c + \tilde{c}_v v_2 + \tilde{c}_{v2} v_2^2 + c_{inc}) s_2 + \lambda(\frac{s_1}{v_1} + \frac{s_2}{v_2} - t) \tag{35}$$

It is seen that the additional c_{inc} in the Lagrangian will disappear when the partial derivatives (16)-(18) are computed, and hence the optimum remains unchanged. The conclusion is that also combinations of level tangent road sections with sections of small gradients has the optimal speed profile of constant speed.

5 Optimal speed on steep gradients

In [2] it is argued that slopes with large gradients, i.e. outside the definition in (32), is so rare on common roads that there is no reason to take account for them. However, in [4, 7, 6] it is shown that there is a potential to save some extra per cent of fuel by controlling the vehicle speed in such slopes. Analytic solutions to the motion of the model presented in Section 2 will here be used to find the optimal speed profiles for large gradients. The type of road sections that will be studied is depicted in Figure 4.

5.1 Downhill slopes

For steep downhill slopes the vehicle will accelerate even though the engine does not produce any work. The motion of a vehicle accelerating in a downhill slope with fuel injection cut off will now be studied. Assuming no fueling, i.e. $\delta(t) = 0$, fixed gear, and constant inclination the vehicle motion (10) can be written as

$$\dot{v}(t) = c_c + c_v v(t) + c_{v2} v^2(t) \tag{36}$$

This ordinary differential equation can be solved by separating variables writing (36) as

$$\frac{1}{c_c + c_v v + c_{v2} v^2} dv = dt, \; c_c + c_v v + c_{v2} v^2 \neq 0 \tag{37}$$

Integrating both sides gives

$$\int \frac{1}{c_c + c_v v + c_{v2} v^2} dv = \int dt + c \tag{38}$$

where c is a constant. For typical values of the model parameters, when the vehicle is traveling downhill, $4c_{v2}c_c < c_v^2$, which means that the integrals are

$$\frac{1}{\sqrt{-4c_{v2}c_c + c_v^2}} \ln \left| \frac{2c_{v2}v + c_v - \sqrt{-4c_{v2}c_c + c_v^2}}{2c_{v2}v + c_v + \sqrt{-4c_{v2}c_c + c_v^2}} \right| = t + c \tag{39}$$

From this equation the speed can be solved for and the result is

$$v(t) = \frac{a(c_v - \sqrt{k}) - (c_v + \sqrt{k}) e^{\sqrt{k}(t+c)}}{2c_{v2} e^{\sqrt{k}(t+c)} - a 2c_{v2}} \tag{40}$$

The constant c is determined from the intitial velocity $v(0)$, $k = c_v^2 - 4c_c c_{v2}$, and $a = 1$ if the initial speed is above the stationary speed and $a = -1$ if below the stationary speed.

Solving Equation (40) for c gives

$$c = \frac{1}{\sqrt{k}} \ln \left(\frac{a(c_v - \sqrt{k}) + v(0) a 2c_{v2}}{v(0) 2c_{v2} + c_v + \sqrt{k}} \right) \tag{41}$$

As seen in Equation (40), given an initial speed at the beginning of the slope, the speed at each time instant in the slope can be calculated. In order to calculate the speed at the end of the slope, the time for that point has to be known. The time it takes to travel the slope

can be calculated from the following expression for the distance of the slope.

$$
\begin{aligned}
s = \int_{t_0}^{t_1} v(t)dt = a\left(c_v - \sqrt{k}\right)\int_{t_0}^{t_1} \frac{1}{2c_{v2}e^{\sqrt{k}c}e^{\sqrt{k}t} - 2ac_{v2}}dt \\
- \left(c_v + \sqrt{k}\right)e^{\sqrt{k}c}\int_{t_0}^{t_1} \frac{e^{\sqrt{k}t}}{2c_{v2}e^{\sqrt{k}c}e^{\sqrt{k}t} - 2ac_{v2}}dt = \\
a\left(c_v - \sqrt{k}\right)\left[\frac{1}{-2ac_{v2}\sqrt{k}}\left(\sqrt{k}t - \ln\left|-2ac_{v2} + 2c_{v2}e^{\sqrt{k}c}e^{\sqrt{k}t}\right|\right)\right]_{t_0}^{t_1} \\
- \left(c_v + \sqrt{k}\right)e^{\sqrt{k}c}\left[\frac{1}{\sqrt{k}2c_{v2}e^{\sqrt{k}c}}\ln\left|-2ac_{v2} + 2c_{v2}e^{\sqrt{k}c}e^{\sqrt{k}t}\right|\right]_{t_0}^{t_1} \qquad (42)
\end{aligned}
$$

Given the start time t_0, start velocity $v(t_0)$, and the total length s, the end time t_1 can be calculated solving equation (42).

When a vehicle has accelerated in a steep downhill slope such as depicted in Figure 4, it has to decelerate to cruising speed again once the level section is reached. The optimal way to decelerate is to cut the fuel injection to decelerate as fast as possible. This will be shown mathematically in Section 6, but it can also be argued intuitively as follows. Any amount of fuel that is injected when driving faster than the cruising speed is used when the vehicle is subject to higher resistance, which decreases the total efficiency. Hence, in order to decelerate on level road the fuel injection is cut off. For typical model parameters in this case $4c_{v2}c_c > c_v^2$ and the integrals in (38) then becomes

$$\frac{2}{\sqrt{k}}\arctan\left(\frac{2c_{v2}v + c_v}{\sqrt{k}}\right) = t + c \qquad (43)$$

where $k = 4c_c c_{v2} - c_v^2$. The speed is then

$$v(t) = \frac{1}{2c_{v2}}\left(\sqrt{k}\tan\left(\frac{\sqrt{k}}{2}(t+c)\right) - c_v\right) \qquad (44)$$

The constant c is given from initial conditions as

$$c = \frac{2}{\sqrt{k}}\arctan\left(\frac{1}{\sqrt{k}}(2c_{v2}v(0) + c_v)\right) \qquad (45)$$

Typical solutions to the speeds as given by Equations (40) and (44) are depicted in Figure 5 - Figure 8. A simulation of a truck driving in a slope as depicted in Figure 4 is presented in Figure 9. Note that for such a short downhill slope as 400 m, the deceleration before and after the slope as well as the acceleration in the slope is nearly linear. The reason for slowing down before the slope is to keep an average speed equal to the cruising speed on the level sections.

5.2 Analytical solutions for optimal speed profiles

As can be seen in Figure 9, during deceleration with fuel cut off on level sections, it is a good approximation to consider speed as a linear function of position. Also the

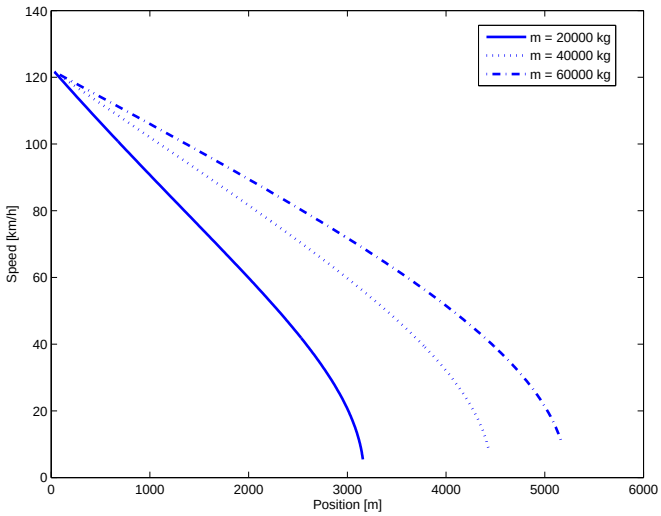

Figure 5: *Deceleration on level road when fueling is zero. For all three vehicle weights the motion is almost linear for a large part of the operating range.*

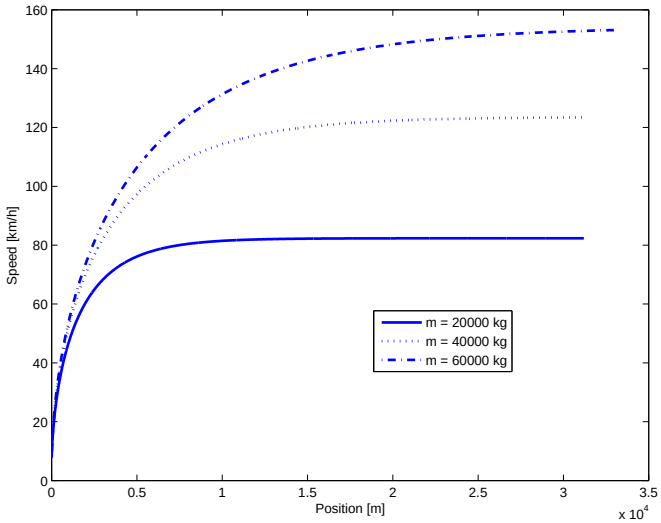

Figure 6: *Acceleration on 2% downhill slope with zero fueling. Note that it takes more than 10 km to reach a stationary speed.*

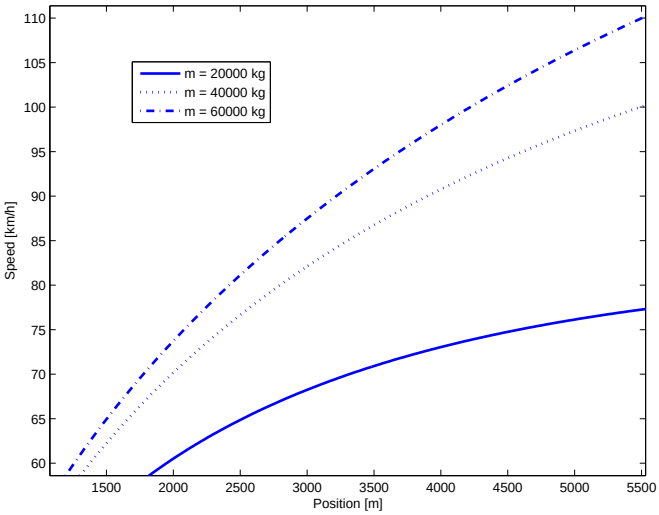

Figure 7: *Acceleration on 2% downhill slope with zero fueling. A zoom in of the previous figure. For speeds around cruising speed the acceleration can be approximated as linear.*

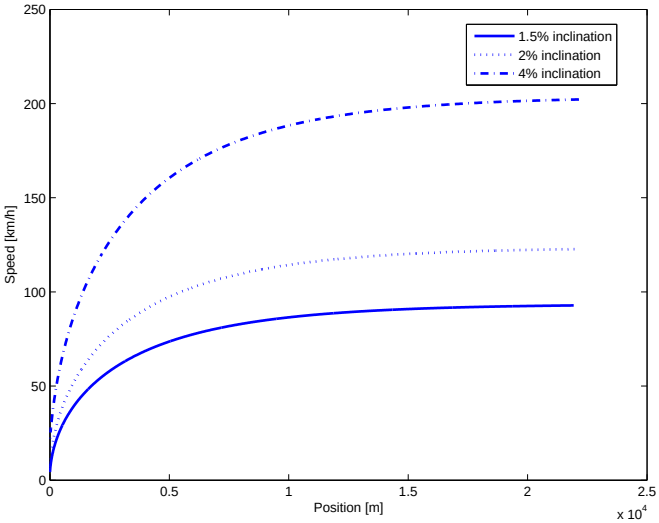

Figure 8: *Acceleration of a 40 ton truck with zero fueling for different inclinations. Note that it takes more than 10 km to reach a stationary speed.*

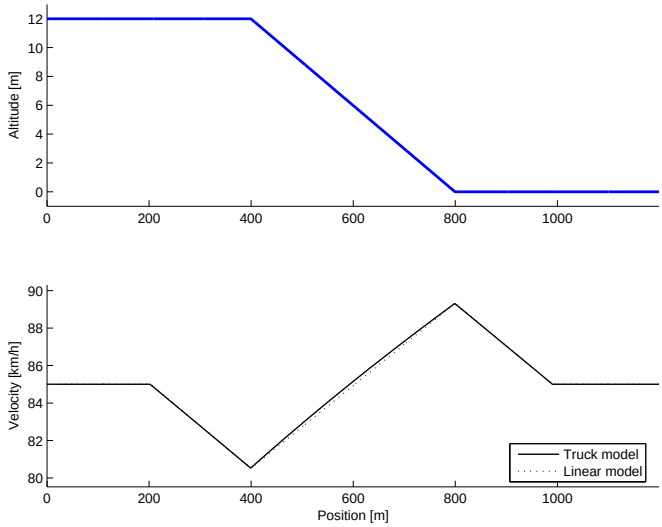

Figure 9: *Typical speed profile when driving with an average speed of 85 km/h on a level section, followed by a steep downhill slope, and ending with a level section. The inclination in the slope is 3%. There is no fuel injection during the part from 200m to 1000m.*

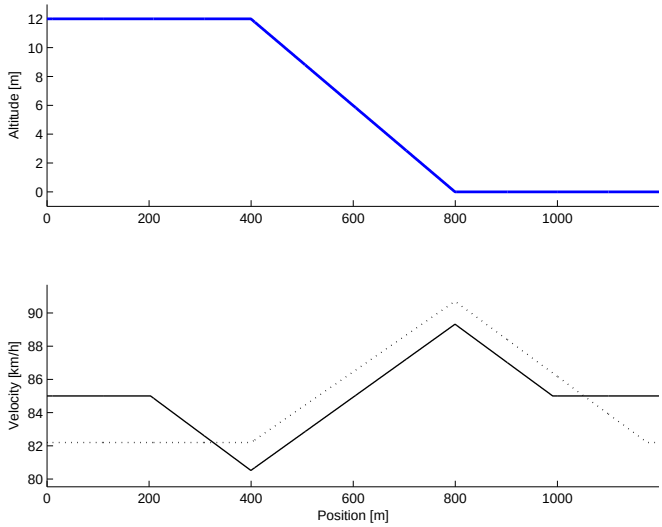

Figure 10: *Two different speed profiles with the same average speed. Both profiles assumes that speed is a linear function of position during deceleration and acceleration. The distance traveled in fuel cut off mode is equal in both cases and hence the dotted profile has the lowest fuel consumption.*

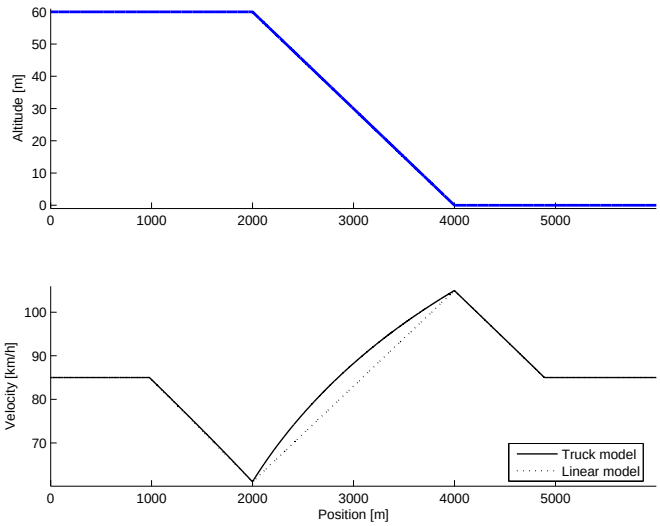

Figure 11: *Typical speed profile when driving with an average speed of 85 km/h on a level section, followed by a steep downhill slope, and ending with a level section. The inclination in the slope is 3%. There is no fuel injection during the part from 1000m to about 5000m.*

acceleration with fuel cut off in the slope can be approximated as linear. In the simulation in Figure 9 the cruising speed was chosen to equal the desired average speed on the total distance. The point where the fuel injection is cut off is chosen so that the average speed is the desired. Of course there are other speed profiles that have the same average speed. For example, a lower cruising speed on the level sections and going into fuel cut off later can have the same average speed, see Figure 10. Using linear approximations for the decelerations and acceleration it is seen that the distance traveled in fuel cut off mode is equal for the different profiles. This means that the profile with lower cruising speed in the level sections has the lowest fuel consumption. As can be seen in Figure 9 the linear approximations of the speed profiles are valid for the case studied.

When studying long slopes such as the one depicted in Figure 11, it is seen that the linear approximation of vehicle speed during the acceleration no longer is very good. However, the linear approximation during deceleration is still good as expected, see Figure 5. The exponential behavior of the speed during the acceleration, see Equation (40), means that the gain in speed in the slope will be lower the higher the initial speed is. Comparing the previous two strategies, this means that using the strategy of cruising at a lower speed and going into fuel cut off mode later, will result in a shorter distance in fuel cut off mode, and hence the decrease in fuel consumption will be lesser. However comparing the two strategies as in Figure 12, the strategy with lower cruising speed still has the lowest consumption on the total distance.

So far it has been shown that the optimal way to drive in downhill slopes is to cruise at constant speed all the way to the crest of the downhill slope, then go into fuel cut off mode, let the vehicle accelerate in the slope, and last decelerate on the level section

down to cruising speed again. Compared to other strategies, the gain in speed in the slope is used to lower the cruising speed on the level sections, and thereby reducing the fuel consumption. However, simulations also show that the gain in fuel consumption varies little between different strategies.

The discussion up till now has assumed that there are no limitations on vehicle speed. However, in a realistic case the speed must be limited due to safety and legislation reasons. For such cases the brakes have to be used to limit the speed in steep downhill slopes. As the brakes transform kinetic energy into heat, all brake usage is a waste of energy. For fuel optimal driving it is hence desirable to find speed profiles that minimize the brake usage. If the optimal speed profile not considering speed limits has a higher velocity than allowed, the strategy can be modified. The new optimal profile is then to cut the fuel injection at a time such that the vehicle reaches the maximum allowed speed at the end of the slope without using the brakes, see Figure 13. Using the analytic solution (40), (42), for vehicle acceleration in the slope and a linear approximation of deceleration on level road, the point of going into fuel cut off can be calculated from a desired speed at the end of the slope.

As mentioned earlier, the difference in fuel consumption for different speed profiles is moderate for the simulation cases presented if not considering speed limitation. Typically, the fuel savings using the optimal strategy as presented in Figure 10 and Figure 12 is in the order of 1-2% for the simulated road profile. However, taking account for speed limits and adjusting the policy as described above, see Figure13, the fuel savings are above 10%.

So far, road sections consisting of level road, and one down hill slope of constant inclination have been examplified. A real road could be considered as a sequence of sections with constant inclination. The problem of finding the optimal speed profile for such sequences can be solved using the same strategy as above adding the constraint that the speed at the end of one section must equal the initial speed of the following section. The parameter to optimize is then the constant speed on the sections of level road and small inclinations.

Another observation can bee made. When looking at numerical solutions to optimal driving as presented in, e.g. [6, 8, 9], there is often oscillations in the control inputs and in some cases also the vehicle speed, and this often occurs close to switch points similar to those in e.g. Figures 9 -12. Using the results presented here it is easier to understand if numerical solutions to optimal control problems are subject to numerical or other errors.

6 Derivation of optimal controls

Up till now it has been argued with an intuitive reasoning what the optimal controls are, namely: 1) At level road or in small gradients the optimal engine fueling is the one that corresponds to a constant vehicle speed. 2) In steep downhill slopes fuel injection is cut off. Before the slope the fuel injection in some cases was cut off in order to minimize brake usage. After the slope fuel injection remained cut off until cruising speed was reached. 3) In long downhill slopes the brakes might have to be applied in order not to exceed the speed limit. For completeness it will in this section be mathematically proven that the above stated optimal controls also are the mathematically optimal controls.

Using the change of variables $ds = vdt$ the problem considered can be formulated as

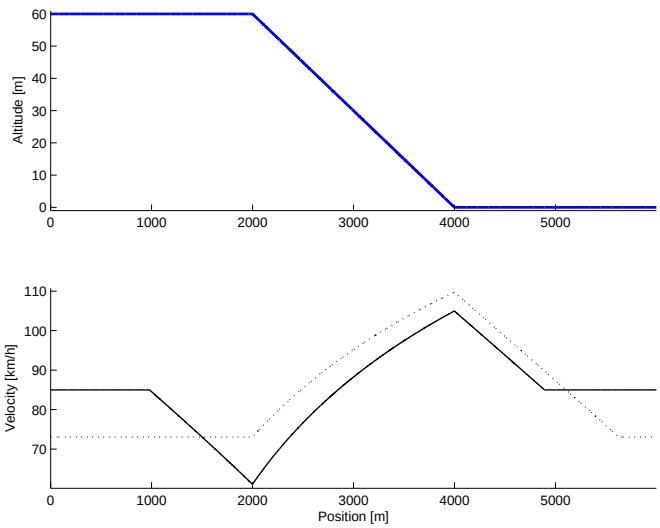

Figure 12: *Two different speed profiles with the same average speed. The distance with fuel cut off is shorter for the dotted profile than the solid profile, but the lower cruising speed still results in a lower over all fuel consumption.*

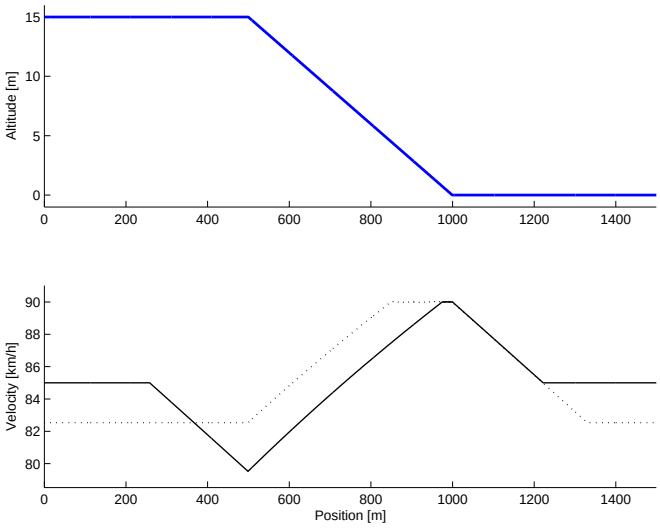

Figure 13: *Using an optimal strategy disregarding speed limits is no longer optimal when speed limitation is introduced. In this case the speed is limited to 90 km/h. The old optimal strategy, dashed line, has to use the brakes at the end of the slope. The new optimal policy, solid line, cuts the fuel injection at a time such that the maximum allowed speed is reached at the end of the slope without using the brakes.*

the following optimal control problem [1]

$$\begin{aligned} &\min \int_{s_0}^{s_f} L(s)ds \\ &x'(s) = f(x,u) \\ &x(s_0) = x_0, \qquad \psi(x(s_f)) = 0 \\ &C(x(s)) \leq 0 \end{aligned} \tag{46}$$

where in this case $L(s) = \delta(s)$, the states are $x^T = \begin{bmatrix} v & t \end{bmatrix}$, i.e. vehicle speed and traveled time. The control variables are $u^T = \begin{bmatrix} \delta & F_b \end{bmatrix}$, i.e. fueling and braking force. The state constraints at position s_f are given by ψ and the path constraint is $C = v(s) - V_{max}$, where V_{max} is the maximum allowed speed. The system dynamics are as in (10) considering c_C as a function of inclination α. Using a fixed gear and also considering the braking force $F_b(s)$ the dynamics are

$$\begin{aligned} v'(s) &= \tfrac{1}{v}\left(c_\delta \delta(s) + c_v v(s) + c_c + c_{v2} v^2(s) - F_b\right) \\ t'(s) &= \tfrac{1}{v(s)} \end{aligned} \tag{47}$$

where ' denotes differentiation with respect to position. The Hamiltonian that is to be minimized [1] is

$$H = L + \lambda^T f + \mu C \tag{48}$$

which in this case is

$$H = \delta + \frac{\lambda_1}{v}\left(c_\delta \delta + c_v v + c_c + c_{v2} v^2 - F_b\right) + \lambda_2 \frac{1}{v} + \mu(v - V_{\max}) \tag{49}$$

The dynamics of the adjoint variables are

$$\lambda' = -H_x^T \tag{50}$$

which in this case is

$$\lambda_1' = \frac{\lambda_1}{v^2}\left(c_\delta \delta + c_v v + c_c + c_{v2} v^2 - F_b\right) - \frac{\lambda_1}{v}\left(c_v + 2c_{v2} v\right) + \frac{\lambda_2}{v^2} - \mu \tag{51}$$

and

$$\lambda_2' = 0 \tag{52}$$

It now is convenient to change variables according to

$$p = 1 + \frac{c_\delta}{v}\lambda_1, \qquad p' = \lambda_1' \ \frac{c_\delta}{v} - \lambda_1 \frac{c_\delta}{v^2} v' \tag{53}$$

which gives the Hamiltonian

$$H = p\delta + \frac{p-1}{c_\delta}\left(c_c + c_v v + c_{v2} v^2\right) - \frac{p-1}{c_\delta} F_b + \frac{\lambda_2}{v} \tag{54}$$

and the adjoint dynamics

$$p' = \frac{p-1}{v^2}\left(-c_v v - 2c_{v2} v^2\right) + \frac{\lambda_2 c_\delta}{v^3} - \mu \frac{c_\delta}{v} \tag{55}$$

Note that the adjoint dynamic is unstable in the causal direction and hence should be simulated in the acausal direction, i.e. time should be reversed when simulating p. Doing so (55) becomes

$$p' = -\frac{p-1}{v^2}\left(-c_v v - 2c_{v2}v^2\right) - \frac{\lambda_2 c_\delta}{v^3} + \mu\frac{c_\delta}{v} \tag{56}$$

The optimal controls are found by minimizing the Hamiltonian (54). It is seen that there are a few choices of optimal control listed below:

- If $p < 0$, $\delta = \delta_{\max}$, i.e. maximum fueling
- If $p = 0$, δ is arbitrary, i.e. partial fueling
- If $p > 0$, $\delta = \delta_{\min}$, i.e. no fueling
- If $p < 1$, $F_b = F_{b,\min}$, i.e. no braking
- If $p = 1$, F_b is arbitrary, i.e. partial braking
- If $p > 1$, $F_b = F_{b,max}$, i.e. maximum braking

The cases of $p = 0$ and $p = 1$ will now be treated. When cruising, i.e. driving on level roads or in small gradients it is not expected that fueling reaches the limits of δ_{max} or δ_{min}. Hence, for cruising at lower speed than the speed limit V_{max}, $p = p' = \mu = 0$ and (56) becomes

$$0 = \frac{1}{v^2}\left(-c_v v - 2c_{v2}v^2\right) - \frac{\lambda_2 c_\delta}{v^3} \tag{57}$$

Since λ_2 is constant, the speed is constant when fueling is not in the limit. This constant speed is given by the above equation and is dependant on the constant λ_2. The value of λ_2 is chosen such that the end constraint on traveled time is fulfilled. Note that since $c_v < 0$, $c_{v2} < 0$, and $c_\delta > 0$, the adjoint variable $\lambda_2 > 0$.

In an instant of partial braking $p = 1$ and (56) would become

$$p' = -\frac{\lambda_2 c_\delta}{v^3} + \mu\frac{c_\delta}{v} \tag{58}$$

When the speed is below the speed limit $\mu = 0$ which gives $p' < 0$. Hence, as long as the speed is below the speed limit p will not stay at $p = 1$ and therefore the conclusion can be drawn that the brakes never will be used in such cases. During sections of partial braking $p' = 0$ and (56) becomes

$$0 = -\frac{\lambda_2 c_\delta}{v^3} + \mu\frac{c_\delta}{v} \tag{59}$$

and the speed $v = V_{max}$. To conclude, the possible choices of optimal controls are: 1) partial fueling such that the vehicle speed is constant. 2) zero fueling used to decelerate on level road or in small gradients or to accelerate in large gradients. 3) Maximum fueling in and in the neighborhood of steep uphill slopes. 4) Partial braking in steep downhill slopes when the vehicle speed is equal to the speed limit.

7 Conclusions

Optimal speed profiles for heavy trucks driving important test road profiles have been presented. The method has been based on analytic solution for linear road segments, and the continuous connection of such solutions. An important effect of that strategy is that the problem of finding the optimal speed trajectory is reduced to a parametric optimization problem of finding the positions for switching between optimal control inputs. This reduces the dimension of the problem significantly compared to other methods. Further, it provides a way of validation of solutions to optimal driving subject to numerical or other errors. The more important conclusions are on a behavioral level. It was shown that it is optimal to keep a constant speed on level road and in small gradients. For large gradients in downhill slopes several interesting conclusions can be drawn. The first is that it is optimal for most cases to drive at cruising speed to the beginning of the slope, then cut the fuel injection and let the vehicle accelerate down the slope, and then decelerate after the slope down to cruising speed again. The acceleration in the downhill slope can be used to lower the speed on level sections while still keeping a desired average speed over the total distance. However, considering a more realistic case where there is a top speed limit, there is an interesting switch in the optimal strategy. The optimal speed profile is now to cut the fuel injection at a point before the downhill slope such that the vehicle will reach the maximum allowed speed at the end of the slope. The point where to cut the fuel injection can be calculated from the presented analytical solutions of the vehicle motion. Thus, the most important contribution is to provide insight into proper strategies for standard cases like up- and downhill slopes, hills and depressions, and that these base strategies can be continuously connected to a complete strategy while still keeping explicit parameter dependence.

Acknowledgments

The Swedish Energy Agency and the Swedish Foundation for Strategic Research are gratefully acknowledged for their funding.

Contact

Anders Fröberg, Division of Vehicular Systems, Department of Electrical Engineering, Linköpings Universitet, SE-581 83 Linköping, Sweden, Telephone: +46-13-284066. Fax: +46-13-282035. E-mail: froberg@isy.liu.se

Bibliography

[1] Arthur E. Bryson and Yu-Chi Ho. *Applied optimal control.* Taylor and Francis, 1975.

[2] David J. Chang and Edward K. Morlok. Vehicle speed profiles to minimize work and fuel consumption. *Journal of transportation engineering*, 131(3):173–182, 2005.

[3] A. Fröberg, E. Hellström, and L Nielsen. Explicit fuel optimal speed profiles for heavy trucks on a set of topographic road profiles. *SAE Technical Paper Series, 2006-01-1071,* 2006.

[4] A. Fröberg, L. Nielsen, L-G. Hedström, and M. Pettersson. Controlling gear engagement and disengagement on heavy trucks for minimization of fuel consumption. *IFAC World Congress. Prague, Czech Republic*, 2005.

[5] I.M. Gelfand and S.V. Fomin. *Calculus of variations.* Dover, 2000.

[6] E. Hellström, A. Fröberg, and L. Nielsen. A real-time fuel-optimal cruise controller for heavy trucks using road topography information. *SAE Technical paper series*, (2006-01-0008), 2006.

[7] Erik Hellström. *Explicit use of road topography for model predictive cruise control in heavy trucks.* Masters thesis, LiTH-ISY-EX-05/3660-SE, Linköping Institute of Technology, Linköping, 2005.

[8] J.N. Hooker. Optimal control of automobiles for fuel economy. *Transportation Science*, 17(2), May 1983.

[9] J.N. Hooker. Optimal driving for single-vehicle fuel economy. *Transportation Research part a,* 22(3), May 1988.

[10] U. Kiencke and L. Nielsen. *Automotive Control Systems, 2nd ed.* Springer-Verlag, 2005.

[11] F. Lattemann, K. Neiss, S. Terwen, and T. Connolly. The predictive cruise control -a system to reduce fuel consumption of heavy duty trucks. *SAE Technical paper series*, (2004-01-2616), 2004.

[12] Tony Sandberg. *Heavy Truck Modeling for Fuel Consumption Simulations and Measurments.* Licentiate thesis, LiU-TEK-LIC-2001:61, Linköping Institute of Technology, Linköping, 2001.

[13] S. Terwen, M. Back, and V Krebs. Predictive powertrain control for heavy duty trucks. *First IFAC Symposium on Advances in Automotive Control*, 2004.

Paper F

OPTIMAL CONTROL UTILIZING ANALYTICAL SOLUTIONS FOR HEAVY TRUCK CRUISE CONTROL[1]

Anders Fröberg[⋆]**, Lars Nielsen**[⋆]

[⋆] *Dep. of Electrical Engineering, Linköpings universitet,*
SE-*581 83 Linköping, Sweden.* {froberg, lars}@isy.liu.se.

Abstract

The problem addressed is how to control vehicle speed over a given distance on a given time such that fuel consumption is minimized. Analytical expressions for the necessary optimality conditions are derived. These expressions are essential for the understanding of the decisive parameters affecting fuel optimal driving and the analytical optimality conditions make it possible to see how each parameter affects the optimal solution. Optimal solutions for an affine engine torque model are compared to solutions for a piece-wise affine model, and it is shown that small non-linearities have significant effect on the optimal control strategy. The solutions for the non linear engine model has a smoother character but also requires longer prediction horizons.

Assuming a continuously variable transmission, optimal gear ratio control is presented, and it is shown how the maximum fueling function is essential for the solution. It is also shown that the gear ratio never is chosen such that engine speed exceeds the speed of maximum engine power. Those results are then extended to include a discrete stepped transmission, and it is demonstrated how gear shifting losses affect optimal gear shifting positions.

The theory presented is a good base to formalize the intuition of fuel efficient driving. To show this, optimal solutions are presented in simulations of some constructed test road profiles, where the typical behavior of an optimal solution is pointed out, and also which parameters that are decisive for the fuel minimization problem. This is then used to design a simple low-complexity computationally efficient rule-based look ahead cruise controller, and it is demonstrated that simple parametrized quantitative rules have potential for significant fuel savings.

[1] This is an edited version of the technical report [4], Optimal Control Utilizing Analytical Solutions for Heavy Truck Cruise Control.

1 Introduction

Fuel cost is a large part of the operating cost of heavy trucks. Hence there has been an increasing interest in predictive cruise controllers that minimizes fuel consumption [19, 5, 11]. Some early work in finding fuel optimal speed profiles for automobiles is reported in [16, 8]. Other related work regarding passenger cars in urban traffic has shown on a large potential to use speed control to minimize fuel consumption [14]. Similar methods as discussed in this paper has earlier been used on rail vehicles [13].

The scenario studied here concerns heavy trucks used for long haulage and the goal is to control vehicle speed over a given distance on a given time such that fuel consumption is minimized. It is assumed that road topography ahead of the vehicle is known and the resulting problem will be referred to as look ahead cruise control. In a practical case road topograghy can be extracted using for example a navigation system with 3D maps or collected data. The differences between optimal solutions for a linear engine torque model and a non linear engine torque model is investigated. The non linear model is here modeled as a piece-wise affine, PWA, function. Optimal gear shifting is also studied, both with a simplified transmission model with continuously variable gear ratio, and for a discrete step transmission.

Based on the modeling, the optimality conditions for the fuel minimization problem become analytical expressions. From these expressions the effect of each parameter can be studied which is important to gain knowledge of what factors that affect fuel consumption. For example, the optimal control derived here can be used as an aid when analyzing and validating the behavior of numerical controllers as described in [6] and [7]. The results are also the basis for formalizing an intuitive optimal driving behavior which can be used for design of simple rule based controllers. In this paper the effect of other traffic is not explicitly considered. However, one way to handle such situations is to consider other traffic as an extra constraint on vehicle speed. In [17] a method is presented that optimizes vehicle speed when approaching a slower vehicle.

The paper is organized as follows. The fuel minimization problem is formulated in Section 2. Under the assumption of an affine engine torque model and a fixed gear ratio, necessary conditions for optimal fueling is derived in Section 3. In Section 4 a piece-wise affine, PWA, model is used to capture the non linearities in the engine characteristics. Assuming a continuously variable transmission, optimal gear ratio is derived in Section 5 and the results are then extended to include a discrete stepped transmission. The optimality conditions for the different modeling choices are used to find optimal solutions for a few illustrative constructed road profiles, and simulation results are presented in Section 6. It is also demonstrated in Section 8 that the derived expressions can be used to design a low-complexity computationally efficient rule-based look ahead cruise controller.

2 Problem formulation

The problem to be solved is to minimize fuel consumption over a given distance s_f with specified travel time T_t. With notation according to Table 1 this is written as

$$\min \quad \int_0^{s_f} \frac{\delta n_{cyl} i}{2\pi n_r r} ds \tag{1}$$

$$\text{s.t.} \quad \int_0^{s_f} \frac{1}{v} ds = T_t \tag{2}$$

The vehicle is modeled as in [3], and [10], and can be written as

$$\dot{v} = \frac{1}{J}\left(F_{prop} - F_{air} - F_{roll} - F_{slope} - F_b\right) \tag{3}$$

where the variables and parameters are selected according to Table 1, and the forces and inertias are set according to Table 2. Losses in different parts of the driveline are easily modeled as lumped losses by modifying the coefficients of engine friction losses and vehicle resistance forces. Measured engine torque from a real engine is given in Figure 1. It is there seen that an affine model of engine torque is a good first approximation, but for a detailed analysis the non linearities should be included.

Variables and parameters	Description
α	Road slope $[rad]$
δ	Engine fueling $[kg/stroke]$
η	Transmission efficiency
ω_e	Engine speed $[rad/s]$
ρ	Air density $[kg/m^3]$
θ_e	Crank shaft angle $[rad]$
A	Front area $[m^2]$
$c_{e\delta}$, $c_{e\omega}$, c_{ec}	Engine torque coefficients
c_d	Air drag coefficient
c_{r1}, c_{r2}, c_{r3}	Rolling resistance coefficients
F_b	Brake force
g	Gravitational acceleration
i	Gear ratio
J_e	Engine inertia $[kgm]$
J_d	Lumped drivline inertia $[kgm]$
m	Vehicle mass $[kg]$
n_{cyl}	Number of cylinders
n_r	Revolutions per stroke
r	Wheel radius $[m]$
s	Traveled distance $[m]$

Table 1: *Variables and parameters for the truck model.*

Quantity	Equation	Description
$J(i(t))$	$m + J_e i^2 \eta \frac{1}{r^2} + \frac{J_d}{r^2}$	Vehicle Inertia
$F_{air}(v(t))$	$\frac{1}{2}\rho c_d A v^2$	Air resistance
$F_{prop}(\delta(t), \omega_e(t), i(t))$	$\frac{i\eta}{r}(f_\delta(\delta) + f_\omega(\omega_e) + c_{ec})$	Propulsive force
$F_{roll}(v(t))$	$m(c_{r1} + c_{r2}v + c_{r3}v^2)$	Rolling resistance
$F_{slope}(\alpha(s(t)))$	$mg\sin\alpha(s)$	Force due to road slope

Table 2: *Vehicle forces and inertias.*

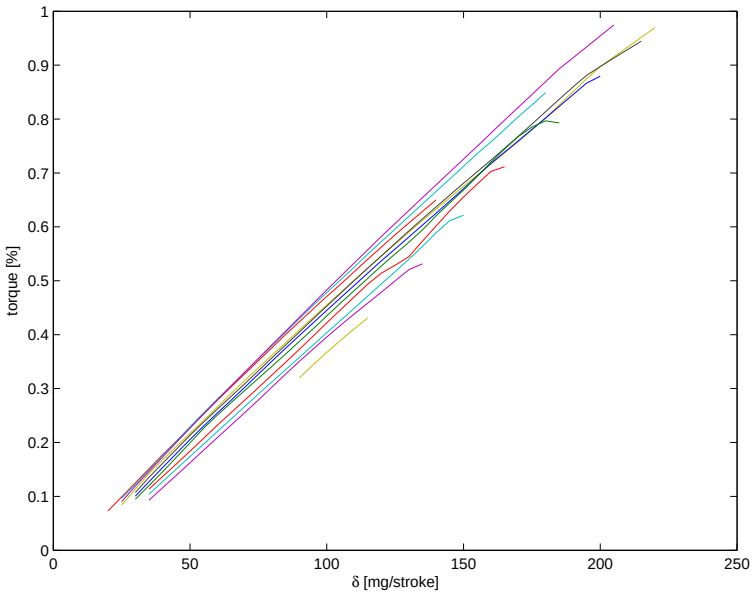

Figure 1: *Measured engine torque. Each line represents a given engine speed.*

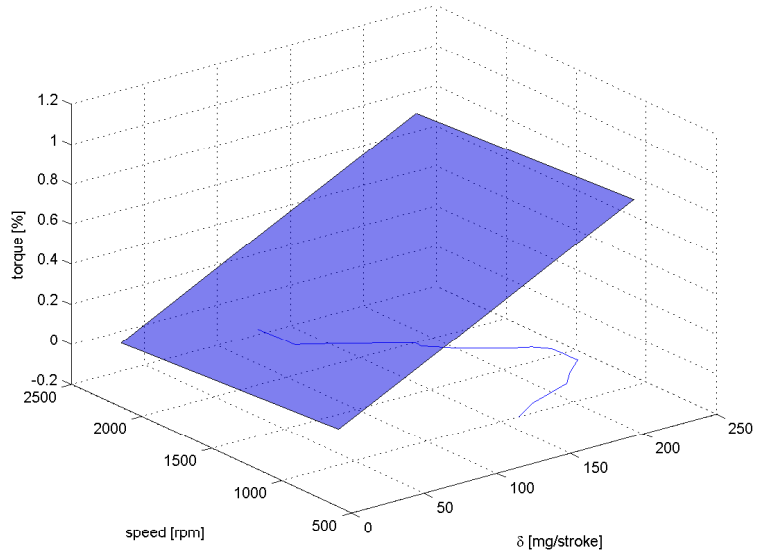

Figure 2: *Affine approximation of engine torque. A maximum fueling function is also plotted as function of engine speed.*

3 Optimal fueling -Affine engine characteristics

It will first be assumed that engine torque can be approximated as an affine function. With inspiration from the measured data in Figure 1, the model depicted in Figure 2 is constructed. Note that engine torque in Table 2 is $T_e = f_\delta(\delta) + f_\omega(\omega_e) + c_{ec}$. Using $\omega_e = \frac{iv}{r}$, the affine approximation of engine torque gives that F_{prop} in Table 2 is written as

$$F_{prop} = \frac{i\eta}{r}(c_{e\delta}\delta + c_{e\omega}\frac{iv}{r} + c_{ec}) \tag{4}$$

In Figure 2 the maximum fueling function for a real engine is plotted. That function will here firstly be approximated as an affine function of engine speed, but later a more exact quadratic function will be used. Again using $\omega_e = \frac{iv}{r}$ this can be written as

$$C_\delta = \delta - (c_{\omega con}i\frac{v}{r} + c_{ccon}) \leq 0 \tag{5}$$

and it is assumed that $\delta \geq 0$.

Since road slope is a function of position it is convenient to change independent variable from time t to position s,

$$\frac{d}{ds} = \frac{1}{v}\frac{d}{dt} \tag{6}$$

Let the states x of the system be vehicle speed v and traveled time T, i.e. $x = [v, T]^T$.

Neglecting engine inertia the system dynamics becomes

$$\begin{aligned}\frac{dv}{ds} &= \frac{1}{v}\Big(c_\delta i\delta + c_\omega i^2\frac{v}{r} + c_e i \\ &\quad + c_c + c_v v + c_{v2}v^2 + c_\alpha \sin\alpha(s)\Big) = f_v \qquad (7)\\ \frac{dT}{ds} &= \frac{1}{v} = f_T \qquad (8)\end{aligned}$$

where the model coefficients can be derived from those given in Tabel 1.

The fuel minimization problem will be solved with optimal control theory which is thoroughly described in the classic textbook [1], and that notation will here be followed. The function to be minimized, (1), with constraints (5), (7), (8), are used to construct the following Hamiltonian

$$H = \delta i + \lambda_v f_v + \lambda_T f_T + \mu_\delta C_\delta \qquad (9)$$

where $\frac{n_{cyl}}{2\pi n_r r}$ are included in the multipliers. When the constraint C_δ is inactive $\mu_\delta = 0$, and when the constraint is active $\mu_\delta \geq 0$. The dynamics of the adjoint state variables are $\frac{d\lambda}{ds} = -H_x^T$, i.e.

$$\begin{aligned}\frac{d\lambda_v}{ds} &= \frac{\lambda_v}{v^2}(c_\delta i\delta + c_e i + c_c - c_{v2}v^2 + c_\alpha \sin\alpha) \\ &\quad + \frac{\lambda_T}{v^2} + \mu_\delta c_{\omega con}\frac{i}{r} \qquad (10)\\ \frac{d\lambda_T}{ds} &= 0 \qquad (11)\end{aligned}$$

As in [12] the optimal fueling control is found by minimizing H with respect to the control variable δ. Since the Hamiltonian is linear in δ the optimal control sequence will consist of sections of maximum fueling, minimum fueling or sections where $\frac{dH}{d\delta} = 0$. The latter sections are called singular arcs. Differentiating the Hamiltonian gives

$$\frac{dH}{d\delta} = i(1 + \frac{\lambda_v c_\delta}{v}) + \mu_\delta \qquad (12)$$

For sections of singular arcs where $C_\delta < 0$, i.e. $\mu_\delta = 0$, it is seen in (12) that $\lambda_v = -\frac{v}{c_\delta}$. It must also hold that $\frac{d}{ds}(\frac{dH}{d\delta}) = 0$ which gives

$$\begin{aligned}\frac{d}{ds}(\frac{\lambda_v c_\delta}{v}) &= \frac{d\lambda_v}{ds}\frac{c_\delta}{v} - \frac{\lambda_v c_\delta}{v^2}f_v \\ &= \frac{\lambda_v c_\delta}{v^3}(-c_\omega\frac{i^2 v}{r} - c_v v - 2c_{v2}v^2) + \frac{\lambda_T c_\delta}{v^3} = 0 \qquad (13)\end{aligned}$$

Putting (12) equal to zero, solving for λ_v, and inserting into (13) gives the following dependency between v and λ_T

$$\frac{v^2}{c_\delta}(c_\omega\frac{i^2}{r} + c_v + 2c_{v2}v) + \lambda_T = 0 \qquad (14)$$

Since λ_T is constant, (11), the system must be in stationarity during singular arcs, i.e. v is constant, and since (14) and $\lambda_v = -\frac{v}{c_\delta}$, λ_v must be constant. The constant λ_T is determined

by that the constraint on total travel time (2) is fulfilled. Given initial and end conditions on the states v and T, the complete problem to solve thus consists of Equations (2), (5), (7), (8), (10)-(12), (14).

3.1 Solution characteristics

As mentioned above, the optimal control sequence consists of maximum fueling, zero fueling and, singular arcs where fueling δ is chosen such that vehicle speed is stationary. Obviously, due to the nature of the vehicle resistance forces, the global optimal solution will be stationary, i.e. constant speed, whenever it is possible, i.e. whenever the road gradient is small enough. Road gradient is considered small if maximum fueling is enough to keep constant speed in an uphill slope and if zero fueling does not result in acceleration in a down hill slope, [2]. Such small enough gradients will here be defined. Consider the model (7) and let fueling $\delta = 0$. It is seen that for all inclination angles

$$\tilde{\alpha}_d \in \{\tilde{\alpha}_d : c_\omega i^2 \frac{v}{r} + c_e i + c_c + c_v v + c_{v2} v^2 + c_\alpha \sin\tilde{\alpha}_d > 0\} \tag{15}$$

the vehicle will accelerate even though the engine does not produce any work. The limit for the set $\tilde{\alpha}_d$ is found by setting equality in (15) resulting in

$$\begin{aligned} \alpha_d &= \arcsin \frac{c_\omega i^2 \frac{v}{r} + c_e i + c_c + c_v v + c_{v2} v^2}{-c_\alpha} \\ &= \arcsin \frac{\frac{c_{e\omega} \eta i^2 v}{r^2} + \frac{c_{ec} \eta i}{r} - m c_{r1} - m c_{r2} v - m c_{r3} v^2 - \frac{1}{2}\rho c_d A v^2}{mg} \end{aligned} \tag{16}$$

that of course is a negative angle, $\alpha_d < 0$, for realistic vehicle parameters. For uphill slopes the vehicle will accelerate when using maximum fueling δ_{max} for angles

$$\tilde{\alpha}_u \in \{\tilde{\alpha}_u : c_\delta i \delta_{max} + c_\omega i^2 \frac{v}{r} + c_e i + c_c + c_v v + c_{v2} v^2 + c_\alpha \sin\tilde{\alpha}_u > 0\} \tag{17}$$

and the limit for the set is

$$\begin{aligned} \alpha_u &= \arcsin \frac{c_\delta i \delta_{max} + c_\omega i^2 \frac{v}{r} + c_e i + c_c + c_v v + c_{v2} v^2}{-c_\alpha} \\ &= \arcsin \frac{\frac{c_{e\delta} \eta i}{r} \delta_{max} + \frac{c_{e\omega} \eta i^2 v}{r^2} + \frac{c_{ec} \eta i}{r} - m c_{r1} - m c_{r2} v - m c_{r3} v^2 - \frac{1}{2}\rho c_d A v^2}{mg} \end{aligned} \tag{18}$$

that is a positive angle, $\alpha_u > 0$.

Using Equations (16) and (18) the following definition can be made

Definition *Small gradients are all gradients with inclination* α *such that*

$$\alpha_d < \alpha < \alpha_u \tag{19}$$

Other gradients are referred to as steep gradients.

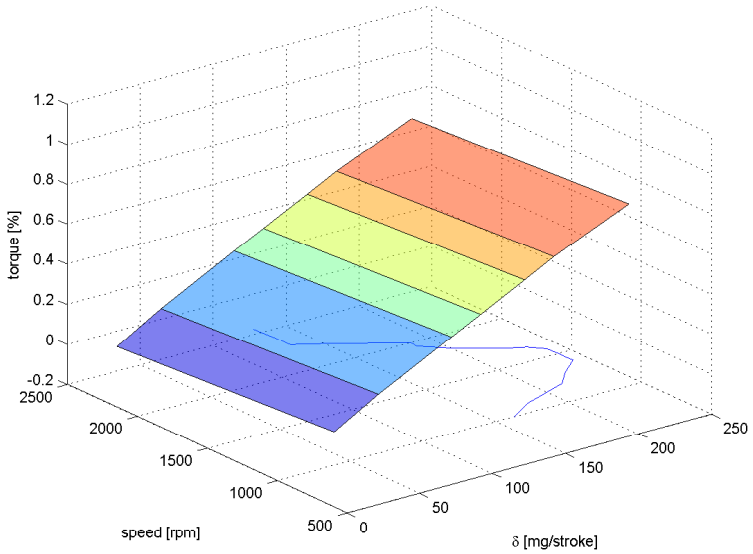

Figure 3: *Engine torque as a piece-wise affine function of fueling. Maximum fueling is plotted as function of engine speed.*

To conclude, there are three possible control settings for optimal fueling, i.e. maximum fueling, fuel cut-off, and to control fueling such that vehicle speed is constant.

The adjoint variable λ_v responds to future changes in inclination α, and for steep slopes maximum or minimum fueling respectively is not enough to keep λ_v stationary. As seen in (12) $\frac{dH}{d\delta}$ depends on λ_v and hence λ_v is important for the control switch points. An optimal solution will thus consists of constant fueling for flat road and small gradients, but in and in a neighborhood of steep uphill slopes it will be optimal to use maximum fueling, and, in and in a neighborhood of steep downhill slopes it will be optimal to cut off the fuel injection. The importance of the adjoint variable λ_v will be stressed later and in Section 6.5 it will be used for a discussion on the sensitivity of the optimal solution.

4 PWA engine characteristics

To better approximate the engine characteristics the engine torque will now be modeled as a piece-wise affine function of fueling δ, see Figure 3 for a hypothetic example. Let fueling be divided in N regions, see Figure 4 for a schematic depiction. When the engine is operated in region n the propulsive force F_{prop} in Table 2 is written

$$F_{prop} = \frac{i\eta}{r}\left(\sum_{i=1}^{n-1}(k_{\delta,i}-k_{\delta,i+1})\delta_{max,i}+k_{\delta,n}\delta+k_{\omega e}\omega_e+k\right) \tag{20}$$

When operating in fueling region n the vehicle dynamics can be written in the form (7) with obvious changes to the parameters, e.g. let $c_\delta = c_{\delta,n} = \frac{\eta k_{\delta,n}}{Jr}$. Differentiating the

Hamiltonian with respect to fueling now gives

$$\frac{dH}{d\delta} = i(1 + \frac{\lambda_v c_{\delta,n}}{v}) + \mu_\delta \tag{21}$$

Considering only the operating region where the engine is currently operating, optimal control can be derived as in Section 3, i.e. fueling can be in the limit of the region or fueling can be such that vehicle speed is constant. Each engine region can be associated with a constant speed solution as in Equation (14), i.e. the solution to

$$\frac{v^2}{c_{\delta,n}}(c_\omega \frac{i^2}{r} + c_v + 2c_{v2}v) + \lambda_T = 0 \tag{22}$$

For each engine operating region n, limit angles can be defined as in Equation (19) by modifying Equations (16) and (18) giving

$$\alpha_{d,n} < \alpha < \alpha_{u,n} \tag{23}$$

4.1 Concave engine map

Now consider a concave torque characteristic, i.e. $c_{\delta,i} > c_{\delta,i+1}$. From (21) it is seen that when

$$-\frac{1}{c_{\delta,i+1}} < \frac{\lambda_v}{v} < -\frac{1}{c_{\delta,i}} \tag{24}$$

it will hold that $\frac{dH}{d\delta_i} < 0$ and $\frac{dH}{d\delta_{i+1}} > 0$. Since both v and λ_v are continuous functions the optimal control sequence will consist of a period where fueling is on the border of fueling region i and $i+1$. This means that there is never an immediate change from constant speed to maximum or minimum fueling, but the solution will consist of a "smoother" change to the upper or lower limit of fueling. With $c_{\delta,i} > c_{\delta,i+1}$ the corresponding stationary solution given by (22) will be $v_i > v_{i+1}$. This means that some downhill slopes will have constant speed solutions with higher speed than for flat road and some uphill slopes will have constant speed solutions that is lower than for flat road.

4.2 Non concave engine map

For the approximation in Figure 3 the requirement $c_{\delta,i} > c_{\delta,i+1}$ is not fulfilled for all i, i.e. the approximation is not concave. For such a case further reasoning needs to be done in order to find the optimal control. An example fuel-torque characteristic is depicted in Figure 4. Let the torque characteristic have slope $c_{\delta,i}$ in the respective region. Consider a case where cruising at constant speed at flat road implicates $i = 1$, i.e. a fueling value in region 1. When a steep uphill slope is approached there is some distance where for example $1 + \frac{\lambda_v c_{\delta,i}}{v} > 0$ for $i = 2,4$ and $1 + \frac{\lambda_v c_{\delta,i}}{v} < 0$ for $i = 1,3$. For such a position, if considering only region 1 and 2 fueling would be chosen at the border between those regions. Considering only region 3 and 4 would in the same way give a fueling in the border between those regions. There is hence two candidate values of fueling to use. To decide which one that is optimal an approximation to the torque characteristics that reduces the number of fueling regions can be used. Such an approximation is marked as

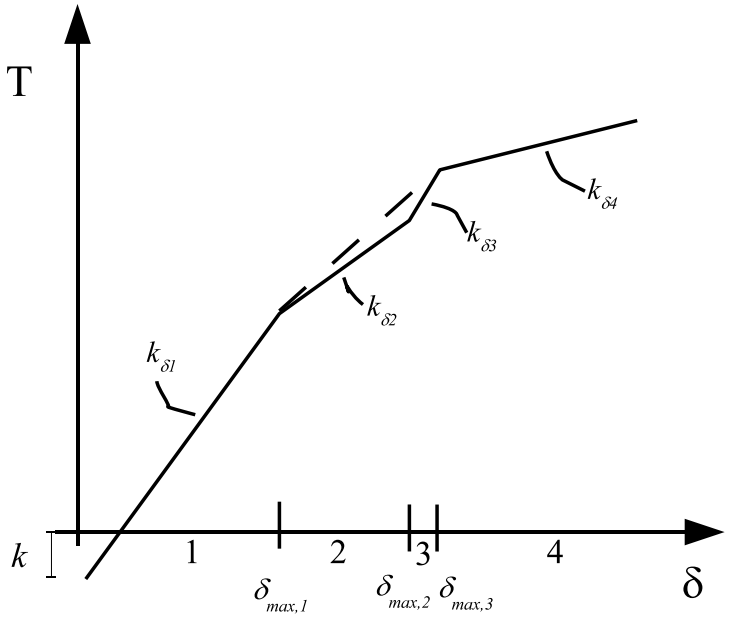

Figure 4: *piece-wise affine approximation of engine characteristics.*

a dashed line in Figure 4. In this way the fueling-torque characteristics is transformed into a concave function and the choice of fueling is uniquely decided by considering (24). Similar reasoning can be made for downhill slopes.

4.3 Non linear engine speed characteristics

To further improve the approximation of the engine characteristics, non-linearities in engine speed dimension could also be considered. One way is to consider engine torque as a piece-wise affine function of both speed and fueling.

Let engine speed be divided in M regions and let fueling be divided in N regions. When the engine is operated in region (m,n) the propulsive force F_{prop} in Table 2 is written

$$\begin{aligned} F_{prop} &= \frac{i\eta}{r}\left(\sum_{i=1}^{n-1}(k_{\delta,i}-k_{\delta,i+1})\delta_{max,i}+k_{\delta,n}\delta+\right. \\ &\qquad \left.\sum_{j=1}^{m-1}(k_{\omega e,j}-k_{\omega e,j+1})\omega_{emax,j}+k_{\omega e,m}\omega_e+k\right) \end{aligned} \tag{25}$$

See Figure 5 for an hypothetic engine model with $M=8, N=6$.

Differentiating the Hamiltonian with respect to fueling gives the same result as in (21).

Considering only the operating region where the engine is currently operating, optimal control can be derived as in Section 3, i.e. fueling can be in the limit of the region or

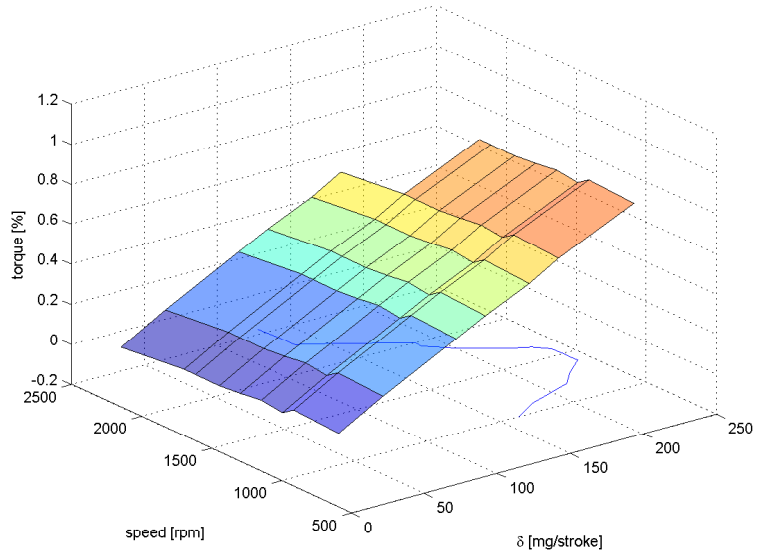

Figure 5: *piece-wise affine approximation of engine characteristics. Maximum fueling is plotted as function of engine speed.*

fueling can be such that vehicle speed is constant. Each engine region can be associated with a constant speed solution as in Equation (14), i.e. the solution to

$$\frac{v^2}{c_{\delta,n}}(c_{\omega,m}\frac{i^2}{r}+c_v+2c_{v2}v)+\lambda_T=0 \tag{26}$$

For each engine operating region $[m,n]$, limit angles can be defined as in Equation (19) by modifying Equations (16) and (18) giving

$$\alpha_{d,m,n}<\alpha<\alpha_{u,m,m} \tag{27}$$

Modeling engine torque as a piece-wise affine function of engine speed gives a Hamiltonian that is not differentiable with respect to v. This means that λ_v will have a discontinuity in the switch point between different engine speed regions. How this can be treated is described in Chapter 3.6 in [1]. However, accounting for the non-linearities in the speed dimension does not affect the principal behavior of the optimal control given by (21) in the sense that the optimal fueling also in this case is in the border of fueling regions or such that vehicle speed is constant. However, both the vehicle dynamics (7) and the adjoint dynamics (10) is affected by the engine characteristics in the speed dimension, which means that the optimal control switch points depends on it. Since the optimal fueling behavior in principal is not affected by the modeling in the speed dimension the remaining of this paper only considers nonlinearities in the fueling dimension.

A non-concave engine torque can require some care in finding the global optimal solution. One such case is treated in [9]. That case is when the desired average speed

corresponds to an inefficient engine operating point. Then it can be optimal to switch between two other cruising speeds resulting in correct average speed. This can be studied using Equation (26). For a given λ_T it can be the case that no region has a feasible constant speed solution corresponding to desired average speed. In such a case the optimal solution consists of switching between different cruising speeds.

Other ways than (25) to make a PWA approximation of the engine map can be more close to the real characteristics. For example one can use a triangular mesh or a bilinear function of engine speed and fueling. However, such approximations would still keep the problem in input affine form and the principal results discussed so far would not be changed.

5 Optimal gear ratio control

Not only fueling control but also gear choice affects the fuel consumption considerably. Although there are high-power applications for which continuously variable transmissions are used [15, 18], the most common transmission for heavy trucks are the discrete step transmission. As a first attempt to study fuel optimal gear shifting, gear ratio i is assumed to be continuously variable and fulfilling $0 < i_{min} \leq i \leq i_{max}$. Later, those results will be used to derive solutions for a stepped transmission.

5.1 Optimal gear ratio - affine maximum fueling

Again study the model with affine engine characteristics (4) from Section 3. Maximum fueling will here be modeled as an affine function of engine speed by using $\omega_e = \frac{iv}{r}$ in (5). Although this is a too simple model to resemble the measured function in Figure 2 the results are illustrative and a base for the more accurate quadratic model that will be used in Section 5.2.

The gear ratio can be varied between a lower and upper limit, i.e., it has to fulfill the following constraints

$$C_{imax} = i - i_{max} \leq 0 \quad (28)$$

$$C_{imin} = i_{min} - i \leq 0 \quad (29)$$

When choosing gear ratio the engine speed must also be kept within limits, i.e.

$$C_{\omega min} = \omega_{min} - \frac{iv}{r} \leq 0 \quad (30)$$

$$C_{\omega max} = \frac{iv}{r} - \omega_{max} \leq 0 \quad (31)$$

The constraints (28)-(31) are adjoined to the Hamiltonian with respective Lagrange multipliers μ_{imax}, μ_{imin}, $\mu_{\omega min}$, and $\mu_{\omega max}$.

$$H = \delta i + \lambda_v f_v + \lambda_T f_T + \mu_\delta C_\delta + \mu_{imax} C_{imax} + \mu_{imin} C_{imin} + \mu_{\omega min} C_{\omega mix} + \mu_{\omega max} C_{\omega max} \quad (32)$$

Differentiating the Hamiltonian (32) with respect to i gives

$$\frac{dH}{di} = \delta(1+\frac{\lambda_v c_\delta}{v}) + 2c_\omega \frac{\lambda_v}{r} i + c_e \frac{\lambda_v}{v} - \mu_\delta c_{\omega con} \frac{v}{r} + \mu_{imax} - \mu_{imin} - \mu_{\omega min} \frac{v}{r} + \mu_{\omega max} \frac{v}{r} \quad (33)$$

During sections of constant speed, i.e. for flat road and small gradients, fueling is not in the limit, i.e. $\mu_\delta = 0$. Then Equation (12) gives $1+\frac{\lambda_v c_\delta}{v} = 0$. Also assume that gear ratio and engine speed is within allowed limits, i.e. the respective $\mu = 0$. The condition $\frac{dH}{di} = 0$ then gives the optimal gear ratio

$$i_{opt} = -\frac{c_e}{c_\omega} \frac{r}{2v} \quad (34)$$

For typical engine characteristics, see Figure 1, $c_e, c_\omega < 0$ or $c_\omega < 0$ and c_e is small. Both situations result in that i_{opt} given by (34) is smaller than i_{min}, and hence, considering limits on i the resulting optimal solution is $i_{opt} = i_{min}$. This minimizes engine speed and hence engine friction.

Assuming that engine speed limits and gear ratio limits are not reached, i.e. $\mu_{\omega min} = \mu_{\omega max} = \mu_{imin} = \mu_{imax} = 0$, optimal gear ratio during sections of maximum fueling is found by combining Equations (5), (12), and, (33), using $\frac{dH}{d\delta} = \frac{dH}{di} = 0$, which gives

$$\begin{aligned} \frac{dH}{di} &= c_{con}(1+\frac{\lambda_v c_\delta}{v}) + c_e \frac{\lambda_v}{v} \\ &\quad + \frac{2}{r}(c_{\omega con} v (1+\frac{\lambda_v c_\delta}{v}) + c_\omega \lambda_v) i = 0 \end{aligned} \quad (35)$$

The optimal gear ratio given by Equation (35) is

$$i_{opt} = -\frac{c_{con}(1+\frac{\lambda_v c_\delta}{v}) + c_e \frac{\lambda_v}{v}}{\frac{2}{r}(c_{\omega con} v (1+\frac{\lambda_v c_\delta}{v}) + c_\omega \lambda_v)} \quad (36)$$

Recall that $1+\frac{\lambda_v c_\delta}{v} < 0$ during sections where maximum fueling is used. It will be shown later in simulations that $1+\frac{\lambda_v c_\delta}{v}$ gets a large magnitude in steep uphill slopes resulting in high gear ratios. Before and after the slope a low gear is used as given by (34). For the model considered $c_{con} c_\delta$ is about 7 times c_e, giving high gear ratios in steep uphill slopes. However, large magnitudes on $c_{\omega con}$ limits the gear ratio to a lower gear ratio.

5.2 Optimal gear ratio - quadratic maximum fueling

To make a better approximation of maximum fueling than (5) the following quadratic model is used

$$C_\delta = \delta - (a_0 + a_1 \frac{iv}{r} + a_2 (\frac{iv}{r})^2) \leq 0 \quad (37)$$

Another choice could be to make a piece-wise affine model, but then the Hamiltonian will not be differentiable with respect to vehicle speed.

The optimal gear ratio is now given from

$$\frac{dH}{di} = \delta(1+\frac{\lambda_v c_\delta}{v}) + 2c_\omega\frac{\lambda_v}{r}i + c_e\frac{\lambda_v}{v} - \mu_\delta(a_1+2a_2\frac{iv}{r})\frac{v}{r} + \mu_{imax} - \mu_{imin} - \mu_{\omega min}\frac{v}{r} + \mu_{\omega max}\frac{v}{r} = 0 \quad (38)$$

When using maximum fueling and assuming that gear ratio limits as well as engine speed limits are not reached, optimal gear ratio is found by combining Equations (12), (37), and (38), which gives

$$3a_2\frac{v^2}{r^2}(1+\frac{\lambda_v c_\delta}{v})i^2 + \left(2a_1\frac{v}{r}(1+\frac{\lambda_v c_\delta}{v}) + 2c_\omega\frac{\lambda_v}{r}\right)i + a_0(1+\frac{\lambda_v c_\delta}{v}) + c_e\frac{\lambda_v}{v} = k_2 i^2 + k_1 i + k_o = 0 \quad (39)$$

Now the optimal gear ratio is

$$i_{opt} = -\frac{k_1}{2k_2} \pm \sqrt{\left(\frac{k_1}{2k_2}\right)^2 - \frac{k_o}{k_2}} \quad (40)$$

Typically, only the solution with the plus sign before the square root gives physically feasible solutions.

Plots of optimal gear solutions. In Figure 6 the solution to Equation (39) is plotted as a function of the decisive variable $1+\frac{\lambda_v c_\delta}{v}$ and vehicle speed v. The lowest possible gear ratio for the vehicle studied is 3.42. Recall that during sections of constant speed $1+\frac{\lambda_v c_\delta}{v} = 0$. Consider the case where cruising speed is 85 km/h and the vehicle is approaching a steep uphill slope. During acceleration before the slope speed will increase and the term $1+\frac{\lambda_v c_\delta}{v}$ will decrease, i.e. the operating point will move downwards to the right in Figure 6. One conclusion that can be drawn from this figure is that it will never be optimal to change gear during the acceleration phase before a steep uphill slope. When the vehicle starts to climb the hill speed will decrease, shifting the operating point to the left, and the operating point enters the region for a possible gear change.

Another thing to notice in Figure 6 is that for large magnitudes of $1+\frac{\lambda_v c_\delta}{v}$ the optimal gear ratio is approximately a function of vehicle speed since the gear ratio contours are almost vertical. As will be shown later in simulations that region is reached when maximum fueling has been used for a longer period of time, i.e. for relatively long or steep uphill slopes.

For any given vehicle speed it is equivalent to see engine speed ω_e as control variable instead of gear ratio i using $\omega_e = \frac{vi}{r}$. Using this substitution in Equation (39) optimal engine speed can be calculated and a contour plot of the achieved result is plotted in Figure 7. It can be seen in the area to the left of the dotted line in Figure 7 that optimal engine speed very well can be described as a function of the decisive variable $1+\frac{\lambda_v c_\delta}{v}$, since the lines are almost horizontal. To the right of the dotted line the solution is restricted by the minimum allowed gear ratio, compare with Figure 6. As will be shown later in simulations the magnitude of the decisive expression $1+\frac{\lambda_v c_\delta}{v}$ depends highly on the length and inclination of uphill slopes. A longer or steeper slope results in larger magnitude of

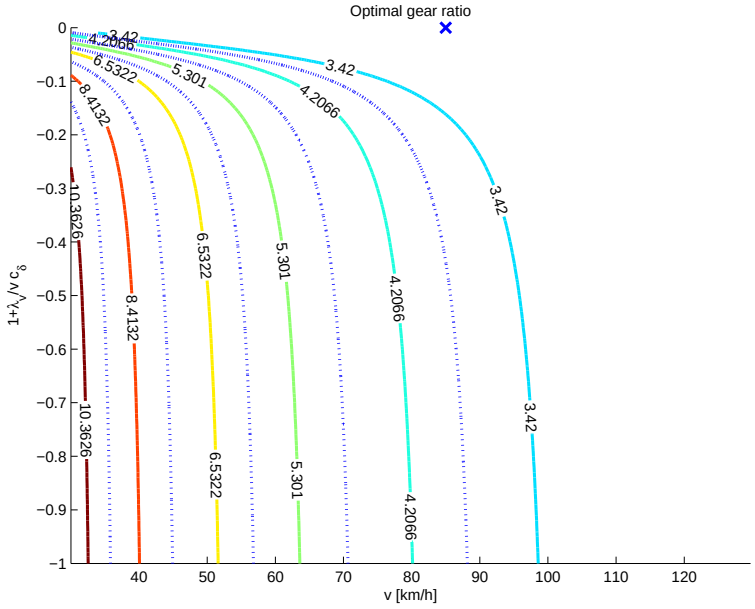

Figure 6: *Contour plot of the optimal gear ratio, i, given by Equation (39). The operating point for stationary vehicle speed at 85 km/h is marked by a cross. The contours are drawn at gear ratio levels corresponding to a discrete step transmission. The dashed lines are the optimal gear shifting points for a discrete step transmission.*

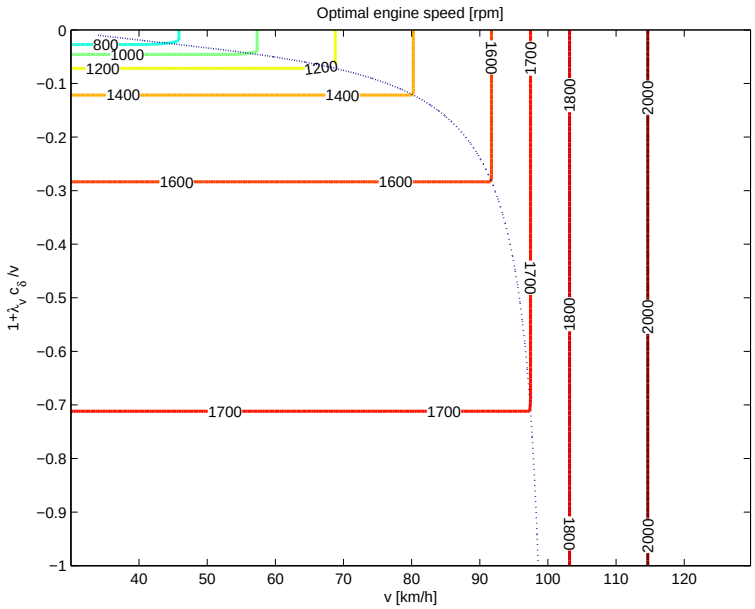

Figure 7: *Contour plot of optimal engine speed.*

$1+\frac{\lambda_v c_\delta}{v}$, which means that optimal engine speed is a function of length and steepness of the slope.

Further analysis and implications of optimality. If the quadratic maximum fueling function is linearized it can be compared with the result in (36). The linearization of the quadratic model in the point ω_0 is

$$C_\delta = \delta - (a_0 - a_2\omega_0^2 + (a_1 + 2a_2\omega_0)\omega) \leq 0 \tag{41}$$

Considering (36) and assuming that $1+\frac{\lambda_v c_\delta}{v}$ has a large magnitude, i_{opt} can be approximated as

$$i_{opt} = -\frac{c_{con}}{\frac{2}{r}c_{\omega con}v} \tag{42}$$

Again using engine speed as an equivalent control instead of gear ratio, using the substitution $\omega_e = \frac{vi}{r}$, an optimal engine speed can be calculated for every vehicle speed. Rewriting (42) to optimal engine speed gives

$$\omega_{opt} = -\frac{c_{con}}{2c_{\omega con}} = -\frac{a_0 - a_2\omega_0^2}{2(a_1 + 2a_2\omega_0)} \tag{43}$$

There is one engine speed $\omega_0 = \omega^*$ where $\omega^* = -\frac{a_0 - a_2\omega^{*2}}{2(a_1+2a_2\omega^*)}$. For $\omega_0 < \omega^*$ it holds that $\omega_{opt} > \omega^*$ and for $\omega_0 > \omega^*$ it holds that $\omega_{opt} < \omega^*$. Hence it is never beneficial to operate at a higher engine speed than ω^*. Rewriting (43) the optimal engine speed is found by solving the following equation

$$3a_2\omega_{opt}^2 + 2a_1\omega_{opt} + a_0 = 0 \tag{44}$$

Using $\omega_e = \frac{vi}{r}$ this expression is quite similar to (39). It will now be shown that when $\left|\frac{\lambda_v c_\delta}{v}\right| >> 1$, optimal engine speed goes to the same engine speed as where maximum torque to the wheels are delivered. The torque delivered by the engine to the wheels is

$$T_w = \frac{r\omega_e}{v}\eta T_e = \frac{r\omega_e}{v}\eta(c_{e\delta}(a_0 + a_1\omega_e + a_2\omega_e^2) + c_{e\omega}\omega_e + c_{ec}) \tag{45}$$

This equation is differentiated with respect to ω_e to find the engine speed that gives maximum torque to the wheels. This is also the engine speed where the engine produces maximum power.

$$\frac{dT_w}{d\omega_e} = \frac{r\eta}{v}(c_{e\delta}(a_0 + 2a_1\omega_e + 3a_2\omega_e^2) + 2c_{e\omega}\omega_e + c_{ec}) = 0 \tag{46}$$

Consider Equation (39), notice that when $\left|\frac{\lambda_v c_\delta}{v}\right| >> 1$, the optimal engine speed goes to the solution of Equation (46). Also, since $|c_{e\delta}| >> |c_{e\omega}|, |c_{ec}|$, this solution is close to the solution of Equation (44). For the engine considered and the quadratic maximum fueling function, maximum engine torque and maximum wheel torque (maximum engine power) are plotted in Figure 8. The conclusion from this is that the character of the maximum fueling function is decisive for the optimal gear choice.

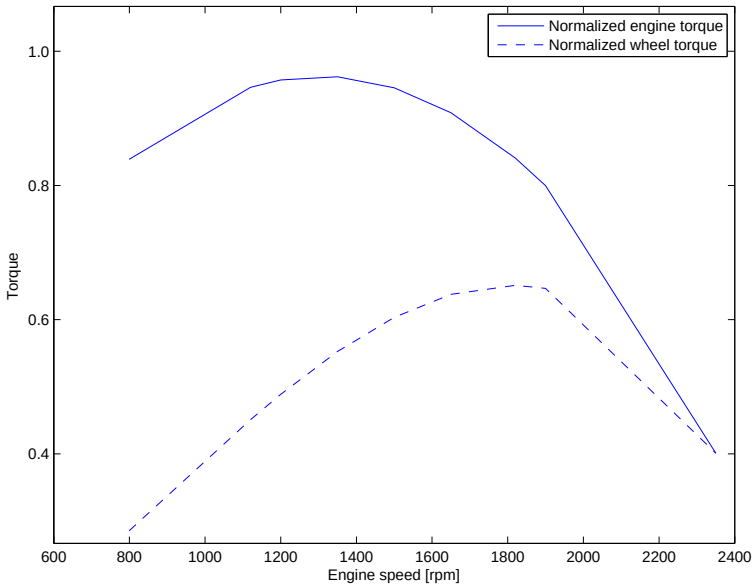

Figure 8: *Maximum engine torque and maximum wheel torque. At about 1800 rpm the engine delivers maximum torque to the wheels.*

5.3 Discrete step transmission

Since discrete step transmissions are the most commonly used transmission for heavy trucks it is interesting to see how the optimal solution would be if the gear ratio belongs to a set of discrete numbers $i \in \{i_1, i_2, \ldots, i_n\}$. For this case Equation (33) can no longer be used directly to find the optimal gear ratio.

As a first attempt to model the gear shift process it will be assumed that a gear shift is carried out instantaneously but possibly with a discontinuity in vehicle speed. For vehicles with mechanical solutions such as for example dual clutch transmissions there is no disruption in torque during a gear shift, and hence it is feasible to model the gear shifting without any speed loss. Using the more common manual transmissions there is a disruption in torque, and such gear shifts will, except in steep downhills, result in a decrease in speed. Suppose that a gear shift occurs at position $s = s_i$ for a set of gear shifting positions $s_i \in \{s_1, \ldots, s_{N-1}\}$, and let the speed just before the shift be $v(s_{i-})$, let the speed just after the shift be $v(s_{i+})$, and let the decrease in speed during the shift be v_s. The shift is then modeled as

$$v(s_{i-}) - v(s_{i+}) = v_s \tag{47}$$

One way to handle the discontinuity in this problem is to consider both fueling and gear choice as control variables. The optimal control is then found by searching for the control that minimizes the Hamiltonian at every position, see the discussion on the maximum principle in [12]. Another approach that will be used here is described in [1]. Then only fueling is considered as a control variable that is found from $\partial H/\partial u = 0$. This leads to a formulation with switching between different system dynamics functions when switching

gear. The optimal control problem formulation with discontinuities in the system equations and in the state variables, as described in Chapter 3.7 in [1] is used here. The gear shifting function

$$\varphi = v(s_{i-}) - v(s_{i+}) - v_s = 0 \tag{48}$$

is adjoined to the performance criteria with multiplier ϑ. Let

$$\phi = \vartheta\varphi \tag{49}$$

and the Hamiltonian be the combination of the Hamiltonians for each interval

$$H^{(i)} = L^{(i)} + \lambda^T f^{(i)} \tag{50}$$

For $N-1$ shifts the performance criteria is

$$J = \sum_{j=1}^{N-1} \vartheta^{(j)T}\varphi^{(j)} + \sum_{i=1}^{N} \int_{s_{i-1}+}^{s_i-} (L^{(i)} + \lambda^T f^{(i)} - \lambda^T \frac{dx}{ds})ds \tag{51}$$

It is shown in [1] that necessary conditions for optimality is

$$\frac{d\lambda}{ds} = -\left(\frac{\partial H^{(i)}}{\partial x}\right)^T, \; s_{i-1}+ < s < s_i - \tag{52}$$

$$\lambda^T(s_i-) = \frac{\partial \phi}{\partial x(s_i-)} \tag{53}$$

$$\lambda^T(s_i+) = -\frac{\partial \phi}{\partial x(s_i+)} \tag{54}$$

$$H^{(i)}(s_i-) - H^{(i+1)}(s_i+) = 0 \tag{55}$$

For the case (48) $\lambda_v(s_i-) = \lambda_v(s_i+) = \vartheta_i$, i.e. the adjoint variable λ_v is continuous over a gear shift.

Since λ_v is continuous and gear ratio should be chosen such that the Hamiltonian is minimized at each position, a change in gear can only occur when the Hamiltonian evaluated for two nearby gears equal each other, i.e. $H(i_i, v(s_i-)) = H(i_{i+1}, v(s_i+))$. For zero speed loss at shifting points, i.e. $v_s = 0$, the resulting gear shifting points are marked with dashed lines in Figure 6. The optimal solution with a stepped transmission will of course be quite similar to the continuously variable ratio solution in the sense that the gear ratio is chosen such that the engine speed is on average close to the continuous case. See Figure 9 for a depiction of typical gear shifting points when the speed loss of a gear shift is set to 0.1 m/s.

5.4 Optimal gear ratio for PWA engine characteristics

For non-linear engine characteristics it is interesting to study gear choice also when fueling is not in the limit. For a PWA model as (25) each engine region can be analyzed separately as in Section 5.1. During constant speed sections each region $\{m,n\}$ has an optimal gear ratio as in (34)

$$i_{opt} = -\frac{c_{e,m,n}}{c_{\omega,m}}\frac{r}{2v} \tag{56}$$

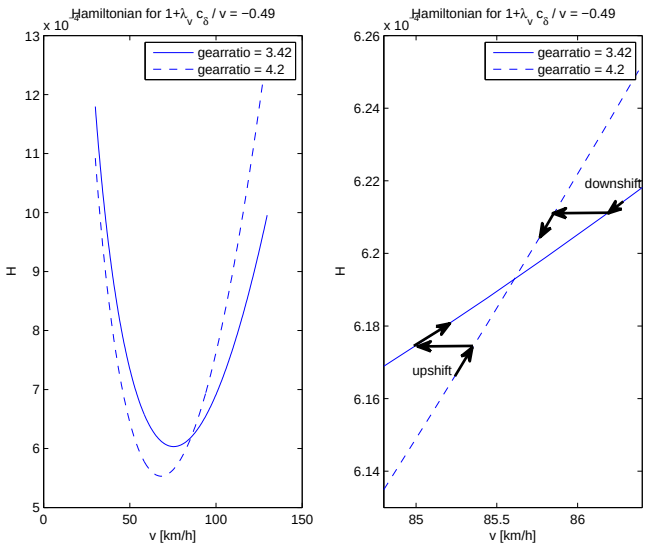

Figure 9: *To the left, the Hamiltonian evaluated for a fixed ratio of λ_v/v and for the two highest gears. To the right, a zoom in of the left plot. The arrows indicates where downshift and upshift occurs when the speed loss of a gear shift is set to 0.1 m/s*

In most cases the optimal gear ratio for each region is such that the engine speed is in the border of the regions. This means that there are some operating points that have to be considered and the optimal gear ratio is chosen such that engine efficiency is maximized. Again, if searching for optimal gear ratio during non stationary sections the engine torque has to be modeled such that the Hamiltonian is differentiable with respect to speed.

6 Simulations

The results from previous sections will now be demonstrated in simulations of some constructed road profiles. Both affine and piece wise affine engine models will be used, but all simulations will use the quadratic maximum fueling function (37). Also results from both continuous variable transmission as well as discrete stepped transmission will be presented. The road profiles will consist of flat road followed by an uphill slope or a downhill slope of constant gradient, and then flat road again. For such road segments the slope α will have a discontinuity when changing from flat road to slope. If there is such a discontinuity at a given position s_d it is according to theory possible that the Hamiltonian and/or the adjoint variables have a discontinuity at that position. For simulation it is important to decide whether or not the adjoint variables have discontinuities, and it will here be shown that that is not the case. A general condition that decides at which position s_1 such an event occurs can be formulated as in [1] as a so called interior boundary condition

$$N(x(s_1), s_1) = 0 \tag{57}$$

In Chapter 3.5 in [1] the influence on H and λ from such an event is derived to be

$$\lambda^T(s_1-) = \lambda^T(s_1+) + \pi^T \frac{\partial N}{\partial x(s_1)} \quad (58)$$

$$H(s_1-) = H(s_1+) - \pi^T \frac{\partial N}{\partial s_1} \quad (59)$$

where π are constant multipliers. Since road slope is a function of position the condition that decides when a discontinuity in α occurs can be formulated as

$$N(s) = s_1 - s = 0 \quad (60)$$

For the condition (60) it is seen from (58) that there is no discontinuity in the adjoint variables λ since the condition is independent of the states.

6.1 Optimal solutions for uphill and downhill slopes

Optimal solutions of example simulations are seen in Figures 10, 11 and, 12. All simulations are of a 40 ton truck with λ_T chosen such that cruising speed at flat road is 85 km/h. In Figure 10 the engine model is piece-wise affine in fueling dimension and affine in speed dimension, see Figure 3. Assuming a continuously variable transmission both fueling and gear ratio is optimized. As expected from Section 5.2 and especially Equations (39) and (46), for long steep slopes the gear ratio is chosen such that the engine speed is close to 1800 rpm, the point of engine maximum power. Also as mentioned in Section 5.2 in connection to Figure 6, starting at 85 km/h before the slope there is no change in gear ratio during the acceleration phase before the slope. Notice also that the acceleration from about position 300 m to 2400 m is done using fueling in the border between the two upper fueling regions. Then, between about 2400 m to 5200 m maximum fueling is used, and from 5200 m to 6900 m fueling is again in the border between the two upper fueling regions.

In Figure 11 a simulation of the PWA engine model is done in a 500 m slope of -6% slope. The vehicle cruises at constant speed from start to about 800 m where the fueling is lowered to the border between fueling region 2 and 3. During that part it begins to decelerate and at about 2400 m the fuel injection is again lowered to the border between region 1 and 2. It is worth noting that the fuel injection is never cut off totally as it would have been done for an affine engine torque model.

6.2 Affine and piece-wise affine modeling

In Figure 12 three simulations are presented. The solid line is a simulation of the affine engine torque model with no gear optimization. The dashed line is with the PWA engine torque model with no gear optimization. The dotted line is also with the PWA model but now with gear optimization. As expected the affine model only uses two modes of fueling, i.e. such that constant speed is kept to about 2300 m, and then maximum fueling is used until 5300 m where speed is kept constant again. The simulation with the PWA model start accelerating earlier and uses only maximum fueling from about 3900 m to about 4200 m. The gradual change in fueling for the PWA model gives a smoother control but

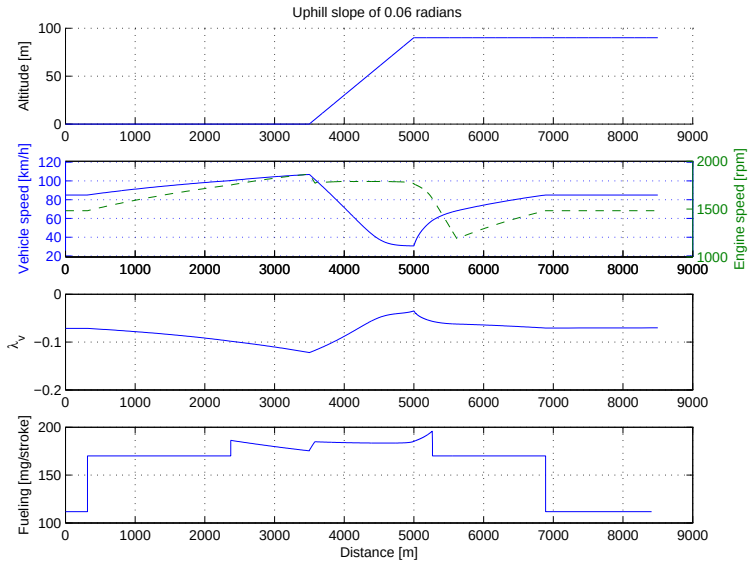

Figure 10: *Uphill slope of 1500 m 6 percent inclination. Both fueling and gear ratio is optimized.*

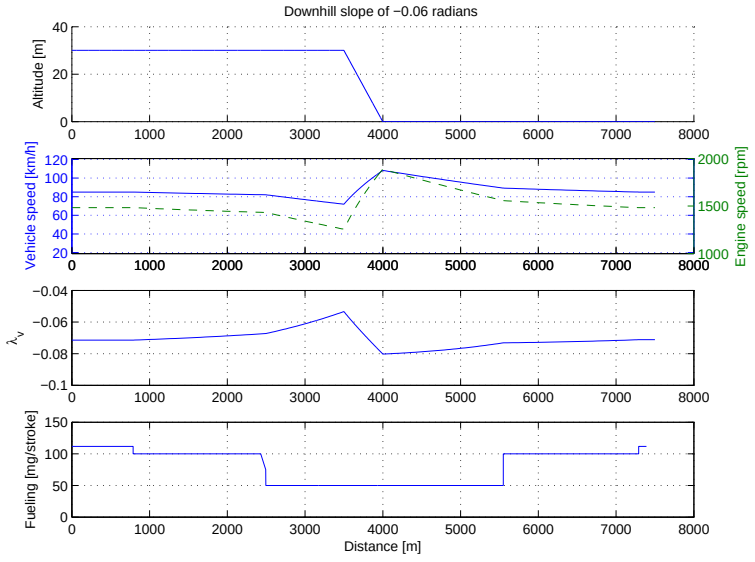

Figure 11: *Downhill slope of 500 m -6 percent inclination. Both fueling and gear ratio is optimized.*

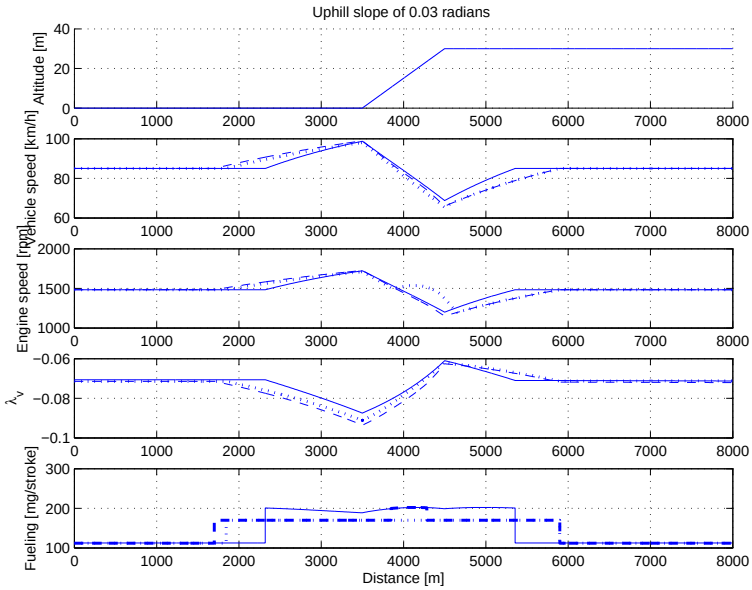

Figure 12: *Three simulations in a 1000 m 3 percent uphill slope. Solid line is an affine engine torque model. Dashed line is PWA engine torque model. Dotted line is PWA engine torque model with gear optimization.*

also requires about 500 m longer prediction horizon than the affine model. When also gear ratio is optimized the PWA model never uses maximum fueling.

6.3 Continuously variable gear ratio optimization

To study optimal choice of gear ratio three simulations of the affine engine torque model is presented in Figure 13. The optimal engine speed given by Equation (39) for the three simulations are there shown as functions of vehicle speed and the decisive variable $1+\frac{\lambda_v c_\delta}{v}$. One simulation, the "inner arc", is of a 1000 m 3 % uphill slope. In that simulation the optimal gear ratio just about reaches the lowest feasible gear ratio. The other simulations is of a 600 m 6 % uphill slope and a 1500 m 6 % uphill slope. In the latter simulation the vehicle is able to keep a constant speed of about 30 km/h at some part of the slope. As mentioned earlier the magnitude of $1+\frac{\lambda_v c_\delta}{v}$ gets larger the longer and steeper the slope is. Hence, optimal engine speed is a function of length and steepness of the slope.

In Figure 14 the same simulation as in Figure 10 with the PWA modeled engine is depicted. Only the part in the upper fueling region is shown. Note that the optimal engine speed, being around the line 1780 rpm, is higher than for the affine engine, Figure 13, where it was around 1650 rpm, and closer to maximum engine power, Figure 8 where the maximum is around 1800 rpm.

The result from Figures 6 and 7 could be used to define gear shifting points that is dependent on speed and for example length and slope of hills. If the vehicle is approach-

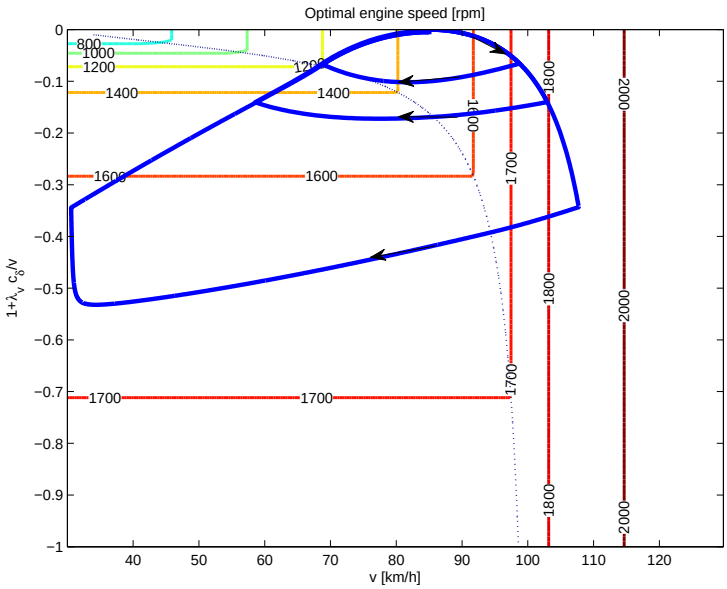

Figure 13: *Optimal gear ratios. One simualation of a 1000 m 3 % uphill slope where the optimal gear ratio just about reaches the lowest feasible gear ratio. The next, the "middle" arc is a simulation of a 600 m 6 % uphill slope. The "outer" arc is a simulation of a 1500 m 6 % uphill slope.*

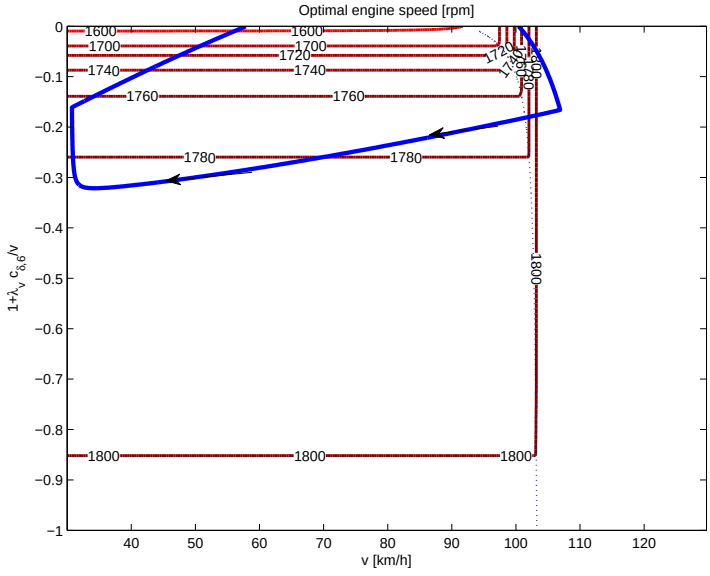

Figure 14: *Optimal engine speed for the highest fueling region of the PWA modeled engine. A simulation of a 1500 m 6 % slope is plotted. Compare with Figure 13.*

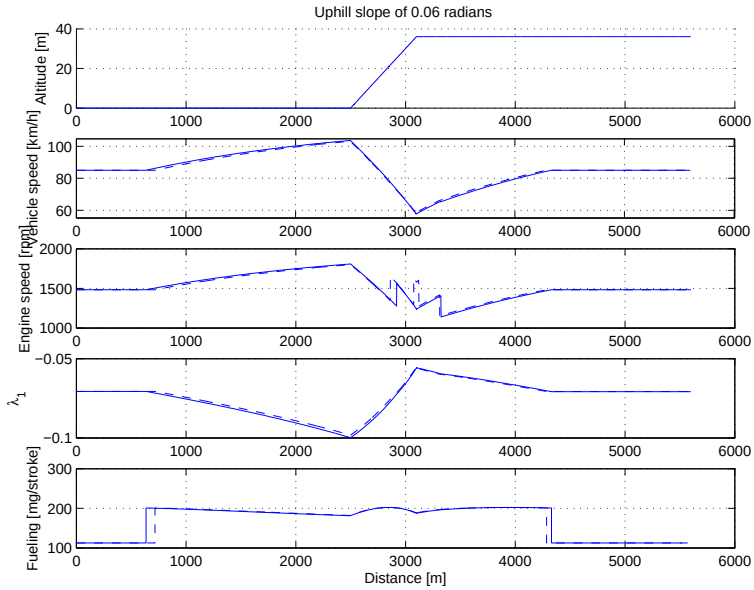

Figure 15: *Simulations with an affine engine and stepped transmission in a 6% 600 m uphill slope. The engine speed is on average close to the continuous ratio solution in Figure 13. Dashed line corresponds to a simulation without a speed loss during the gear shifts, and solid line corresponds to a simulation with 0.1 m/s speed loss during the gear shifts. Note that without gear shift losses an extra gear shift occurs near the top of the hill.*

ing a long and or steep slope the magnitude of $1 + \frac{\lambda_v c_\delta}{v}$ will get larger leading to a higher optimal engine speed during the slope. Looking at the simulations in for example Figure 13 it is seen that during the uphill slope, the retardation phase, the optimal engine speed has small variations with a mean value depending on the speed at the start of the slope. Hence, an approximative gear shifting strategy could be designed based on the speed when starting to climb a hill.

6.4 Discrete stepped transmission

Last, two simulations of a stepped transmission is presented. See Figure 15 for example simulations in a 6% 600 m uphill slope. The dashed lines in the figure corresponds to a simulation without a speed loss during the gear shifts, and the solid lines corresponds to a 0.1 m/s speed loss during shifts. This is a typical value if it is assumed that the engine is incapable to propel the vehicle for about 0.5 s during the shift. Note that the simulation without gear shifting losses performs an extra gear shift near the top of the hill. Note also that the engine speed is on average close to the continuous ratio solution in Figure 13.

6.5 Interpretation of the Lagrange variables

Looking at the Hamiltonian (9), it is seen that it is proportional to amount of fuel used per distance, i.e. [kg/m]. This means that the Lagrange variable λ_v is proportional to amount of fuel divided by velocity, i.e. [kg/(m/s)]. Since λ_v is decisive for the optimal control it is interesting to interpret the value of it. In [1] it is shown that for the augmented performance criteria $\bar{J} = \int_{s_0}^{s_f} (\delta i + \lambda^T (f - \frac{dx}{ds}))ds$, the variation in the performance criteria $\delta\bar{J}$ due to a variation in initial conditions $\delta x(s_0)$ is

$$\delta\bar{J} = \lambda^T(s_0)\delta x(s_0) + \int_{s_0}^{s_f} \frac{\partial H}{\partial u}\delta u ds \tag{61}$$

where u is the control vector $[\delta\ i]^T$. Hence, $\lambda^T(s_0)$ is the gradient of $\bar{J}$ with respect to initial conditions while holding $u(s)$ constant. Of course the position s_0 can be taken anywhere which means that λ at every position is a measure of how much the total cost would be affected by a change in x at that position. The variable λ_v thus is a measure of how much fuel consumption would change if the speed v is varied. Since λ_v is negative a raise in vehicle speed by 1 m/s at position s_0 will result in a decreased total cost given by the value of $\lambda_v(s_0)$. A decrease of speed by 1 m/s would increase the total cost by the same amount.

Now, looking at the simulations above in for example Figures 10 and 11, it is seen that for an uphill slope a change in speed in the beginning of the slope has the highest influence on the total consumption. In the same way the speed at the end of a down hill slope is most critical to the total fuel consumption.

The influence from a change in vehicle speed on the total cost, $\lambda_v(s_0)\delta v(s_0)$, can be written as

$$\frac{\lambda_v(s_0)}{v(s_0)} v(s_0)\delta v(s_0) \tag{62}$$

Remember that the term λ_v/v is decisive for both optimal fueling and for optimal gear ratio. Rewriting (61) the first part is (62). Since $v\delta v$ is a measure of change in kinetic energy, λ_v/v is a measure of how the total cost is affected to a change in kinetic energy. Looking at Figure 13 it is seen that the point most sensitive to a change in kinetic energy does not coincide with the point most sensitive to a change in vehicle speed. Instead of the beginning of the slope now a point somewhere in the middle of the slope is most critical, i.e. the lowest point of the respective arc. However, as mentioned earlier, the decisive factor $1 + \frac{\lambda_v c_\delta}{v}$ has small variations during the slope which means that the sensitivity to a change in kinetic energy is approximately constant during the slope.

6.6 Speed limits

Speed limits is a state variable inequality constraint. Optimal control with such constraints are treated in Section 3.11 in [1]. An upper speed limit is derived by the following constraint

$$C_v = v - V_{max} \leq 0 \tag{63}$$

In [1] the method to handle the type of constraint as (63) are to differentiate until the control variable appears explicitly. For the model (7) this means that the derivative $C_v' = \frac{d}{ds}C_v$ is adjoined to the Hamiltonian (9) with the multiplier μ_v resulting in

$$H = \delta i + (\lambda_v + \mu_v) f_v + \lambda_T f_T + \mu_\delta C_\delta \tag{64}$$

At the entry point of a constrained arc the adjoint variable λ_v is discontinuous but continuous at the exit point. However, instead of solving the optimal control problem as before the constrained solution can intuitively be found from the unconstrained solution. Consider the cases presented so far. If there had been an upper speed constraint present the solution after the position of leaving the constrained arc would follow the unconstrained solution. For example, after a steep downhill slope where the unconstrained solution exceeds the speed limit at the end of the slope, the constrained solution could be found in the same way as before, by setting the speed at the end of the slope to the maximum allowed speed. The value of λ_v is then given by the fact that both λ_v and v should reach their respective stationary values at the same position. Since λ_v has a discontinuity at the entry point of the constrained arc there is no easy way to decide the value of λ_v at that point. However, among all solutions that fulfills the necessary conditions for optimality, (10)-(13), the most fuel efficient solution is to start to decelerate before the slope at a position such that the upper speed limit is reached exactly at the end of the slope. This is of course then the solution that minimizes brake usage, and hence minimizes the total fuel consumption.

For uphill slopes the reasoning can be done in the same way such that maximum allowed speed is reached exactly at the beginning of the slope if the unconstrained solution exceeds the speed limit at that position. An example simulation with an affine engine torque model is plotted in Figure 16 where the maximum allowed speed was 90 km/h. If Figure 16 is compared to an unconstrained simulation of the same slope in Figure 13 it is seen that in the constrained simulation the optimal gear ratio in the slope is higher resulting in about 100 rpm higher engine speed than in the unconstrained case.

6.7 Discussion

The optimal strategies presented above is a compromise between running the engine at efficient operating points and minimizing air and roll resistance. For the affine engine model (4) the optimal fueling strategy has the character of bang-bang control. This strategy minimizes vehicle speed variations and hence air and roll resistance losses. When using the non linear model (20) the engine efficiency decreases in the upper fueling region. Hence the optimal solution in for example Figure 12 starts to accelerate earlier than when using an affine model. Using this strategy, vehicle losses for the driving mission is increased but the distance of maximum fueling, where engine efficiency is low, is shortened. Looking in the same figure it is also seen that, by optimizing gear ratio, the upper fueling region is avoided, though the higher gear ratio gives increased engine friction.

7 Sensitivity analysis

For an implementation in a vehicle it is interesting to see how uncertainties in parameters will affect the optimal strategy and thereby the total fuel consumption. Using a given

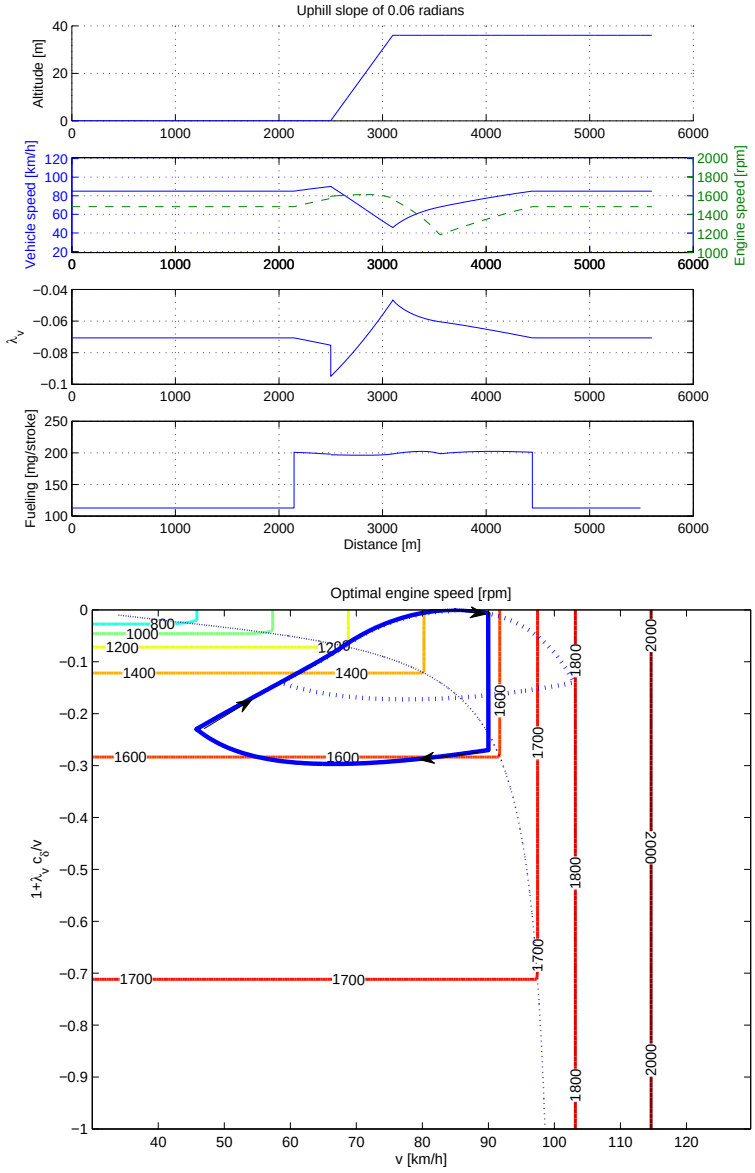

Figure 16: *Simulation in a 6 % 600 m uphill slope with maximum allowed speed of 90 km/h, solid line. The unconstrained solution from Figure 13 of the same simulation case is also plotted in the lower plot, dotted line.*

Coefficient	Sensitivity, $\alpha = -0.03$ $\delta = 0$ mg/stroke	Sensitivity, $\alpha = 0$ $\delta = 113$ mg/stroke	Sensitivity, $\alpha = 0.03$ $\delta = 220$ mg/stroke
c_δ	0.00	323	-1.48
c_ω	-0.12	-49	0.11
c_e	0.079	32	-0.076
c_c	-0.42	-171	0.40
c_v	0.00	0.00	0.00
c_{v2}	-0.33	-135	0.32
c_α	1.78	0.00	1.72
α	1.78	0.00	1.72

Table 3: *Senstivity of vehicle dynamics to model coefficients. The sensitivity is calculated for a 40 ton truck cruising at 85 km/h*

fueling strategy and gear choice, an error in a parameter estimation will result in a different speed profile than predicted. To see how much such a change will affect the total cost the discussion in Section 6.5 can be used. As mentioned, λ_v is a measure of how much the total fuel consumption is affected by a change in vehicle speed. Thus, to estimate how a parameter change influences the total fuel consumption it is sufficient to study how a parameter change affects vehicle speed. The sensitivity of a function $f(x)$ to x at the point x_0 is computed as $(\partial f/\partial x)|_{x_0}/(x_0/f(x_0))$. In Table 3 the sensitivity of the vehicle dynamics, i.e. the right hand side of Equation (7), to the model coefficients, is presented. Road slope has the highest significance on the total fuel consumption. The second highest influence has c_δ, and the third highest influence has c_c and c_{v2}. Note that if the drive line inertias J_e and J_d are neglected in the total vehicle inertia, see Table 2, $c_\delta = (i\eta c_{e\delta})/(mr)$, $c_{v2} = (0.5\rho c_d A + mc_{r3})/m$, $c_c = (i\eta c_{ec} + mc_{r1})/m$, and $c_\alpha = g$. This means for example that a fault in vehicle mass or fuel-torque characteristic has equal importance. However, a fault in road slope has the most significant influence on the total cost.

One parameter known to be difficult to measure is vehicle mass and therefor it is of special interest to study. To see how a fault in vehicle mass affects the optimal solution two simulations has been performed with masses 40 tons and 44 tons, see Figure 17. It is there seen that if the vehicle mass is underestimated, the vehicle will start to accelerate too late and shift to lower gear too late which can lead to a necessary extra gear shift which of course gives an increase in fuel consumption. In a downhill slope it is of course also worse to underestimate the mass than to overestimate since an underestimate leads to a later deceleration before the slope, which in turn leads to a higher speed in the slope. In presence of speed limits this leads to unnecessary braking and an increase of total fuel consumption.

8 Rule based predictive cruise control

There are several ways to use the presented optimality conditions in attempts towards an on-line controller. Looking at the vehicle dynamics in the time domain, vehicle speed can be solved analytically, as in [2], on constant grades for both constant fueling and maximum fueling. Given the equations for vehicle speed and the constraint on total travel

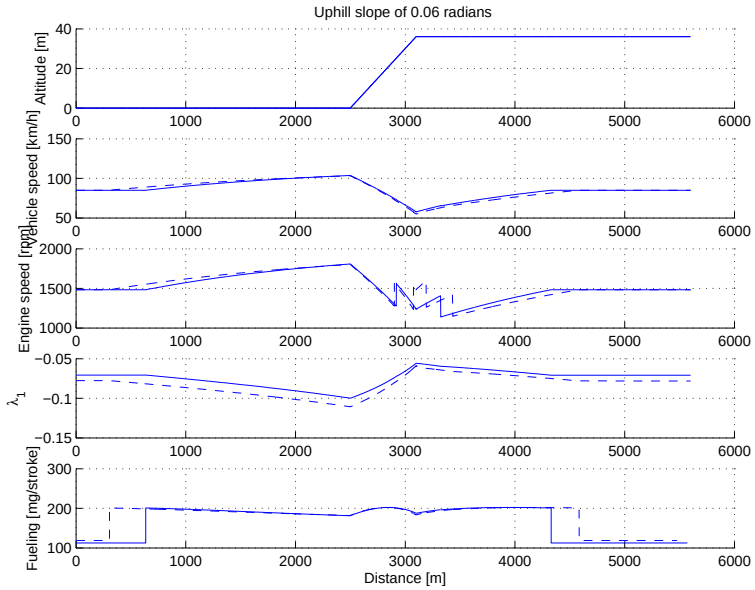

Figure 17: *Simulation in a 6 % 600 m uphill slope with masses 44 tons (dashed lines) and 40 tons (solid lines).*

time, the problem of finding optimal controls is that of finding optimal control switching points, by solving a system of nonlinear equations [2].

Another approach to utilize the analytical solutions to the vehicle motion will here be used as part of an on-line predictive cruise controller. One advantage is that the assumption that the road grade is piece-wise constant can be dropped.

To demonstrate the possibility to significantly save fuel using the second approach, a simple rule based predictive cruise controller has been implemented. For simplicity the controller is based on the results using an affine engine torque model as in Section 3. It would be possible to make further improvements using a controller based on non-linear engine characteristics and optimize gear choice. However, the purpose here is only to demonstrate the magnitude of the savings that can be done using the presented material. In [5] the possible savings of gear choice is presented.

8.1 Optimization criterion

The idea for an on-line controller is to locate upcoming steep hills, compare different fueling strategies with respect to a criterion over a prediction horizon, use the best strategy over a sampling distance, and then re-evaluate the criterion at the next sampling point. Closed loop control is achieved by recalculating optimal controls at every sample point.

An idea for criterion could be to use the Hamiltonian (9). Over short horizons it might however not be a good idea to try to control the average speed to a given value. For example, if the road mostly consists of downhill slopes during the prediction horizon it is often better for the total driving mission to have a higher speed than average, and

the opposite for sections of mostly uphill slopes. Influenced by (9) the criterion for a prediction horizon from $s = 0$ to $s = S_p$ could be chosen as

$$\tilde{J} = \int_0^{S_p} \delta i ds + \lambda_T \int_0^{S_p} f_T ds \tag{65}$$

The first term is proportional to the fuel consumed while driving the distance S_p and the second term accounts for the travel time. The time penalty λ_T is obtained by solving Equation (14) using a desired stationary speed v_{ref} on flat roads and small gradients. For this criterion to be useful it has to be modified to account for the speed at the end of horizon. As known from Section 3 the optimal solution consists of constant speed, maximum fueling, and fuel cut off. Using (65) will result in a strategy that uses fuel cut off at the end of the prediction horizon.

Handling residual cost at end of horizon. One way to deal with this could be to constrain the solution to a given speed, e.g. $v(S_p) = v_{ref}$, at the end of the horizon. However, this is not a good idea if for example the end of horizon is in a slope. The way chosen here to deal with the problem of finite horizon is as follows: Assume flat road after S_p, let S_{vref} be the position where the reference speed v_{ref} is reached after S_p when using either maximum fueling or fuel cut off depending on if the speed at S_p is less than or greater than v_{ref}. By defining a function Δ as

$$\Delta = \int_{S_P}^{S_{vref}} \delta i ds + \lambda_T \int_{S_P}^{S_{vref}} f_T ds \tag{66}$$

the criterion (65) can be chosen as

$$J = \int_0^{S_p} \delta i ds + \lambda_T \int_0^{S_p} f_T ds + \Delta \tag{67}$$

The function Δ then follows from the solution to the vehicles longitudinal dynamics. When using fuel cut off on flat road the vehicle dynamics (7) in the time domain becomes

$$\dot{v} = c_e i + c_c + (c_\omega \frac{i^2}{r} + c_v)v + c_{v2}v^2 \tag{68}$$

Using maximum fueling modeled as $\delta_{max} = c_{con} + c_{\omega con}\frac{i}{r}v + c_{\omega 2con}\frac{i^2}{r^2}v^2$ results in

$$\dot{v} = c_\delta i c_{con} + c_e i + c_c + (c_\delta c_{\omega con}\frac{i^2}{r} + c_\omega \frac{i^2}{r} + c_v)v + (c_\delta c_{\omega 2con}\frac{i^3}{r^2} + c_{v2})v^2 \tag{69}$$

Both Equation (68) and (69) are in the form

$$\dot{v} = c_0 + c_1 v + c_2 v^2 \tag{70}$$

This differential equation can be solved by separating variables as

$$\frac{1}{c_0 + c_1 v + c_2 v^2} dv = dt,\ c_0 + c_1 v + c_2 v^2 \neq 0 \tag{71}$$

Integrating both sides give

$$\int \frac{1}{c_0 + c_1 v + c_2 v^2} dv = \int dt \tag{72}$$

This equation has two different solutions depending on the coefficients. When accelerating the coefficients are such that the solution to (72) is

$$\frac{1}{\sqrt{-4c_2c_0 + c_1^2}} \ln \left| \frac{2c_2 v + c_1 - \sqrt{-4c_2c_0 + c_1^2}}{2c_2 v + c_1 + \sqrt{-4c_2c_0 + c_1^2}} \right| = t + k \tag{73}$$

The solution to this equation is

$$v(t) = \frac{-(c_1 - \sqrt{c_1^2 - 4c_0c_2}) - (c_1 + \sqrt{c_1^2 - 4c_0c_2}) e^{\sqrt{c_1^2 - 4c_0c_2}(t+k)}}{2c_2 e^{\sqrt{c_1^2 - 4c_0c_2}(t+k)} + 2c_2} \tag{74}$$

and k is chosen such that initial conditions are satisfied. When decelerating the coefficients are such that the solution to (72) is

$$\frac{2}{\sqrt{4c_0c_2 - c_1^2}} \arctan \left(\frac{2c_2 v + c_1}{\sqrt{4c_0c_2 - c_1^2}} \right) = t + k \tag{75}$$

and also here k is determined by initial conditions. The vehicle speed given by this equation is

$$v(t) = \frac{1}{2c_2} \left(\sqrt{4c_0c_2 - c_1^2} \tan \left(\frac{\sqrt{4c_0c_2 - c_1^2}}{2} (t+k) \right) - c_1 \right) \tag{76}$$

Now, from (73) or (75) the time required for v to reach v_{ref} can be calculated. Given time, distance can be calculated by integrating speed. The distance traveled, $s = \int v dt$, during acceleration to v_{ref}, is given from the integral of (74) which is

$$\begin{aligned} \int \frac{-(c_1 - \sqrt{c_1^2 - 4c_0c_2}) - (c_1 + \sqrt{c_1^2 - 4c_0c_2}) e^{\sqrt{c_1^2 - 4c_0c_2}(t+k)}}{2c_2 e^{\sqrt{c_1^2 - 4c_0c_2}(t+k)} + 2c_2} dt \\ = \frac{\sqrt{c_1^2 - 4c_0c_2} - c_1}{2c_2} t - \frac{\ln \left| 2c_2 (e^{\sqrt{c_1^2 - 4c_0c_2}(k+t)} + 1) \right|}{c_2} \end{aligned} \tag{77}$$

and the distance traveled during deceleration to v_{ref} is given from the integral of (76) which is

$$\begin{aligned} \int \left(\frac{\sqrt{4c_0c_2 - c_1^2}}{2c_2} \tan \left(\frac{\sqrt{4c_0c_2 - c_1^2}}{2} (t+k) \right) - \frac{c_1}{2c_2} \right) dt \\ = -\frac{c_1}{2c_2} t - \frac{\ln \left| \cos \left(\frac{\sqrt{4c_0c_2 - c_1^2}}{2} (t+k) \right) \right|}{c_2} \end{aligned} \tag{78}$$

Now Δ, (66), can be calculated as follows. Given distance the first integral is easily calculated for the different cases of fuel cut off and maximum fueling. The second integral is simply traveled time as given by Equations (73) and (75).

8.2 On-line algorithm

Given the results above, an on-line cruise controller can be formulated. For simplicity, as in [5] the standard cruise controller will be used as actuator. When constant speed is desired, $v = v_{ref}$ is commanded, when maximum fueling is desired, a higher speed than the vehicles present speed will be commanded, and, when fuel cut off is desired, a lower speed than the present speed is commanded. Since the standard cruise controller is of a PID-controller type this strategy will not always lead to the desired fueling but as will be shown in simulations it will be close to desired behavior.

For a realistic case, speed limits has to be imposed such that $V_{min} \leq v \leq V_{max}$. The algorithm is as follows:

1. Check if there are steep slopes within the horizon. If not, send v_{ref} to the cruise controller.

2. If a steep slope is detected, perform two simulations of the vehicle. First simulation: If the first steep slope is an uphill(downhill) slope start using maximum(minimum) fueling and simulate until either v_{ref} or $V_{max}(V_{min})$ is reached. Second simulation: Command constant speed on one sample and then use maximum(minimum) fueling.

3. If $V_{max}(V_{min})$ is reached before v_{ref} is reached after the slope, command v_{ref} to the cruise controller.

4. Compare the two solutions by the performance index (67). Chose control according to the simulation with lowest value of the performance index.

This algorithm is implemented in a simulation environment developed by Erik Hellström [6].

Results from the simulations are shown in Figures 18 - 20. There the above rule-based look-ahead cruise controller, LC, is compared to a standard PID-type cruise controller, CC. The allowed speed range is $80 \leq v \leq 90$ km/h and the reference speed is 85 km/h. The standard cruise controller will not apply the brakes until the upper speed limit is reached. The prediction horizon for the look-ahead controller was set to 1000 m and the sample distance to 50 m. It is seen that the algorithm works as expected from Section 3. In Figure 18 the algorithm starts to accelerate using maximum fueling about 300 m before the slope. The higher speed compared to the standard cruise controller also results in a shorter period on a lower gear. Due to higher average speed for the look ahead cruise controller the fuel consumption is slightly higher compared to the standard cruise controller. However, the trip time is significantly lower. A down hill slope is presented in Figure 19. The look ahead algorithm cut offs the fuel injection and starts to decelerate about 200 m before the slope. This results in a shorter period of braking and significant fuel savings but a small increase in trip time. For a real road consisting of both uphill slopes and downhill slopes, it is expected that the difference in total travel time between the look ahead cruise

controller and the standard cruise controller is moderate. In Figure 20 it is seen that even though the travel time is almost the same for the two controllers the fuel saving is significant for the look ahead controller. It can also be mentioned that the magnitude of the savings is promising even though not quite as high as those reported in [6] using a more sophisticated numerical optimal controller.

9 Conclusions

Analytical expressions for optimality of the fuel optimal cruise control problem have been derived. These expressions are essential for the understanding of the decisive parameters affecting fuel optimal driving, and the analytical optimality conditions makes it possible to see how each parameter affects the optimal solution. It has been shown that the expression $1+\frac{\lambda_v c_\delta}{v}$ is decisive for both optimal fueling and optimal gear selection. For example, it is seen in Equation (12) that the ratio between engine torque to vehicle mass, given by the parameter c_δ, directly affects the optimal control switch points, which also the adjoint variable λ_v and vehicle speed v does. The adjoint variable λ_v reacts to future changes in road slope and from that the control switch points given by (12) also depends on road inclination. This type of analysis lead to the idea of using phase plots with $1+\frac{\lambda_v c_\delta}{v}$ and v on the axes, and this type of plot has been used extensively, see Figures 6, 7, 13, 14, and 16. It has also been shown that, accounting for small non-linearities in the engine torque model, fueling is gradually increased or decreased to the fueling limit, giving a smoother control than achieved for an affine model, see for example Figure 11. This gradual change in control also means that a longer prediction horizon is needed.

The maximum fueling function has strong influence on optimal gear choice. It is shown for a continuously variable transmission that it is never optimal to operate above the engine speed of maximum engine power. Further, for typical cases, see Figure 13, during the acceleration phase before an uphill slope it is never optimal to shift gear, but it can be optimal to stay at a higher gear ratio for a short distance after the slope. From the results in Figure 13 it is seen that for optimal solutions engine speed is approximately constant during the slope, and is determined by the vehicle speed at the beginning of the slope. The optimal vehicle speed at the beginning of the slope mostly depends on the length and inclination of the slope and hence optimal gear shifting is approximatively a function of slope length and inclination. Another point to notice is that for non-linear fuel-torque characteristics, in order to avoid inefficient engine operating points, it can be beneficial to shift gear instead of using maximum fueling.

Optimal solutions for a discrete stepped transmission are close to the continuous gear ratio solutions in the sense that engine speed for the two cases are close. However, it is shown in simulations that modeling of gear shifting losses are important for gear shifting positions.

The theory presented is a good base to formalize the intuition of fuel efficient driving and one example where the analytical optimality expressions can be used is in design of a simple low-complexity computationally efficient rule-based controller. Such a controller has been shown to be able to save a large part of the possible savings achieved with more computationally demanding controllers based on numerical optimization.

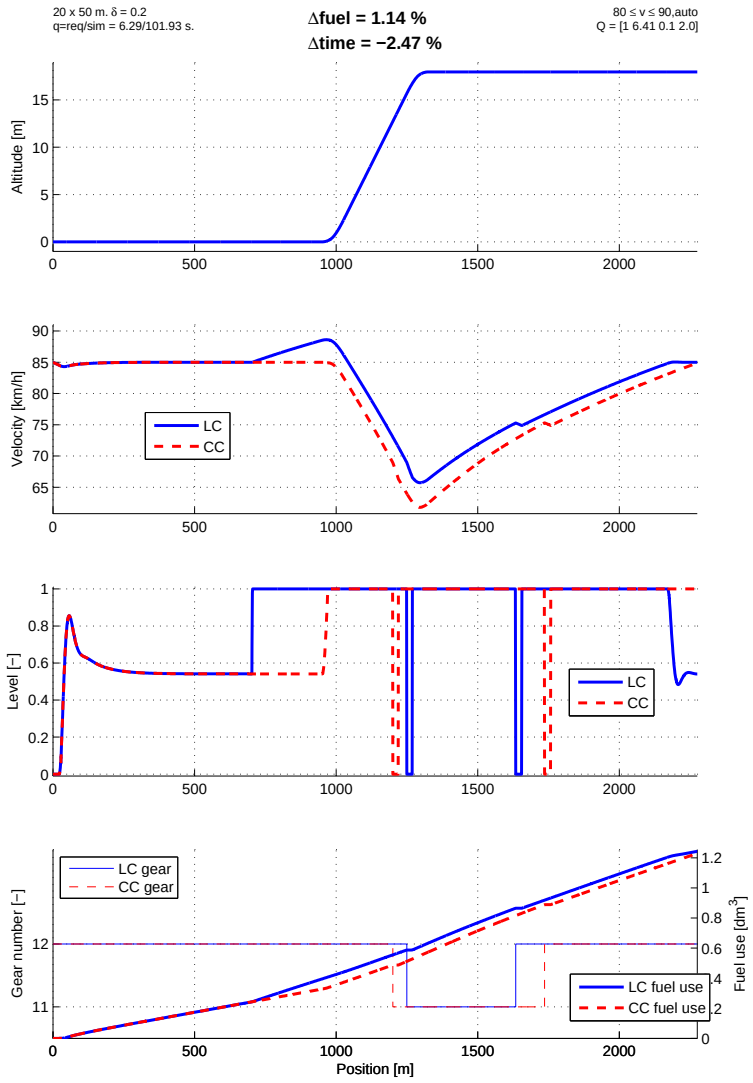

Figure 18: *Rule based algorithm in a 6 % 300 m upphill slope. LC denotes Look-ahead cruise controller and CC denotes the standard cruise controller.*

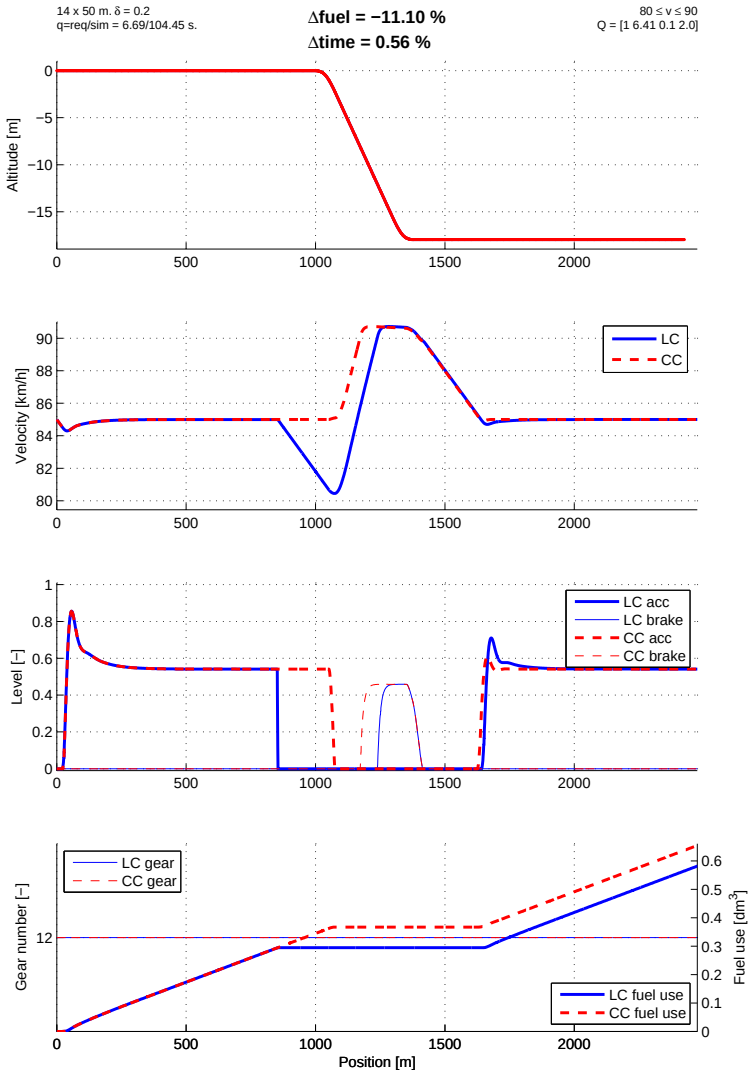

Figure 19: *Rule based algorithm in a -6 % 300 m downhill slope. LC denotes Look-ahead cruise controller and CC denotes the standard cruise controller.*

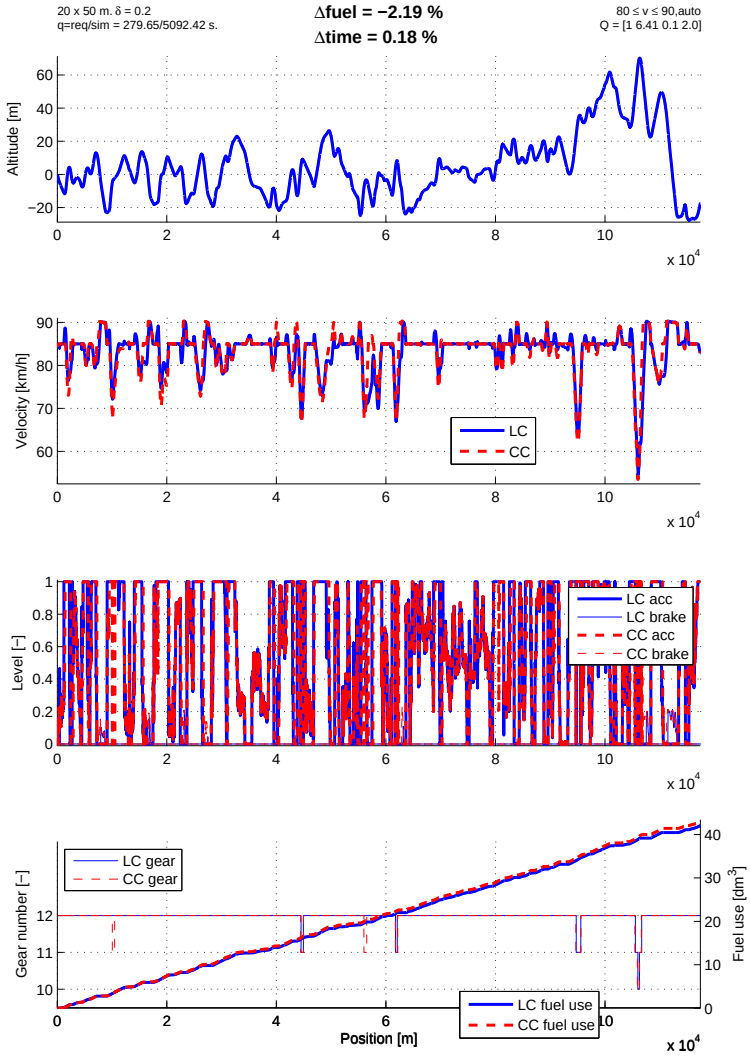

Figure 20: *Simulation of the rule based algorithm on the Highway E4 between the cities Södertälje and Norrköping in Sweden. LC denotes Look-ahead cruise controller and CC denotes the standard cruise controller.*

Bibliography

[1] Arthur E. Bryson and Yu-Chi Ho. *Applied optimal control.* Taylor and Francis, 1975.

[2] A. Fröberg, E. Hellström, and L Nielsen. Explicit fuel optimal speed profiles for heavy trucks on a set of topographic road profiles. *SAE Technical Paper Series, 2006-01-1071*, 2006.

[3] Anders Fröberg and Lars Nielsen. Optimal fuel and gear ratio control for heavy trucks with piece wise affine engine characteristics. Fifth IFAC symposium on advances in automotive control, Monterey Coast, California, 2007.

[4] Anders Fröberg and Lars Nielsen. Optimal control utilizing analytical solutions for heavy truck cruise control. *Technical report, Department of Electrical Engineering, Linköpings Universitet*, LiTH-ISY-R-2842, http://www.vehicular.isy.liu.se/Publications/, 2008.

[5] Erik Hellström, Maria Ivarsson, Jan Åslund, and Lars Nielsen. Look-ahead control for heavy trucks to minimize trip time and fuel consumption. Fifth IFAC Symposium on Advances in Automotive Control, Monterey, CA, USA, 2007.

[6] Erik Hellström. *Look-ahead control of heavy trucks utilizing road topography*. Licentiate thesis, LIU-TEK-LIC-2007:28, Linköping Institute of Technology, Linköping, 2007.

[7] Erik Hellström, Jan Åslund, and Lars Nielsen. Design of a well-behaved algorithm for on-board look-ahead control. *IFAC World Congress, Korea*, 2008.

[8] J.N. Hooker. Optimal driving for single-vehicle fuel economy. *Transportation Research part a*, 22(3), May 1988.

[9] Maria Ivarsson, Jan Åslund, and Lars Nielsen. Optimal speed on small gradients - consequences of a non-linear fuel map. *IFAC World Congress, Korea*, 2008.

[10] U. Kiencke and L. Nielsen. *Automotive Control Systems, 2nd ed.* Springer-Verlag, 2005.

[11] F. Lattemann, K. Neiss, S. Terwen, and T. Connolly. The predictive cruise control -a system to reduce fuel consumption of heavy duty trucks. *SAE Technical paper series*, (2004-01-2616), 2004.

[12] George Leitmann. *The calculus of variations and optimal control.* Plenum press, 1981.

[13] Rongfang Liu and Iakov M. Golovitcher. Energy -efficient operation of rail vehicles. *Transporation research Part A*, 37(10):917–932, 2003.

[14] C. Manzie, H. Watson, and S. Halgamuge. Fuel economy improvements for urban driving: Hybrid vs. intelligent vehicles. *Transportation Research Part C*, (15):1–16, 2007.

[15] S. M. Savaresi, F. L. Taroni, F. Previdi, and S. Bittanti. Control system design on a power-split cvt for high-power agricultural tractors. *IEEE/ASME Transactions on mechatronics*, 9(3):569–579, 2004.

[16] A. B. Schwarzkoopf and R. B. Leipnik. Control of highway vehicles for minimum fuel consumption over varying terrain. *Transportation Research*, 11:279–286, 1977.

[17] A. Sciaretta and L. Guzzella. Fuel-optimal control of rendezvous maneuvers for passenger cars. *Automatisierungstechnik*, 53(6):244–250, 2005.

[18] P. Setlur, J. R. Wagner, D. M. Dawson, and B. Samuels. Nonlinear control of a continuously variable transmission (cvt). *IEEE Transactions on control systems technology*, 11(1):101–108, 2003.

[19] S. Terwen, M. Back, and V Krebs. Predictive powertrain control for heavy duty trucks. *First IFAC Symposium on Advances in Automotive Control*, 2004.